This is to certify that the

thesis entitled

THREE-DIMENSIONAL KINEMATICS OF THE EQUINE TEMPOROMANDIBULAR JOINT

presented by

Stephanie Julie Bonin

has been accepted towards fulfillment
of the requirements for

MS degree in Mechanical Engineering

Major professor

Date 8/29/01

THREE-DIMENSIONAL KINEMATICS OF THE EQUINE TEMPORAL MANDIBULAR JOINT

By

Stephanie Julie Bonin

A THESIS

Submitted to
Michigan State University
in partial fulfillment of the requirements
for the degree of

MASTER OF SCIENCE

Department of Mechanical Engineering

2001

ABSTRACT

THREE-DIMSIONAL KINEMATICS OF THE
EQUINE TEMPORAL MANDIBULAR JOINT

By

Stephanie Julie Bonin

Topics in equine medicine related to the temporomandibular joint (TMJ) receive far less attention than other branches such as lameness, infectious disease and reproduction. Problems with the TMJ can affect a horse's ability to chew and properly digest its food and to perform as an athlete. The anatomy of the equine dentition is such that the constructs of the teeth highly influence the overall motion of the mandible and the grinding capacity during the chewing cycle. Consequently, regular dental exams and treatments are essential to the overall health of the animal. As in most branches of medicine, it is important to first understand normal function prior to analyzing pathologies. This study examines the normal chewing pattern of seven horses while chewing two different feed types: hay and pellets. Retro-reflective spherical markers were adhered to the horse's skull and mandible and a Motion Analysis System recorded the marker locations as the horses chewed hay and pellets. The data were processed with customized software and the three-dimensional displacement and rotations, described as pitch, roll, and yaw, of the mandible relative to the skull were computed. In addition, a virtual tracking marker was created on the mandible and tracked relative to the skull. The mandible was found to have a significantly greater range of motion while chewing hay versus pellets. The mandibular velocity while chewing hay versus pellets was not significantly different.

DENTAL DILEMMA

By Dale Jeffrey

When I was young my teeth came in
They got sharp edges that stole my grin
Somehow they didn't match quite right
And now I've got an overbite.

As if these problems weren't enough
My wolfers made my cheeks so rough
And after they became so sore
They couldn't drag me through the door

There was not a bit that I would take
Nor any rider I could shake
So there I stood within my stall
No one would help me through it all

My caps came in and stuck so tight
They say I colicked in the night
And now I have the wavy mouth
I hear they'll ship me to the south

So…
If you don't want to end up like me
Your equine dentist, you should see

ACKNOWLEDGMENTS

I would like to thank my co-advisor, Dr. Hilary M. Clayton, for her supervision throughout the duration of this project and guidance during the writing of this thesis.

I am grateful for the contributions of my co-advisor Dr. Brian Feeny and committee member Dr. Alan Haddow. Thank you for being part of my committee and advising me during the writing of this document.

I greatly appreciate the assistance of Dr. Thomas Johnson, whose desire to improve the quality of horse's lives lead to this research.

I would also like to express my deepest gratitude to Mr. Joel Lanovaz, whose input made this research possible. Thank you for the valuable contributions and guidance made throughout this project.

Finally, I would like to thank my husband, Dr. Hooman Rezaei for his patience and understanding throughout the time required to complete this thesis.

TABLE OF CONTENTS

LIST OF TABLES

LIST OF FIGURES

1. Introduction:

Prior to discussing modern-day equine dentistry, it is important to understand how and why the horse's dentition evolved to its present state. In this section, the evolution of equine dentition will be briefly discussed, followed by a description of common malocclusions. A description of the anatomy of the TMJ, the skull's bones, and muscles of mastication will follow. Previous equine and human studies that examined the motion of the TMJ will be mentioned next. Finally, a brief discussion of kinematic analysis techniques, a description of the motion capture system, and a statement regarding the research objectives will complete the chapter.

1.1 Equine Dental Evolution:

The evolutionary developments that lead to the modern horse *Equus caballus* began during the Eocene Epoch, which lasted from about 54 million to 38 million years ago. During the early Eocene the first ancestral horse appeared, a hoofed, browsing mammal known technically as *Hyracotherium* but more commonly called eohippus, the "dawn horse." This animal lived on succulent plants that caused little dental wear on its short-crowned teeth. As the years went by, climatic changes resulted in vegetation changes and the descendants of Hyracotherium evolved to adapt to a coarse, grassy diet (Baker and Easley, 1999).

During the remainder of the Eocene, the prime evolutionary changes were in dentition, which appear abruptly in the fossil record. *Orohippus*, a genus from the middle Eocene, and *Epihippus*, a genus from the late Eocene, resembled eohippus in size and limb structure, but the dentition was quite different. The cheek teeth, comprising the four premolars and the three molars found in each half of both jaws, were undergoing changes. In eohippus the premolars and molars were clearly distinct, the molars being larger. In *Orohippus* the fourth premolar had become similar to the molars, and in *Epihippus* the second, third, and fourth premolars had become molar-like. Modern day horses have retained this pattern. The six functional cheek teeth, consisting of the second, third, and fourth premolars and the three molars, are similar in size and shape. This first premolar has become vestigal. It is sometimes present as the "wolf" tooth, in the upper dental arcade, but is essentially non-functional.

In addition to these morphological changes, the individual cusps that characterized the cheek teeth of eohippus had been replaced in *Epihippus* by a system of continuous crests or ridges running the length of the molars and premolars (Encyclopedia Britannica, 2000). As a result, the outer surface of the teeth was no longer covered entirely by enamel; instead a folded layer of cement, enamel, and dentin was exposed to the occlusal surface **(Figure 1)**.

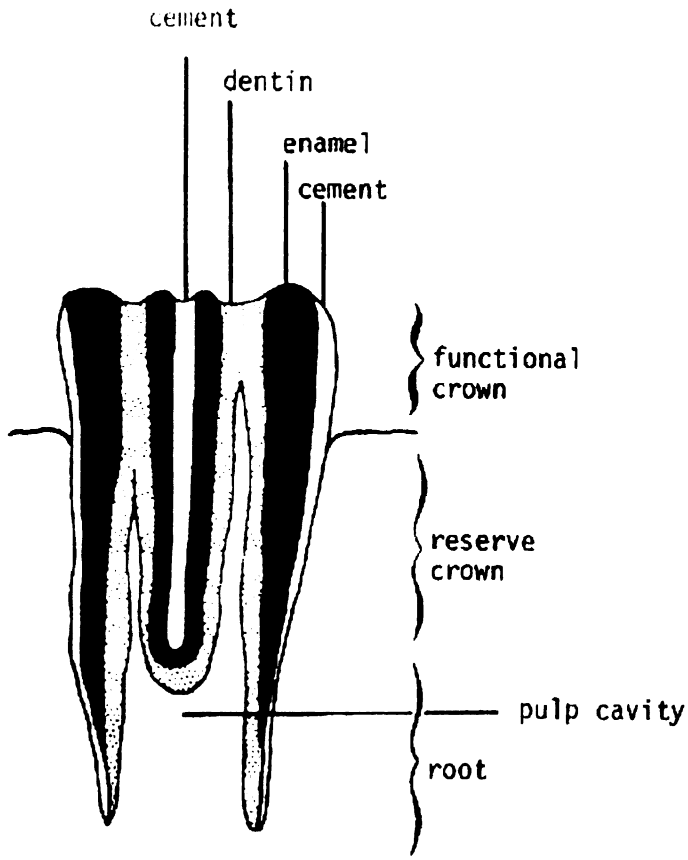

Figure 1: Schematic of a cheek tooth's anatomy

These calcified tissues wear at different rates (enamel slowest, dentin and cementum fastest) creating a permanently irregular occlusal surface that is advantageous in the grinding of coarse fibrous foodstuffs and acts as a self-sharpening mechanism (Baker and Easley, 1999). These changes, which represent adaptations to a more specialized grazing diet, were retained by all subsequent ancestors of the modern horse.

Grass is much coarser than succulent leaves and requires a different kind of tooth structure. Grass contains abrasive silicates, both within the plant and in the soil attached to the roots and lower stems. As equine predecessors increased in size, they were required to forage for longer periods of time to ingest sufficient nutrients to support their larger body mass and the food was ground into smaller particles for more efficient digestion. The changing requirements placed additional demands on the cheek teeth, which developed larger, stronger crests and became adapted to the side-to-side motion of the lower jaw necessary to grind grass blades. Each tooth progressed from being low-crowned (brachydont) to developing an extremely long crown (hypsodont), most of which, in the young animal, was buried beneath the gum line. As grinding wore down the exposed surface, some of the reserve crown grew out. This high-crowned tooth structure assured the animal of having an adequate grinding surface throughout its normal life span. Adaptations in the digestive tract must have occurred as well, but the organs of digestion are not preserved in the fossil record. In modern day horses, the permanent cheek teeth erupt at a rate of 2-3 mm/year, which is similar to the rate of attrition on the occlusal surface of the tooth, provided the horse regularly consumes a fibrous diet such as grass rather than high levels of concentrate food (Baker and Easley, 1999).

1.2 Common Dental Malocclusions:

A horse's teeth erupt constantly throughout its lifetime. The coarse, fibrous nature of the horse's diet wears the surface of the teeth, but the wear patterns are not always symmetrical and dental pathologies frequently occur. Malocclusions, or the improper position and contact between teeth, lead to inefficient chewing, bit discomfort, excessive wear and premature loss of teeth. Many horses will not show overt symptoms of dental problems until it is too late to treat them successfully. Malocclusions of the molars include hooks, ramps, enamel points, sheared molar table, wave complexes, accentuated transverse ridges, and periodontal pockets.

Hooks can develop at the rostral or caudal ends of the molar table. Rostral hooks are dominant upper front premolars overhanging the rostral edge of the lower premolars. They may develop as a result of a horse born with an overbite or they may be a secondary result from molar malocclusions that force the jaw out of alignment (Johnson, 2000). Caudal hooks are dominant lower or upper last molars overhanging the opposing molar. They may develop as a result of a horse born with an underbite or they may be a secondary result from molar malocclusions that force the jaw out of alignment (Johnson, 2000). Both conditions prevent horses from chewing freely from side to side, resulting in improper and excessive molar wear. They can cause extreme discomfort when the position of the head is changed during riding or from interaction with the bit, and the sharp molar points can lacerate soft tissues (Baker and Easley, 1999, Johnson, 2000).

Excessive height of the lower second premolar characterizes a ramp. This condition may occur when the upper second premolar deciduous tooth is retained, preventing normal growth of the permanent premolar (Johnson, 2000). They may also arise from a tooth reduction without correcting the opposing tooth. Ramps also prevent horses from chewing freely from side to side, cause severe discomfort with the bit, and can force the lower jaw forward over time, resulting in an underbite (Johnson, 2000).

Enamel points are sharp points that generally form on the buccal (cheek) side of the upper molars and lingual (tongue) side of the lower molars (Baker and Easley, 1999, Johnson, 2000). They develop over time as the horse reduces the lateral excursion of the mandible during chewing, resulting in the unopposed edge of the tooth getting longer. The unworn enamel forms razor sharp points. Sometimes this progresses to a sheared molar table, which is an extreme angulation of the chewing surface of the molars as seen from the front (Hayes, 1968, Johnson, 2000). This is a more severe condition than sharp enamel points since it precludes lateral motion of the mandible. This becomes a vicious cycle resulting in poor utilization of feed.

Wave complexes are characterized by a series of convex and concave changes of the crowns and occlusal surfaces of the cheek teeth with a reciprocal concave and convex changes on the opposing arcade (Baker and Easley, 1999) resulting in an uneven "wavelike" appearance. This condition often occurs secondary to other malocclusions such as retained deciduous caps, missing teeth, hooks, ramps, etc. Wave complexes cause gradual excessive wear to many molars, resulting in prematurely worn out teeth, periodontal pocketing, decay, and loss of teeth (Johnson, 2000). The horse is prevented from chewing freely from side to side and properly grinding its food.

Enlarged ridges that run across chewing surfaces of molars are accentuated transverse ridges and can result from a shift in jaw alignment. Ridges develop as a result of a harder area in one tooth wearing a soft area in an opposing tooth. This condition can also develop if a horse is not chewing with proper lateral excursion. Excessive wear to opposing molars, reduced front to back motion of the lower jaw, and severe periodontal disease can result (Johnson, 2000).

Periodontal pockets develop when gum disease around a tooth allows a space to develop between the tooth and the surrounding gum. Food collects in the resulting pocket and leads to infection, abscesses, and bone erosion around the teeth, which lose their stability and may fall out (Johnson, 2000). **Figure 2** depicts some of the above malocclusions.

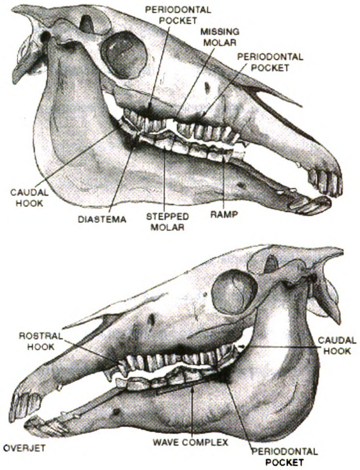

Figure 2: Common Malocclusions

Proper and regular dental treatment can prevent and correct many of these malocclusions.

1.3 Dental Health and Performance:

In order to wear the occlusal surfaces of the teeth sufficiently, the mandible must undergo adequate lateral excursion. When the teeth do not completely abrade against each other, malocclusions, such as sharp enamel point, hooks, and ramps can develop, which can exacerbate the problem by further preventing lateral excursion. This self-propagating cycle can lead to inefficient chewing, poor nutrition, bit discomfort, excessive wear and premature loss of teeth. Many horses will not show symptoms of dental problems until it is too late. In addition, horses experiencing oral pain will not perform up to their best abilities.

Performance horses face further anomalies as they are required to wear a bridle, which includes a bit in their mouth and cavesson (leather strap) fitted snug around their nose to aid in keeping the mouth shut. Pain can result from the bit making harsh and abrupt contact with malocclusions at the rostral end of the cheek teeth and the cavesson prevents the jaws from opening to avoid contact and alleviate the pain.

As a horse is ridden, the rider often changes the position of the horse's head. As the head moves from a somewhat horizontal position to an orientation that is more perpendicular to the ground, the lower jaw may slide relative to the upper jaw. In cases where severe wave mouth or hooks exist, the lower jaw cannot easily slide due to the cheek teeth interfering with each other. In order to comfortably orient the head in the desired position, the mouth must open to allow the lower jaw to slide, however, with a cavesson fitted snuggly over the nose, the jaws are unable to open. Consequently, pain can develop at the TMJ, resulting in head tossing, teeth grinding, and tail swishing, which are often considered training problems rather than medical problems.

1.4 Anatomy of the Temporomandibular Joint:

The temporomandibular joint is classified as a synovial, condylar joint, formed by the condylar process of the mandible that engages with the articular tubercle of the temporal bone. A meniscal cartilage compensates for incongruencies between the two articular surfaces (Rosenstein *et al.,* 2001). The joint capsule it tight and reinforced by an indistinct lateral ligament and an elastic posterior ligament (Sisson and Grossman, 1975). A joint complex, as depicted in **Figure 3**, exists on each side of the skull with independent joint capsules, but the whole arrangement is regarded as constituting a single condylar joint (Dyce *et. al.*, 1987). Movement on one side must be accompanied by a movement, not necessarily identical, on the other side (Dyce *et al.*, 1987). Between the articular surfaces of the mandible and the temporal bone lies a fibrous articular disc that divides the joint cavity into upper and lower compartments, the former being more spacious (Sisson and Grossman, 1975). The complex motion of the joint can be resolved into simpler components; a hinge movement occurs in the lower compartment between the mandible and the disk, while translation of the mandible relative to the skull occurs at the upper compartment. In species where the mandibular movement is simple, such as a dog, the disk is rather thin and poorly developed. In species where lateral grinding movements predominate, the mandibular head is larger, the surface more plateau-like, and the disk thicker as in most herbivores (Dyce *et al.*, 1987). Herbivores employ the cheek teeth for grinding ingested food and the active grinding movement is preceded by lateral displacement. The temporomandibular joint of these animals is situated high above the occlusal plane and the lower teeth are drawn forward over the opposing upper teeth as they approach. This contributes a grinding component that is absent when the joint and occlusal surfaces are more nearly level (Dyce *et al.*, 1987).

1.4.1 Bones of the Skull:

The temporal bone is one of fifteen bones that articulate to form the skull. It forms the greater part of the lateral wall of the cranium and articulates with the zygomatic, occipital, parietal, frontal, and basisphenoid bones by rigid joints called sutures **(Figure 3)**. It also articulates with the mandibular condyle, and the hyoid apparatus. The temporal bone consists of three distinct parts: squamous, tympanic, and petrous (Dyce *et al.*, 1987). The squamous portion of the temporal bone articulates with the mandible at the temporomandibular joint. The mandible is the largest bone of the equine face. The left and right mandibles are firmly joined at the mandibular symphysis that fuses in the foal at 2 to 3 months (Baker and Easley, 1999).

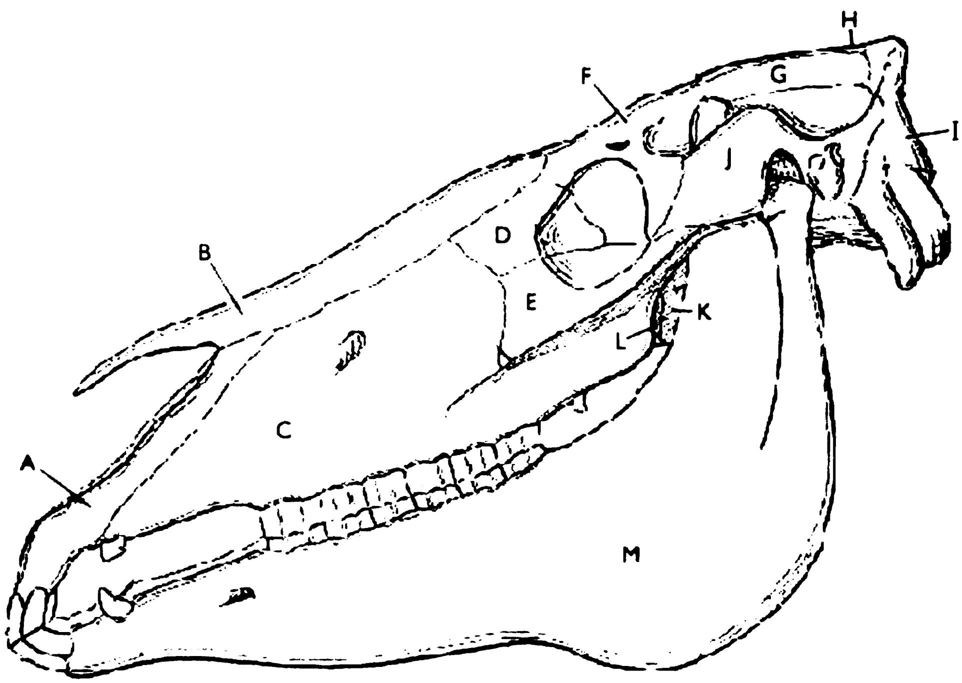

A. Incisive
B. Nasal
C. Maxilla
D. Lacrimal

E. Zygomatic
F. Frontal
G. Parietal
H. Interparietal
I. Occipital

J. Temporal
K. Sphenoid
L. Palatine
M. Mandible

Figure 3: Bones of the Equine skull

1.4.2 Muscles of Mastication:

Six muscle pairs are utilized during chewing. The masseter, which aids in closing the mouth, originates from the facial crest and the zygomatic arch and inserts on the ramus of the mandible. The temporalis originates at the temporal fossa and inserts at the coroniod process of the mandible and acts in closing the mouth. The medial and lateral pterygoids close the mouth and move the mandible rostrally and laterally. They originate from the pterygoid process of the basisphenoid bone, and insert on the medial surface of the mandible. The digastricus muscle, which opens the mouth, originates from the jugular process of the occipital bone and inserts on the ventral border of the mandible. Finally, the occipitomandibularis, another muscle that opens the mouth, originates from the jugular process of the occipital bone, and inserts on the caudal border of the mandible. All muscles of mastication are innervated by the mandibular branch of the trigeminal (V) nerve except for the digastricus, which has dual innervation from the facial (VII) and trigeminal (V) nerves and the occipitomandibularis, which is supplied by the facial (VII) nerve (Sisson and Grossman, 1975).

1.5 Evaluation of TMJ Motion:

Existing studies of TMJ motion in horses and humans are reviewed in this section.

1.5.1 Equine Studies:

Chewing is based upon the repetition of a cyclical movement that results from the coordinated rhythmic contraction of all the muscle groups associated with the opening and closing of the jaws. In studies of the chewing cycle in many species it was found that, with the exception of man, mammals have consistent chewing patterns - consistent both individually and as a species (Baker and Easley, 1999). Few studies exist on qualifying the three-dimensional motion of the equine TMJ.

In 1941, Leue developed a mechanical recorder that attached to the upper and lower jaws of horse's with a stationary notepad and a pen the followed the motion of the mandible (**Figure 4**).

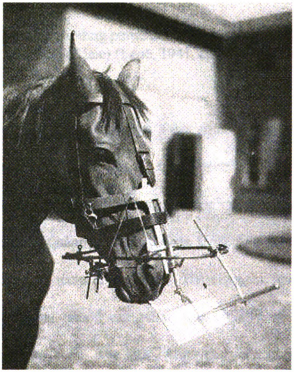

Figure 4: Mechanical recorder utilized to trace grinding patterns (Leue, 1941, cited by Becker, 1962)

Dixon (2000) stated the lateral excursion values from Leue's study were 60 mm, 38 mm, and 23 mm while chewing grass, oats, and bran respectively. Leue, however, did not report these values and the location that these measurements were made is not specified **(Figure 5)**.

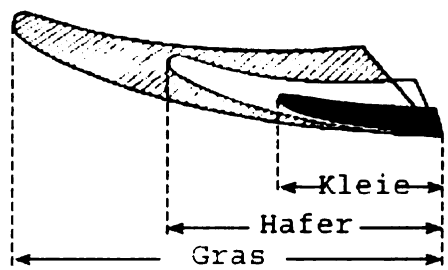

Figure 5: Varying grinding patterns while chewing grass (Gras), hay (Hafer), and bran (Kleie) (Leue, 1941, cited by Becker, 1962)

Leue proposed that bundles of fibrous food such as hay or grass could readily be maintained on the occlusal surface of the mandibular cheek teeth as they moved laterally to their full extent, thereby allowing a complete horizontal grinding movement. However, just a limited quantity of particulate food, such as bran, could be retained on the narrow mandibular occlusal surface. Therefore, a primary vertical mandibular movement, with minimal lateral excursion, was required to maintain particulate food between the occlusal surfaces. The lack of lateral excursion allows the development of enamel overgrowths. Diets high in concentrates also greatly limit the length of time horses chew forages and so further predispose to such enamel overgrowths (Leue, 1941, cited by Dixon *et al.*, 2000).

Baker and Easley (1999) conducted a two-dimensional video analysis of the equine masticatory movements. Their results corresponded to the general masticatory cycle of herbivorous mammals with the chewing cycle being divided into three phases according to the relative displacement of the mandible: the opening stroke (O), the closing stroke (C), and the power stroke (P). **Figure 6** depicts isolated frames from a video recording of equine mastication and **Figure 7** shows the positional changes of the mandible. Note that frames 1- 4 represent the opening stroke, frames 5-6 represent the closing stroke, and frames 7-10 represent the power stroke.

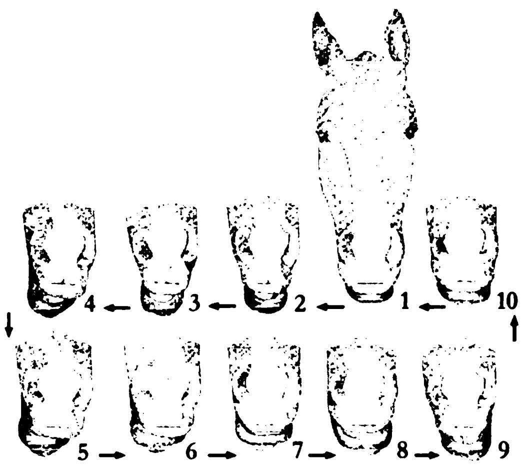

Figure 6: Chewing cycle of a horse reproduced from video recordings (Baker and Easley, 1999, reproduced with permission).

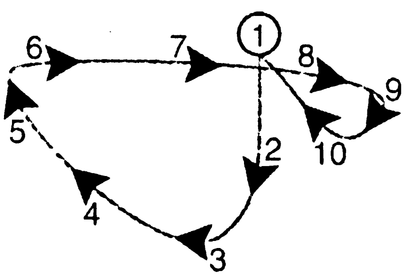

Figure 7: Path of mandible during the chewing cycle (Baker and Easley, 1999, reproduced with permission).

It is evident that Baker and Easley observed the chewing cycles from the front of the horse, however, they did not define the specific plane that the motion was observed in. In addition, the motion was tracked by observing how a point on the lower lip displaced relative to a point on the upper lip. The lips consist of highly mobile soft tissue and cannot be classified as rigid bodies. Therefore, movements of the lips do not accurately represent mandibular motion, though they may indicate the general pattern of movement. In a study by Collinson (1994), the chewing frequency was measured using electromyography in four horses chewing food classified as low, medium, and high fiber. The frequency ranged from 1.14 Hz while chewing food with high fiber content to 1.16 Hz while chewing food with low fiber content. Collinson also measured the absolute velocity of the fourth premolar, which ranged from 85 mm/sec while chewing high-fiber food to 104 mm/sec while chewing low-fiber food. Incisor displacement was reported to be 44-45 mm.

The studies of Leue (1941) and Baker and Easley (1999) were two-dimensional. Previous studies of three-dimensional equine chewing motion have not been discovered.

The arrangement of the teeth within the upper and lower jaws is such that the lateral outward curve of the upper dental arcade is not fully accommodated by the conformation of the lower arcade, i.e. the lower arcade is straighter and the distance between the left and right arcades is less in the mandible than in the upper jaw (**Figure 8**).

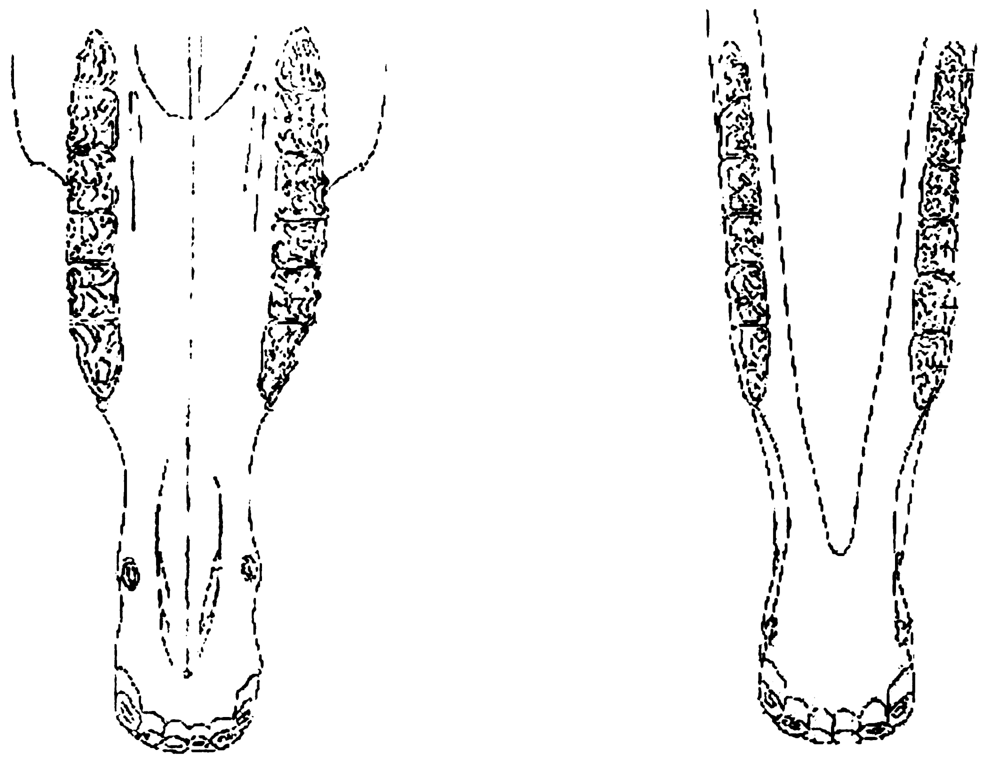

Figure 8: Upper and lower dental arcades

As a consequence of the discrepancy in width between the upper and lower dental arcades, the mandible must move a considerable distance laterally to make complete occlusal contact across the width of the teeth in the upper arcade. Complete occlusal contact is necessary to ensure that the entire molar table receives even and adequate wear.

1.5.2 Human Studies:

Human studies have been performed to evaluate the three-dimensional TMJ motion. Techniques utilized include magnetic resonance imaging (MRI) to acquire sequential images of the joint capsule during opening and closing of the mouth (Chen and Buckwalter, 1992, Koolstra and Van Eijden, 1992), an optoelectronic system that tracks light-emitting diodes (Zhang *et al.* 1995, Ostry *et al.* 1997, Gallo *et al.*, 2000), and magnetometers in which the displacement of magnets on the incisors is detected and recorded (Plesh *et al.*, 1993). Computed tomography allows three-dimensional examination of the TMJ and has been used primarily for morphological examination and to develop mathematical models of the joint (Christiansen *et al.* 1987, Paz *et al.* 1990, Raustia *et al.*, 1990). Similar techniques (radiographic, ultrasound, computed tomography, scintigraphy, and magnetic resonance imaging) have been applied in studies of the equine TMJ, primarily for anatomical purposes and not for motion analysis (Patterson *et al.*, 1989, Warmerdam *et al.*, 1997, Weller *et al.*, 1999, Rosenstein *et al.*, 2001).

1.6 Kinematic Analysis:

A complete understanding of joint kinematics is important in understanding the etiology, pathology, diagnosis, and treatment of joint disorders resulting from injury or disease, in the design of better prosthetic devices, and in the general study of locomotion (Grood and

Suntay, 1983). In order to evaluate joint motion, a set of coordinate systems needs to be established in the segments proximal and distal to the joint. In 1983, Grood and Suntay developed a joint coordinate system that provides a simple geometric description of the three-dimensional rotational and translational motion between rigid bodies. Their coordinate system was applied to the knee and the joint motions were described in a way that provides clinical significance for physicians and orthopaedic surgeons. Joint coordinate systems are created by using markers placed on key anatomical locations such that the axes of the coordinate systems are aligned with anatomical axes of the body segments.

Kadaba *et al.*, (1990) developed a systematic method for lower extremity external marker placement, sometimes called the Helen Hayes method, named after the hospital where the technique was developed. The relatively small number of body surface markers used in the system render it easy to implement in routine clinical gait evaluations to compute the motion at the pelvis, hip, knee, and ankle joints. The markers are used to define a coordinate system for each segment, and axes and planes about which the limb rotations take place.

The author has not encountered any study of TMJ motion, human or animal, that utilizes body surface markers to track the motion.

The location of one coordinate system relative to another is commonly described by Euler angles (or Cardan angles) or by the concept of a helical axis. Euler angles are defined as a set of three finite rotations assumed to take place in sequence to achieve the final orientation from a reference orientation (Kadaba, 1990). The displacement of a segment from one position to another can also be represented as a rotation about and a translation along a particular axis in space called the helical axis or screw axis (Woltring *et al.*, 1985). The motion of the mandible relative to the skull will be defined in this thesis by three successive rotations: pitch, roll, and yaw (Ostry *et al.* 1997, Fredrickson and Drevemo, 1971). This research study used a highly accurate optical motion capture system to track markers attached to the skin overlying bony landmarks on the skull and mandible of horses during chewing. The data describe the three-dimensional motion of the equine TMJ by six degrees of freedom: three translations and three rotations, using Euler angles as the rotational position coordinates.

1.7 Motion Analysis System:

The three-dimensional Optical Motion Capture System from Motion Analysis Corporation is a high performance video/computer-based instrumentation system that tests and measures the movement of objects. This system is commonly utilized for animation production, industrial measurement and control systems, and movement analysis such as gait analysis, sports medicine and performance, product design and development, orthotics and prosthetics, and virtual surgeries.

The Motion Analysis system functions like other videographic systems. Spherical retro-reflective skin markers are placed on the segments of interest (assumed to be rigid bodies) and each marker must be seen by at least two cameras. The action to be measured must take place in a calibrated volume. The coordinates of the skin markers are determined through automatic digitization, where the marker periphery is located through edge detection and the center of the marker is calculated. In the McPhail Equine Performance Center, the Motion Analysis system is typically used for locomotion analysis in horses, but the highly sensitive system with sub-millimeter accuracy can detect and track much smaller motions. This project applies the Motion Analysis system to study the kinematics of TMJ motion during chewing in horses to provide baseline information of characteristic, normal chewing patterns that can be compared to future studies of pathological equine TMJ motion.

1.8 Research Objectives:

The goal of this study is to investigate how horses chew different types of food. The objectives are to describe the normal three-dimensional motion of the equine temporomandibular joint (TMJ) during chewing and to measure differences in the motion while chewing hay versus pellets. The null hypothesis is that there is not a significant difference between the mean values of the variables that measure mandibular motion in horses chewing hay versus pellets. The experimental hypothesis is that the variables investigated are significantly different while chewing hay versus pellets.

2. Materials and Methods:

In this section, the subjects and equipment and their preparation will be described. The data collection procedure and the processing techniques will be discussed next and the data processing protocol will be explained.

2.1 Subjects:

The subjects were seven horses including one Hanoverian, one Quarter Horse, two Thoroughbreds, one Morgan, and two Appaloosas. A veterinary dentist verified that no malocclusions existed in these horses. The horses ranged from 4-15 years old, 480-655 kg, and 155 to 175 cm tall at the withers **(Table 1)**.

Table 1: Description of horses used in the study

Horse No.	Age	Breed	Height (cm)	Mass (kg)
1	5	Thoroughbred	165	534
2	15	Appaloosa	155	515
3	10	Morgan	157	655
4	10	Hanoverian	168	608
5	9	Appaloosa	162	480
6	4	Quarter Horse	165	550
7	8	Thoroughbred	175	649

2.2 Equine Preparation:

Hair was removed with clippers where markers were to be secured, including the forehead, nose, and right and left angle of the mandible, facial crest, articular tubercle, and condylar process. The skin was cleaned with rubbing alcohol to remove dirt and sweat. Twelve tracking markers were glued onto the skin with cyanoacrylate glue (super glue) on the most rigid locations on the skull and mandible (**Figure 9**). These tracking markers were placed on the forehead (8) and nose (9) on the midline of the face, bilaterally on the middle (6) and rostral (7) part of the facial crest, the notch on the mandible for facial vessels (5) and dorsally (3) and ventrally (4) on the caudal aspect of the mandibular ramus. In addition, virtual markers were placed on the right and left articular tubercles of the skull (1) and condylar processes of the mandible (2) on each side. Due to the close proximity of the tubercles and the condylar processes, two standing files were recorded: one with the tracking markers and the articular tubercle virtual markers and a second standing file with the tracking markers and the condylar process virtual markers.

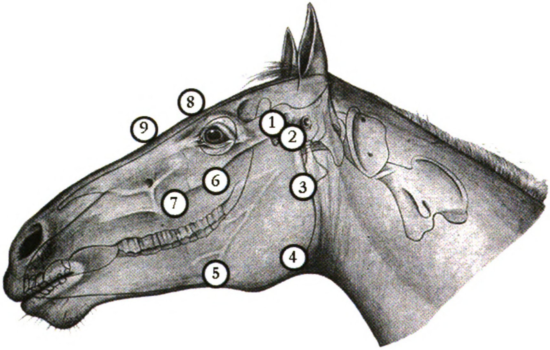

Figure 9: Locations of skin markers

2.3 Equipment Set-Up:

A Motion Analysis system for kinematic analysis (Motion Analysis Corporation, Santa Rosa, CA) was utilized for collecting data. Six Falcon infrared cameras (Motion Analysis Corporation, Santa Rosa, CA) were placed in a semi-circle around of the volume occupied by the horse's head (**Figure 10**).

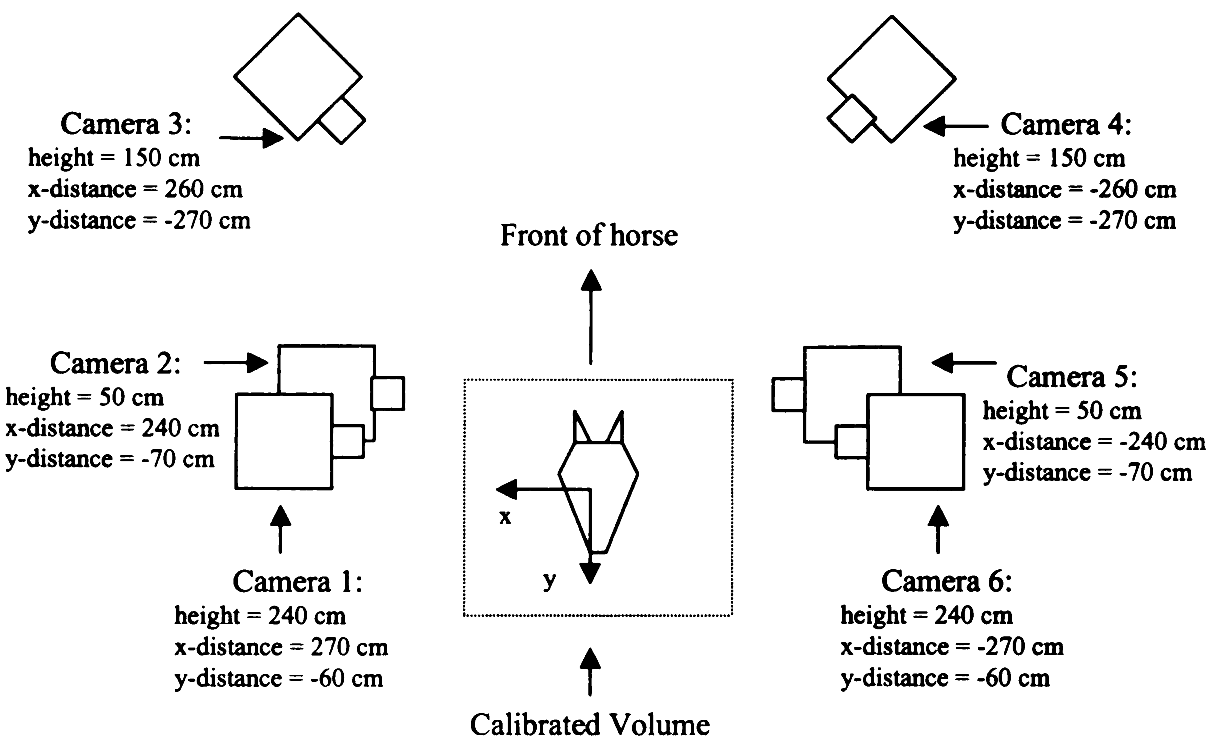

Figure 10: Camera set-up

The aperture and focus were adjusted for each camera to establish the highest quality image. The volume was calibrated according to Motion Analysis specifications. In addition, a video camera was set up to record the data collection process. A time code super imposed on the video image coincided with the time code file generated by the Motion Analysis system.

2.4 Data Collection Procedure:

2.4.1 Standing Files:

The horse stood with its head in the calibrated volume with the tracking markers and the virtual articular tubercle markers in place. Data were collected for one second at 60 Hz while the horse was not chewing. A single frame of data is sufficient for a standing file, however. The articular tubercle markers were removed and the condylar process markers were glued in place. Again, the horse stood in the calibrated volume while data were collected for one second at 60 Hz. The standing files were later utilized to calculate the locations of the articular tubercles and condylar processes from the measured locations of the tracking markers.

2.4.2 Tracking Files:

The virtual markers were removed and the horse was fed hay and pellets in random order while the head was in the calibrated volume. The hay was a mature, first cutting from a field composed of 90% timothy, 10% alfalfa. The pellets and were a commercial concentrated feed commonly fed to horses on a daily basis. The following table provides information on the feed samples:

Table 2: Description of feed types.

Feed Type	Description	Dry Matter	Protein	Fiber	Digestible Energy
Grass Hay	Over-mature first cutting	84.40%	8.70%	44.60%	1.83 Mcal/Kg
Pellets	Purina Horse Chow #100	90.00%	10.00%	30.00%	2.20 Mcal/Kg

Data were collected at 120 Hz while the horse was chewing the sample (**Figure 11**) and a data set was considered acceptable if the horse did not move its head out of the calibrated volume, did not make any rapid movements with its head, and was not in the process of ingesting feed. Upon giving the horse the second feed sample, the horse was allowed to consume the new feed type for at least 2 minutes to ensure that the prior feed type was no longer in the mouth before collecting data with the new feed type. A minimum of 4 chewing cycles per trial and a minimum of 6 trials per feed type were recorded.

Figure 11: Horse standing in calibrated volume, chewing pellet sample

2.5 Data Processing

The x, y, z locations of each marker were acquired every 1/120 second during the data collection. The files were analyzed through a customized MATLAB (The Mathworks, Natick, MA) program in order to determine how the mandible moves relative to the skull. The procedure was as follows:

1) Temporary coordinate systems were created on both the skull and mandible. The skull's origin was the forehead marker and the mandible's origin was the more ventral marker on the right side of the mandibular ramus. These locations were chosen because they appeared to have the least amount of skin displacement relative to the underlying bones during chewing. Skin displacement considerations will be discussed in more detail in section 4.1.

2) Vectors from the local origin to each marker on the segment were determined.

3) A generalized cross validation was performed on the tracked data in order to remove high frequency noise in the data (Woltring, 1986). This technique is a filtering process that fits a cubic spline to the raw data.

4) A transformation matrix and a translation vector were determined using a singular value decomposition method based on Soederkvist and Wedin (1993).

The algorithm by Soederkvist and Wedin (1993) produces a rotation matrix and a translation vector that describe the rotation and translation of the mandibular coordinate system from its neutral position (horse not chewing, obtained from the standing file) to the new orientation at each frame of tracked data. The algorithm determines the motion of a rigid body by using the positions of landmarks in a least-squared sense. The method uses the singular value decomposition of a matrix derived from the positions of the landmarks. Although the skull and mandible are rigid structures, skin displacement relative to the underlying bones occurs; this algorithm was employed because it obtains transformation matrices that minimize high frequency errors that possibly arise from skin displacement and provides a best approximation of the rotation. Matrix transformations will be described in full detail in the next section.

5) Upon smoothing the data and obtaining the transformations to describe the motion of the mandible, an orthogonal coordinate system, based on the skull and mandible anatomy, was established for both the skull and mandible (**Figure 12**). This was done in order to describe the relative motion of the mandible in anatomical terms.

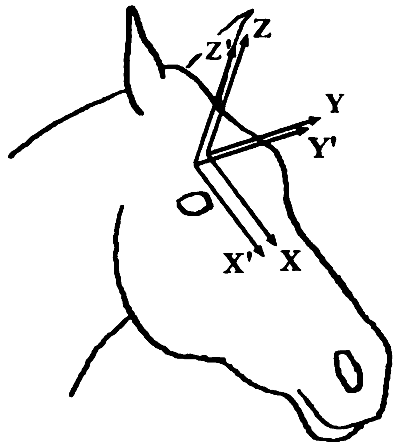

Figure 12: Location of skull and mandible coordinate systems

The techniques used to create these coordinate systems will be discussed in section 2.7.2.

6) Euler angles were directly calculated utilizing techniques from Ramakrishnan and Kadaba (1991). Euler angles will be described in section 2.7.3.

7) A virtual midline-mandible marker was created and tracked relative to the skull's coordinate system. This marker aids in visualizing the mandibular motion and allows comparisons to be made to previous studies. The technique used will be explained in section 2.5.4.

2.5.1 Coordinate Transformations

A rotation transformation matrix and a translation vector are necessary in order to describe the 3-dimensional motion of an object in space. A geometric vector is uniquely represented by an algebraic vector that contains components of the geometric vector in a Cartesian reference frame. The components of a vector, however, are defined in a specific Cartesian reference frame. Consider a second Cartesian x'-y'-z' frame with the same origin as the X-Y-Z frame, as shown in **Figure 13**. Unit x', y', and z' coordinate vectors are denoted by **f**, **g**, and **h**, respectively and unit X, Y, and Z coordinate vectors are denoted by **i**, **j**, and **k**.

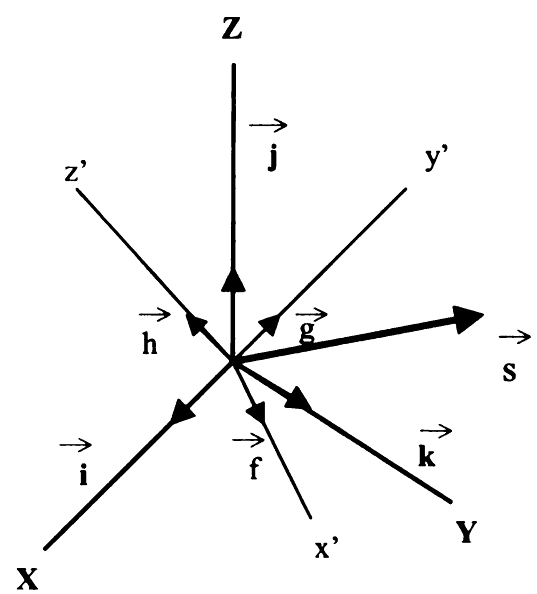

Figure 13: Two Cartesian reference frames with the same origin and rotated with respect to each other

A vector **s** in space can be represented in the X-Y-Z frame as

$$\mathbf{s} = s_x\,\mathbf{i} + s_y\,\mathbf{j} + s_z\,\mathbf{k} \tag{1}$$

or in the x'-y'-z' frame as

$$\mathbf{s} = s_x'\,\mathbf{f} + s_y'\,\mathbf{g} + s_z'\,\mathbf{h} \tag{2}$$

where

$$s_x = s \bullet \mathbf{i} \qquad s_y = s \bullet \mathbf{j} \qquad s_z = s \bullet \mathbf{k} \tag{3}$$

and

$$s_x' = s \bullet \mathbf{f} \qquad s_y' = s \bullet \mathbf{g} \qquad s_z' = s \bullet \mathbf{h} \tag{4}$$

The algebraic vectors that define **s** and **s'** are

$$\mathbf{s} = [s_x, s_y, s_z]^T \tag{5}$$

in the X-Y-Z frame and

$$\mathbf{s}' = [s_x', s_y', s_z']^T \tag{6}$$

in the x'-y'-z' frame.

It is clear that there is a relation between **s** and **s'**, since they are defined by the same geometric vector s. To establish the relationship between **s** and **s'**, the **f**, **g**, and **h** unit vectors are expanded in the terms of the **i**, **j**, and **k** unit vectors as

$$\begin{aligned} \mathbf{f} &= a_{11}\mathbf{i} + a_{21}\mathbf{j} + a_{31}\mathbf{k} \\ \mathbf{g} &= a_{12}\mathbf{i} + a_{22}\mathbf{j} + a_{32}\mathbf{k} \\ \mathbf{h} &= a_{13}\mathbf{i} + a_{23}\mathbf{j} + a_{33}\mathbf{k} \end{aligned} \tag{7}$$

where a_{ij} are the following direction cosines:

$$\begin{aligned} a_{11} &= i \bullet f = \cos\theta\,(\mathbf{i},\mathbf{f}) \\ a_{12} &= i \bullet g = \cos\theta\,(\mathbf{i},\mathbf{g}) \\ a_{13} &= i \bullet h = \cos\theta\,(\mathbf{i},\mathbf{h}) \\ a_{21} &= j \bullet f = \cos\theta\,(\mathbf{j},\mathbf{f}) \\ a_{22} &= j \bullet g = \cos\theta\,(\mathbf{j},\mathbf{g}) \\ a_{23} &= j \bullet h = \cos\theta\,(\mathbf{j},\mathbf{h}) \\ a_{31} &= k \bullet f = \cos\theta\,(\mathbf{k},\mathbf{f}) \end{aligned} \tag{8}$$

$$a_{32} = \mathbf{k} \bullet \mathbf{g} = \cos\theta\,(\mathbf{k},\mathbf{g})$$

$$a_{33} = \mathbf{k} \bullet \mathbf{h} = \cos\theta\,(\mathbf{k},\mathbf{h})$$

Substituting Eq. 7 into Eq. 2 yields

$$\mathbf{s} = (a_{11}s_x' + a_{12}s_y' + a_{13}s_z')\mathbf{i} + (a_{21}s_x' + s_{22}s_y' + a_{23}s_z')\mathbf{j} + (a_{31}s_x' + a_{32}s_y' + a_{33}s_z')\mathbf{k} \quad \textbf{(9)}$$

Equating corresponding right sides of this representation of **s** and **Eq. (1)**,

$$\begin{aligned} s_x &= a_{11}s_x' + a_{12}s_y' + a_{13}s_z' \\ s_y &= a_{21}s_x' + s_{22}s_y' + a_{23}s_z' \\ s_z &= a_{31}s_x' + a_{32}s_y' + a_{33}s_z' \end{aligned} \quad \textbf{(10)}$$

In matrix form, this is

$$\mathbf{s} = \mathbf{A}\mathbf{s}' \quad \textbf{(11)}$$

where **A** is called the direction cosine matrix or rotation transformation matrix:

$$A = \begin{bmatrix} a_{11} & a_{12} & a_{13} \\ a_{21} & a_{22} & a_{23} \\ a_{31} & a_{32} & a_{33} \end{bmatrix} \quad \textbf{(12)}$$

When the origins of the X-Y-Z and x'-y'-z' frames do not coincide, the foregoing analysis is applied between the x'-y'-z' and the translated X-Y-Z frame, as shown in **Figure 14**.

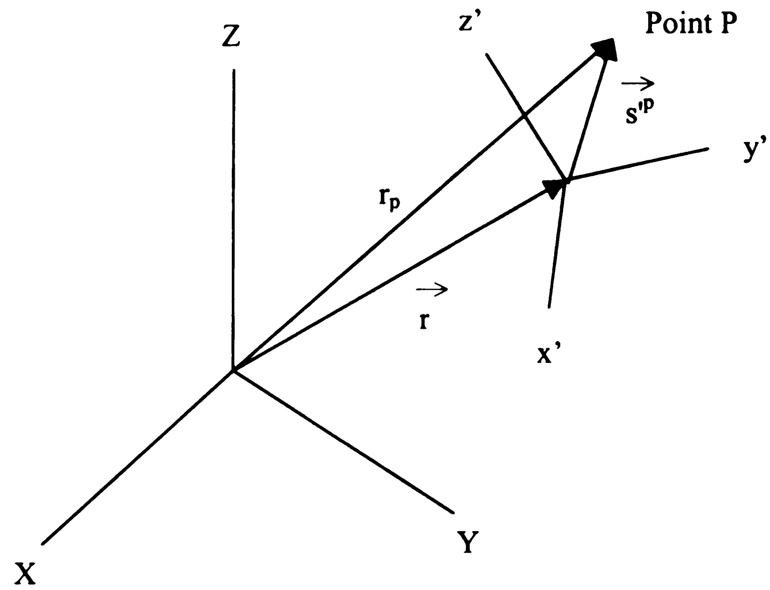

Figure 14: Translation and rotation of a reference frame.

If the algebraic vector $\mathbf{s}'^P$ locates point P in the x'-y'-x' frame, then in the translated X-Y-Z frame, the vector is $\mathbf{A}\mathbf{s}'^P$. Thus,

$$\mathbf{r}^P = \mathbf{r} + \mathbf{A}\mathbf{s}'^P \tag{13}$$

where r is the translation vector from the origin of the X-Y-Z reference frame to the origin of the x'-y'-z' frame.

In the present study, the transformation matrix and translation vector are obtained in order to describe the orientation of the mandible from its neutral (non-chewing) position to the position at each frame.

2.5.2 Coordinate System Development

The skull and mandible are treated as rigid bodies and in order to describe how one moves relative to the other, each needs its own orthogonal coordinate system. The skull and mandible unit vectors are analogous to the **i**, **j**, **k** and **f**, **g**, **h** unit vectors respectively in **Figure 13**.

The tubercle markers were used to establish the y-axis of the skull's coordinate system:

$$J_{skull} = \frac{tubercle\ left - tubercle\ right}{\left| tubercle\ left - tubercle\ right \right|} \tag{14}$$

This establishes a unit vector from the right tubercle to the left tubercle.

Two unit vectors were established along the facial crests, from the mid-facial crest markers to the rostral marker on each side. A temporary I'-axis of the skull was established by averaging the right and left unit vectors:

$$I'_{skull} = \frac{right\ vector + left\ vector}{2} \tag{15}$$

The z and x-axes was determined by utilizing principles of cross products:

$$K_{skull} = I'_{skull} \times J_{skull} \tag{16}$$

$$I_{skull} = J_{skull} \times K_{skull} \tag{17}$$

The origin of the skull was the midpoint between the tubercle markers:

$$Skull\ Origin = \frac{tubercle\ left + tubercle\ right}{2} \tag{18}$$

A similar technique was applied to the mandible where the j-axis was established using the condyle markers:

$$J_{mandible} = \frac{condyle\ left - condyle\ right}{\left| condyle\ left - condyle\ right \right|} \tag{19}$$

The I' axis established for the skull was also used for the mandible:

$$I'_{mandible} = I'_{skull} \tag{20}$$

The z and x-axes was determined by utilizing principals of cross products:

$$K_{mandible} = I'_{mandible} \times J_{mandible} \tag{21}$$

$$I_{mandible} = J_{mandible} \times K_{mandible} \tag{22}$$

The origin of the mandible was the midpoint between the condyle markers:

$$Mandible\ Origin = \frac{condyle\ left + condyle\ right}{2} \tag{23}$$

The motion of the mandible coordinate system relative to the skull coordinate system was described using Euler angles.

2.5.3 Euler Angles

Euler angles are the three successive rotation angles that describe a body's orientation in three-dimensional space. In 1776, the Swiss mathematician Euler first established a series of transformations to describe the motion of a spinning top. Euler angles are sequence dependent, that is, the rotations must occur in a specific order to properly describe a body's orientation. These rotations are typically labeled α, β, and γ and in gait analysis, the rotations have the following definitions and anatomical descriptions:

Step 1: Rotation α (flexion/extension) about the Y-axis

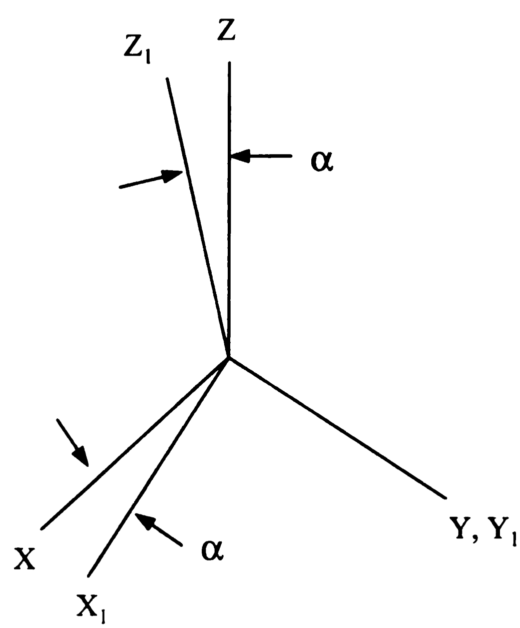

Step 2: Rotation β (ab/adduction) about the X_1-axis (also called the floating axis)

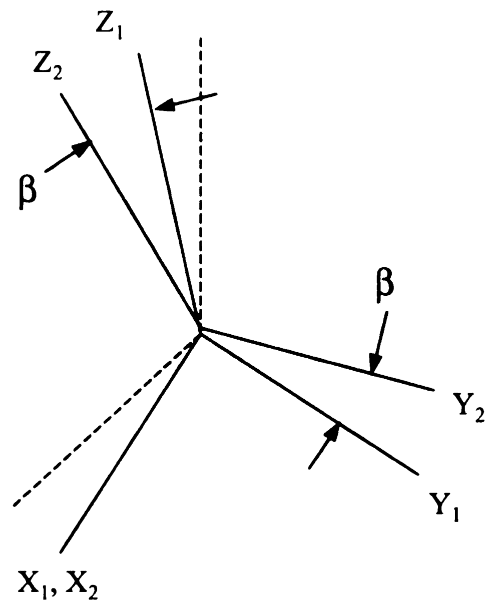

Step 3: Rotation γ (internal/external rotation) about the Z_2-axis

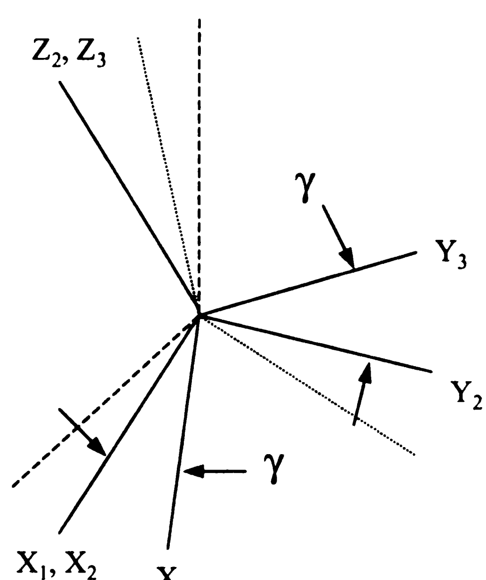

The terminology used in gait analysis is not applicable in describing the motion of the TMJ. Gait analysis terminology describes joint motion of limbs and how they move relative to the midline of the body. In this case, the skull and mandible are on the midline of the body and more appropriate terminology must be used. In a study performed by Ostry *et al.* (1997), the three rotations of the human mandible have been described as pitch, roll, and yaw where pitch is a rotation α about the Y (transverse horizontal) axis, roll is a rotation β about the X_1 (longitudinal) axis, and yaw is a rotation γ about the Z_2 (vertical) axis (**Figure 15**). Fredricson and Drevemo (1971) also used this terminology to describe the equine hoof motion during racing. This is the convention utilized in this study.

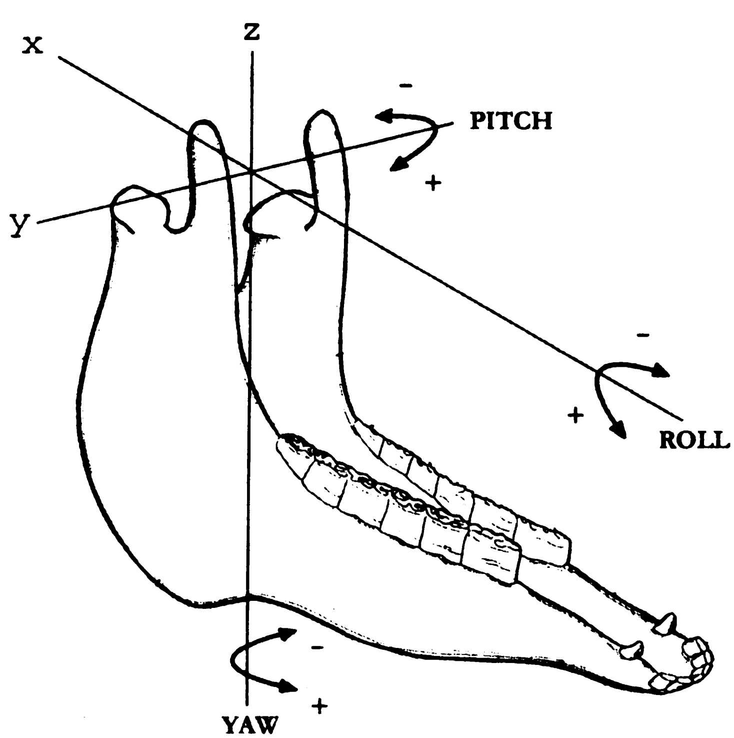

Figure 15: Description of mandibular rotations

Utilizing the convention of right-handed coordinate systems, a positive pitch (rotation α about the y-axis) is defined as opening the jaw and negative pitch is closing the jaw. This is contrary to Ostry's definition, where negative pitch is opening. A positive roll is a counter-clockwise rotation β about the x-axis when viewed from the front of the horse and a negative roll is a clockwise rotation. A positive yaw occurs when the jaw rotates (γ) clockwise about the z-axis when viewed from above the horse and negative yaw is counter-clockwise.

The rotation matrix, R, is established through the following equation:

$$R = Z(\gamma)X(\beta)Y(\alpha) \qquad \textbf{(24)}$$

Setting Eqn. (12) = Eqn.(24), the rotational angles can be calculated:

$$\text{Roll} = \beta = \arcsin(\text{-K mandible} \bullet \text{J skull}) \qquad \textbf{(25)}$$

$$\text{Pitch} = \alpha = \arcsin(\text{K mandible} \bullet \text{I skull}/\cos(\beta)) \qquad \textbf{(26)}$$

$$\text{Yaw} = \gamma = \arcsin(\text{I mandible} \bullet \text{J skull}/\cos(\beta) \qquad \textbf{(27)}$$

2.5.4 Midline-Mandibular Marker Development:

In order to measure the displacement of the mandible, a tracking marker placed on the midline of the mandible would have been ideal. The only bony structure on the midline is at the mandibular symphysis, just caudal to the lower lip. This location, which is in close proximity to the lips, is not suitable for a marker due to the high amount of skin displacement occurs at that location while chewing. Therefore, a virtual marker was created along the midline of the mandible utilizing the average x-coordinates of the rostral facial crest markers (marker #7 in **Figure 16**) and the z-coordinates of the markers placed on the notch (marker #5 in **Figure 16**) on the mandible from the standing file. The y-coordinate was set equal to zero to place this virtual marker on the midline of the mandible.

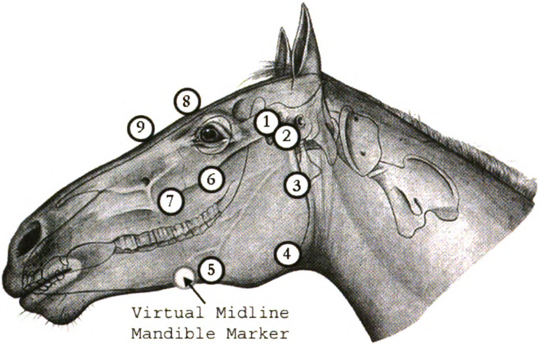

Figure 16: Location of Midline Mandibular Marker

This mandibular marker, originally a static marker represented in mandible coordinates, was first converted into a tracked marker in global coordinates. This was accomplished by multiplying the markers location by the **i-j-k** unit vectors of the tracked mandible coordinate system for each frame of data. The mandible origin was then added to this product in order to represent the midline marker in global coordinates. The marker, now expressed in global coordinates, was represented in the skull's coordinate system in order to observe how the marker moved relative to the skull. This was achieved by creating a vector from the skull origin (located half way between the tubercle markers) to the midline-mandible marker. This vector was then multiplied by the **i-j-k** unit vectors of the skull coordinate system to express the midline marker in terms of the skull coordinate system.

2.6 Data Post-Processing

2.6.1 Cycle Definition

Data were processed for three trials per feed type for each horse. Each trail was defined by three consecutive chewing cycles. The cycles with the least amount of overall head movement were manually selected for each trial as rapid head movement may cause undesirable marker movement. A cycle was defined from one minimum pitch angle to the next. The minimum pitch angle coincides with the mouth being fully closed. As the mouth opens, the pitch angle increases to a maximum value when the mouth is fully opened. The mouth closes again and the pitch angle decreases to a minimum when the mouth is fully closed. Each cycle had several local minimum and maximum pitch angles, therefore, the minimum pitch angle with the largest magnitude was manually selected to define the starting and ending frames of each cycle.

2.6.2 Data Normalization

All tracked and standing files were processed with customized software. The output included the x, y, and z location of the midline-mandibular marker relative to the skull's coordinate system and the three Euler angles and translations that describe the orientation of the mandible, relative to the skull, for each frame of data. In order to normalize the data, the output from the standing files was subtracted from the tracking file output for all trials. The x, y, and z locations of the midline-mandibular marker and the mandible relative to the skull were averaged over the 60 frames of standing file data and subtracted from the x, y, and z values from the tracked files. Likewise, the average of each Euler angle was determined in the standing position and subtracted from the tracked files. This referenced the midline-mandibular marker location, mandible coordinate translation, and Euler angles to their standing positions. The data are referred to as "normalized" to distinguish them from the raw date in the following sections.

2.6.3 Processing Midline-Mandibular Marker Data

A virtual midline-mandibular marker was created to aid in visualizing mandibular motion. From the normalized data, the minimum and maximum x, y, and z values of the midline-mandibular marker data were found for every cycle. The total displacement in the x, y, and z directions was calculated by subtracting the minimum from the maximum values in each direction. The displacements were calculated for every cycle, averaged for each trial, and the three trials were averaged for each horse, as stated in section 2.6.1. The area contained within the path that the midline-mandibular marker described was calculated in the z-y plane for each cycle and averaged in the same manner as the displacements. The absolute velocity of the midline-mandibular marker was calculated and averaged.

2.6.4 Processing Mandibular Coordinate System Data

From the normalized data, the minimum and maximum x, y, and z values of mandible coordinate system data were found for every cycle. The total displacement in the x, y, and z directions was calculated by subtracting the minimum from the maximum values in each direction. The displacements were calculated for every cycle, averaged for each trial, and the three trials were averaged for each horse.

2.6.5 Processing Euler Angle Data

The minimum and maximum values were found for each angle and trial from the normalized data. The total angular displacement for pitch, roll, and yaw were calculated by subtracting the minimum values from the maximum for each cycle and averaged for each horse.

2.6.6 Statistical Analysis:

Three cycles of data were evaluated for each trial and three trials were evaluated for each feed type. The variables investigated were averaged over the three cycles for each trial and the three trials were averaged and standard deviations (SD) determined for each horse (sample size, n, is three). The mean values of the variables of interest while chewing hay and pellets were compared for all horses using a two-tailed paired samples t-test (SPSS, Inc., Chicago, IL). The necessary assumption for applying the paired t-test is that the data have a normal distribution (Triola, 1998). In this study, the sample size for the paired t-test computation, N, is 7, for the number of horses, the standard deviation for the entire population is not known, and the data were plotted and subjectively appeared to have a normal distribution, therefore the normal distribution assumption is not unreasonable. In this test, the t statistic is calculated by:

$$t = \frac{d_{ave}}{SD_d / \sqrt{N}} \qquad (28)$$

where d_{ave} is the mean difference between the average values, for each horse, while chewing hay versus pellets, SD_d is the standard deviation of the differences and N is the number of pairs (7 in this study). The corresponding significance value associated with "t" can be looked up in a t-distribution table or calculated with software. In this study, 7 horses were examined and therefore there were 6 degrees of freedom (N-1). A 95% confidence interval, which is a measure of how certain we are that the interval contains the population parameter, (Triola, 1998) was chosen. The choice of 95% is most common because it provides a good balance between precision and reliability (Triola, 1998). Values were considered significantly different when the confidence parameter, p, was less than 0.05. This significance level indicates that less than 5% of all the tests for significant differences between hay and pellets will be false positive. This level of significance is standard in most studies evaluating biological data. A significant difference in values will reject the null hypothesis, that there is not a significant difference between the mean values of the variables that measure mandibular motion in horses chewing hay versus pellets.

3. Results:

In this chapter, results for the midline mandibular marker, including its motion in all three planes for a horse chewing on the right and left and the differences between chewing hay versus pellets are displayed first. The mean area the marker encompasses, and the mean velocity and cycle duration will follow. Finally, the mean x, y, z and angular displacements for the mandibular coordinate system are provided. The figures illustrating these results are at the end of the chapter.

3.1 General Midline-Mandibular Marker Motion:.

When a horse chews, occlusal contact only occurs between the cheek teeth of the side being chewed on. Therefore, in a chewing cycle, the horse chews on either the left or the right side. During this study, four horses were chewing on the right and three on the left.

The data were plotted in the z-y plane (observing the motion from the front of the horse), the z-x plane (observing from the right of the horse), and the x-y plane (observing from above the horse). These orientations are depicted in **Figure 16**. The z-y plane is the transverse plane, the z-x plane is the sagittal plane, and the x-y plane is the dorsal plane.

The location of the midline-mandibular marker relative to the skull's coordinate system was plotted in all three planes. When the movements of the midline-mandibular marker in the z-y plane are viewed from the front in a horse chewing on the right side (**Figure 17**), the lower jaw starts in the upper-most, closed position (1), then moves clockwise and slightly to the horse's left (i.e. to the right of the graph) to its maximum pitch angle (2).

As the jaw starts to close, it swings to the horse's right (moving to the left of the figure) to the position of maximum lateral excursion for the cycle (3). At this point, the cheek teeth establish contact to grind the food as the jaw slides to the left and upward to return to the starting position (1). Chewing in this direction is considered chewing on the right side because the cheek teeth on the right side of the jaws are utilized for grinding.

A horse chewing on the left starts with the lower jaw in the closed position (1), followed by the jaw moving counter-clockwise, when viewing from the front of the horse, as it opens and moves slightly right to its most open position (2). The jaw then swings to its left-most position as it closes (3) and the left cheek teeth establish contact to grind **(Figure 18)**.

The path that the midline-mandibular marker follows has the same basic geometry while chewing hay and pellets. There is a difference, however, in the mandibular excursion of the cycles for the two feed types. Comparison of the mandibular movements in the z-y plane when chewing hay versus pellets shows that the mandible undergoes more lateral excursion while chewing hay compared to pellets **(Figure 19)**.

When observing the z-x plane of a horse chewing on the left **(Figure 20)**, the midline-mandible marker moves in the negative x and z-directions while the lower jaw opens and positive x and z-directions as the jaw closes. In the x-y plane of a horse chewing on the left **(Figure 21)** this marker moves in the negative x and y-direction during the opening phase. During the closing phase, the maker initially moves in the positive y-direction, then moves in the negative y-direction. The marker moves in the positive x-direction for the duration of the closing phase.

In general, the midline-mandibular marker moved in the negative x- and z-directions (caudoventrally) during the opening phase of the cycle, and in the positive x- and z-directions (rostrodorsally) during closing. The motion in the y-direction depended on if the horse was chewing on the left or right.

Graphs of the location of the midline-mandibular marker for all three planes for all chewing cycles for each horse and feed-type can be found in Appendix A.

Chewing cycles are complicated with many detailed features. To quantify the cycles, mean and standard deviations for x, y, and z displacements, velocities, and areas encompasses by the path of the midline-mandibular markers were calculated and tabulated for all horses while chewing both hay and pellets. The mean values for each variable were compared while chewing hay versus pellets with a paired t-test as described in section 2.6.6. For example, in comparing the statistical difference between the mandibular marker x-displacement while chewing hay versus pellets **(Table 3)**, the difference d between the mean x-displacement value for hay and pellets was determined for each horse. The mean value and the standard deviation (SD_d) of the difference d across the seven horses were used to compute the variable t for the paired t-test **(eqn. 28)**. The bottom row in the tables represents the means across the values entered in the table for the seven horses, and the standard deviations of those numbers. These numbers do not account for the standard deviations in each line of the table and are not used to verify the hypothesis through the paired t-test.

The displacements of the midline-mandibular marker in the x, y, and z-directions were determined for each cycle and averaged (**Table 3**). Based on the paired t-test, the displacements in the x, y, and z directions for the entire group were significantly larger for hay than for pellets, under the assumption that the data have a normal distribution. Consequently, the null hypothesis will be rejected and the experimental hypothesis accepted. Horse #4 varied from the group, however, this did not effect the statistical result.

Table 3: Mean (SD) x, y, and z displacement of the midline-mandibular marker for each horse while chewing hay and pellets

Horse	Mean X-Disp. (SD) (mm)		Mean Y-Disp. (SD) (mm)		Mean Z-Disp. (SD) (mm)	
	HAY	PELLETS	HAY	PELLETS	HAY	PELLETS
1	5.86 (0.56)	3.47 (0.12)	18.83 (1.89)	11.03 (0.22)	13.38 (1.84)	12.05 (0.14)
2	6.76 (2.64)	5.02 (0.60)	23.51 (0.79)	17.91 (0.74)	19.25 (1.24)	17.97 (0.75)
3	7.14 (1.27)	4.71 (0.10)	17.35 (0.73)	12.16 (0.36)	16.44 (0.80)	11.88 (0.23)
4	4.40 (1.06)	4.97 (0.57)	21.74 (0.75)	15.90 (1.96)	11.63 (0.86)	11.88 (1.30)
5	5.34 (1.14)	4.02 (0.54)	16.95 (0.67)	13.58 (0.67)	21.00 (0.26)	18.19 (0.62)
6	7.20 (3.16)	5.58 (0.79)	19.01 (1.37)	17.31 (1.69)	13.67 (0.83)	12.29 (0.72)
7	5.87 (0.41)	4.30 (0.39)	21.73 (2.61)	19.75 (1.72)	15.03 (0.29)	13.23 (0.28)
Total Mean	**6.08 (1.02)**	**4.58 (0.71)**	**19.87 (2.48)**	**15.38 (3.22)**	**15.77 (3.36)**	**13.93 (2.87)**

The area encompassed by the midline-mandibular marker in each cycle, was calculated for the z-y plane and averaged in a similar manner (**Table 4**). The area encompassed when chewing hay was significantly larger than when chewing pellets, rejecting the null hypothesis.

Table 4: Mean area encompassed by each cycle in the z-y plane for hay and pellets

Horse	Mean Area (SD) (mm^2)	
	HAY	PELLETS
1	146.27 (6.95)	94.43 (3.49)
2	306.95 (29.52)	240.75 (5.31)
3	190.77 (3.81)	93.72 (5.58)
4	168.82 (17.29)	119.03 (24.51)
5	237.56 (20.68)	147.60 (14.90)
6	137.29 (10.26)	112.18 (9.24)
7	154.28 (6.26)	100.53 (2.31)
Total Mean	**191.71 (61.71)**	**129.75 (52.38)**

The absolute velocity of the midline-mandibular marker was determined for each cycle and averaged for each horse (**Table 5**). The mean velocities for the hay and pellets were very similar, failing to reject the null hypothesis for this variable only.

Table 5: Mean absolute velocity for all horses for each feed sample.

Horse	Mean Velocity (SD) (mm/s)	
	HAY	PELLETS
1	67.10 (0.80)	56.50 (10.63)
2	87.15 (7.76)	115.79 (11.12)
3	75.07 (3.61)	65.81 (4.12)
4	81.03 (5.19)	77.85 (6.95)
5	77.44 (3.28)	71.87 (0.93)
6	70.56 (9.82)	72.89 (4.06)
7	85.05 (3.88)	92.51 (2.87)
Total Mean	**77.63 (7.35)**	**79.03 (19.60)**

The cycle duration was determined for each cycle and averaged for each horse and the mean frequency was calculated for hay and pellets (**Table 6**). The mean duration for hay was significantly longer than for pellets, rejecting the null hypothesis.

Table 6: Mean cycle duration for all horses for each feed sample

Horse	Mean Cycle Duration (SD) (msec)	
	HAY	PELLETS
1	837.04 (26.25)	675.93 (80.95)
2	1007.41 (209.80)	601.85 (27.82)
3	906.48 (91.89)	698.15 (30.47)
4	722.22 (25.46)	681.48 (27.40)
5	847.22 (12.11)	744.44 (16.90)
6	883.33 (37.37)	717.59 (22.45)
7	725.00 (65.68)	624.07 (11.23)
Total Mean	**846.96 (100.95)**	**677.65 (31.03)**
Mean Frequency (Hz)	**1.18**	**1.48**

3.2 Mandible Coordinate System Displacement:

The location of the origin of the mandible coordinate system was plotted relative to the origin of the skull coordinate system in all three planes. In general, during the opening phase, the mandible tended to move in the positive x- and negative z-directions (rostroventrally) and in the negative x and positive z- directions (caudoventrally) during the closing phase. The motion in the y-direction was highly variable throughout the chewing cycle (**Figures 22-24**).

The three planes for additional sample chewing cycles for each feed-type can be found in Appendix B.

The displacements of the mandible coordinate relative to the skull coordinate system in the x, y, and z-directions were determined for each cycle (**Table 7**). The mean displacements in the x, y, and z directions were significantly larger for hay than for pellets, rejecting the null hypothesis.

Table 7: Mean (SD) x, y, and z displacement of the mandible coordinate system relative to the skull coordinate system for each horse while chewing hay and pellets

Horse	X-Displacement (SD) (mm)		Y-Displacement (SD) (mm)		Z-Displacement (SD) (mm)	
	HAY	PELLETS	HAY	PELLETS	HAY	PELLETS
1	11.01 (1.02)	7.78 (0.63)	3.89 (1.12)	2.82 (0.74)	2.70 (0.17)	2.91 (0.75)
2	19.45 (2.97)	13.03 (3.50)	17.09 (2.06)	10.74 (2.48)	4.43 (0.98)	4.05 (0.61)
3	18.24 (1.79)	12.42 (0.45)	6.59 (1.09)	4.79 (0.64)	5.64 (0.78)	4.00 (0.51)
4	6.99 (1.01)	6.85 (0.96)	9.04 (0.67)	7.69 (1.39)	3.12 (0.51)	2.83 (0.11)
5	23.24 (1.40)	18.84 (2.07)	12.09 (0.86)	8.69 (0.51)	4.87 (0.46)	2.74 (0.97)
6	12.36 (1.87)	13.72 (0.99)	8.86 (2.04)	9.44 (1.02)	4.64 (1.69)	4.04 (0.40)
7	12.90 (1.94)	9.58 (1.26)	15.47 (3.80)	13.56 (1.32)	5.19 (2.23)	3.64 (0.46)
Total Mean	**14.88 (5.62)**	**11.75 (4.10)**	**10.43 (4.73)**	**8.25 (3.60)**	**4.37 (1.08)**	**3.46 (0.61)**

3.3 Euler Angles:

The three Euler angles were plotted for all trials. The beginning and end of each cycle were defined from the pitch angles. The beginning of the first cycle was defined by the first minimum value in the trial, which corresponds with the jaw in its fully closed position. The lower jaw opens (positive pitch) until a maximum is reached, which corresponds with the fully open position. The jaw then begins to close (negative slope) until the next minimum value is reached where the mouth is closed again and the first cycle is complete. The pattern was repeated twice to define cycles 2 and 3. The cycles were defined for each trial and all angles were plotted within the defined ranges (**Figure 25**).

Euler angles for all horses can be found in Appendix C.

The maximum and minimum angles were averaged for each trial and the angular displacements were determined for each horse (**Table 8**). The mean range of motion for pitch, roll, and yaw were significantly larger for hay than for pellets, rejecting the null hypothesis.

Table 8: Mean range of Euler angles for all horses chewing hay and pellets

Horse	Pitch Range (SD) (Degrees)		Roll Range (SD) (Degrees)		Yaw Range (SD) (Degrees)	
	HAY	PELLETS	HAY	PELLETS	HAY	PELLETS
1	2.94 (0.47)	2.61 (0.02)	0.81 (0.09)	0.68 (0.14)	3.81 (0.47)	2.27 (0.89)
2	5.47 (0.25)	4.80 (0.87)	2.37 (0.41)	1.20 (0.31)	3.70 (0.46)	3.44 (0.31)
3	4.94 (0.42)	3.54 (0.10)	1.81 (0.13)	1.35 (0.08)	4.44 (0.17)	2.89 (0.07)
4	2.51 (0.04)	2.64 (0.29)	1.16 (0.13)	0.69 (0.19)	4.35 (0.55)	3.45 (0.12)
5	7.17 (0.06)	5.87 (0.54)	1.81 (0.15)	1.26 (0.11)	4.47 (0.18)	2.86 (0.17)
6	4.42 (0.13)	4.32 (0.15)	1.54 (0.20)	1.09 (0.10)	3.67 (0.12)	2.81 (0.28)
7	4.07 (0.27)	3.09 (0.15)	1.44 (0.05)	1.03 (0.08)	2.94 (0.20)	2.53 (0.22)
Total Mean	**4.50 (1.57)**	**3.84 (1.22)**	**1.56 (0.50)**	**1.04 (0.27)**	**3.91 (0.55)**	**2.89 (0.44)**

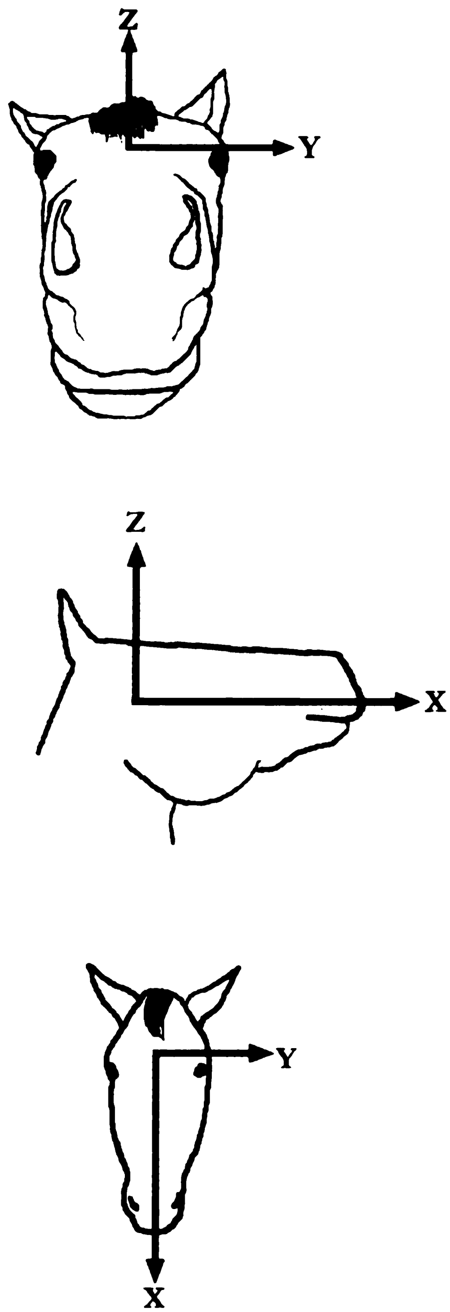

Figure 17: The three planes the data are described in

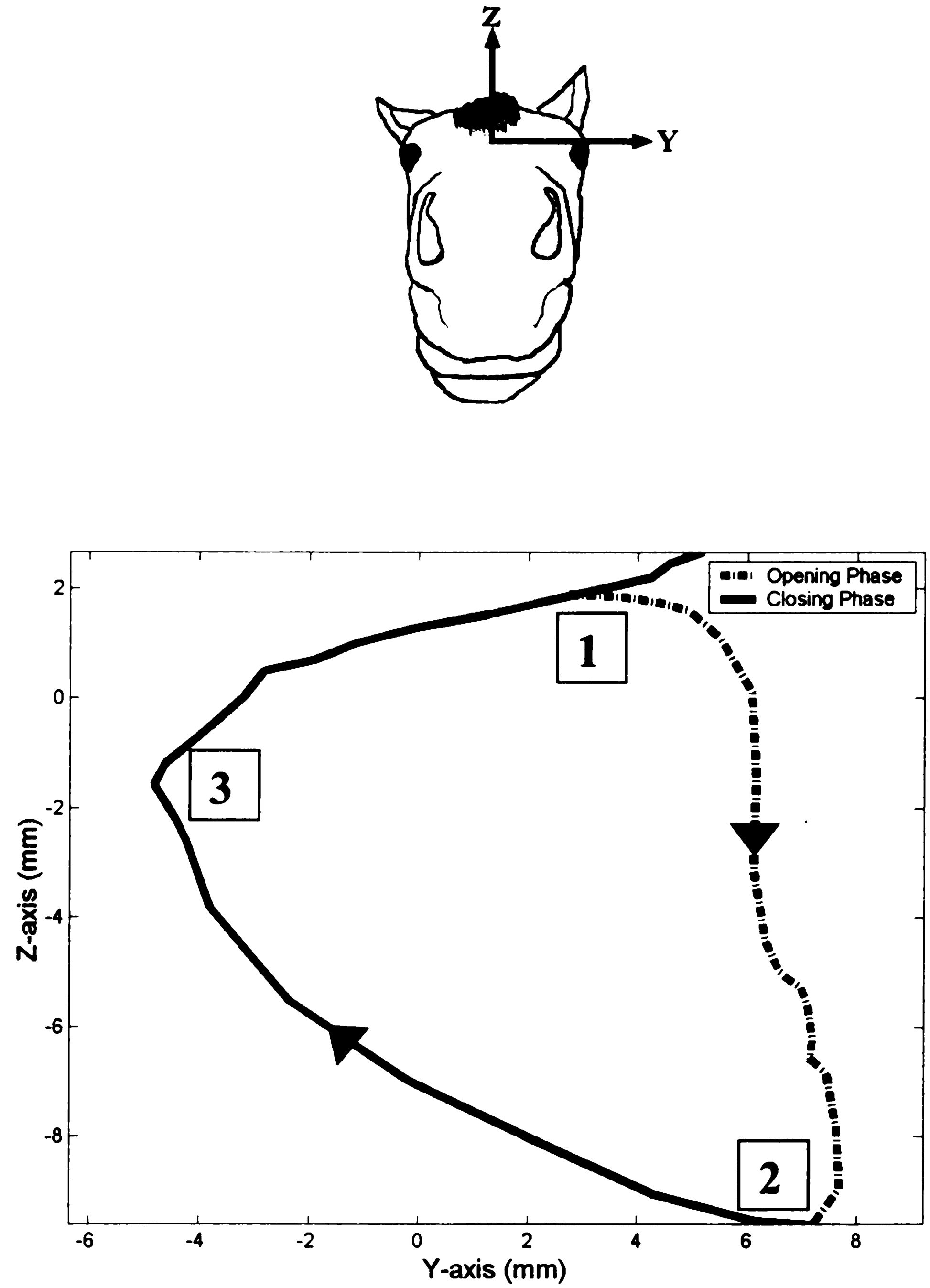

Figure 18: Normalized midline-mandibular marker location in the z-y plane from one chewing cycle viewed from the front of a horse #1 chewing hay on the right. Number 1 = lower jaw in closed position, number 2 = maximum pitch angle, number 3 = maximum lateral excursion. Arrows indicate the direction the mandible moves.

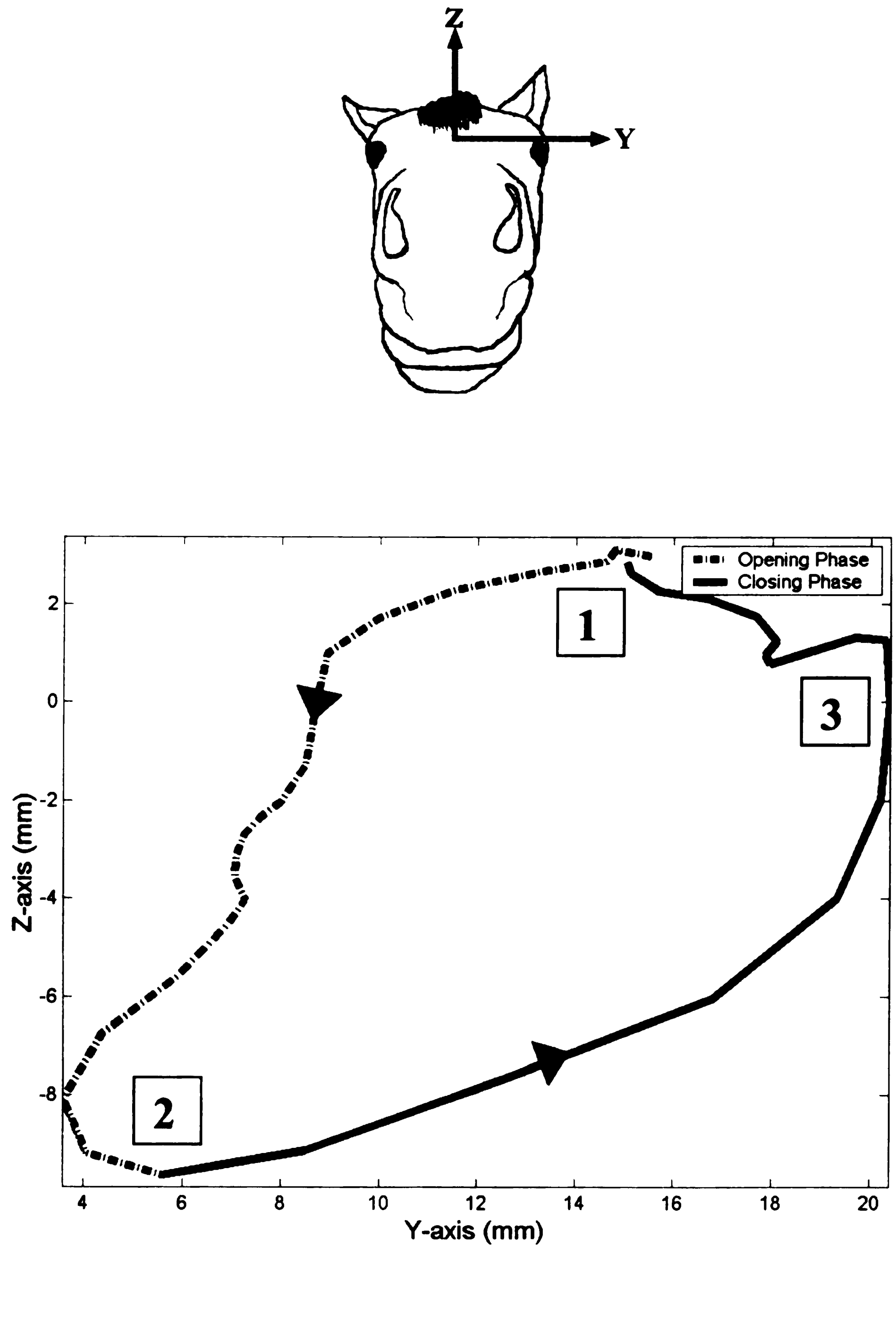

Figure 19: Normalized midline-mandibular marker location from one chewing cycle viewed in the z-y plane of a horse #4 chewing hay on the left
Number 1 = lower jaw in closed position, number 2 = maximum pitch angle, number 3 = maximum lateral excursion. Arrows indicate the direction the mandible moves.

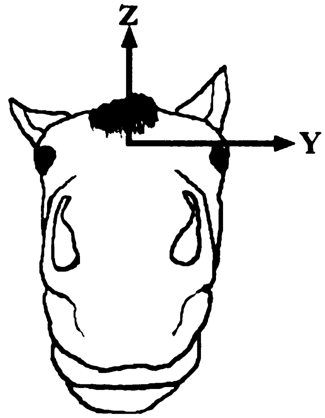

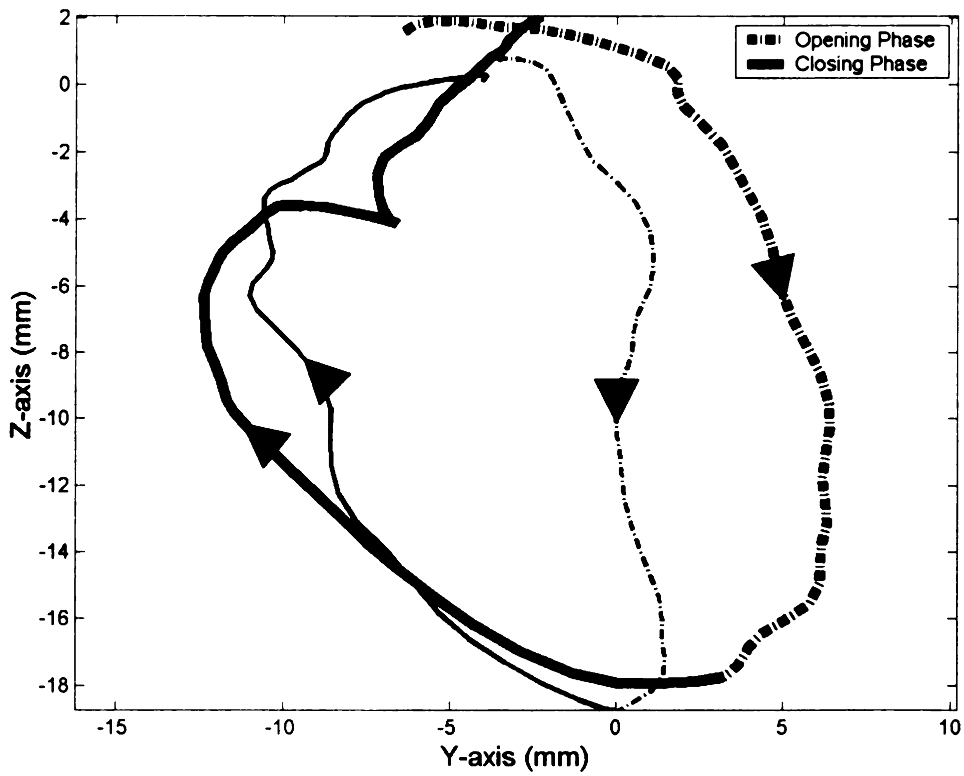

Figure 20: Normalized midline-mandibular marker viewed in the z-y plane from one chewing cycle of hay (thicker line) and pellets (thinner line) from horse #5 chewing on the right. Arrows indicate the direction the mandible moves.

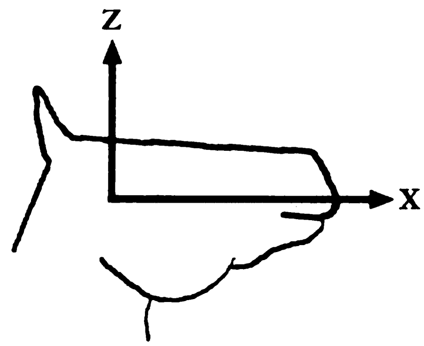

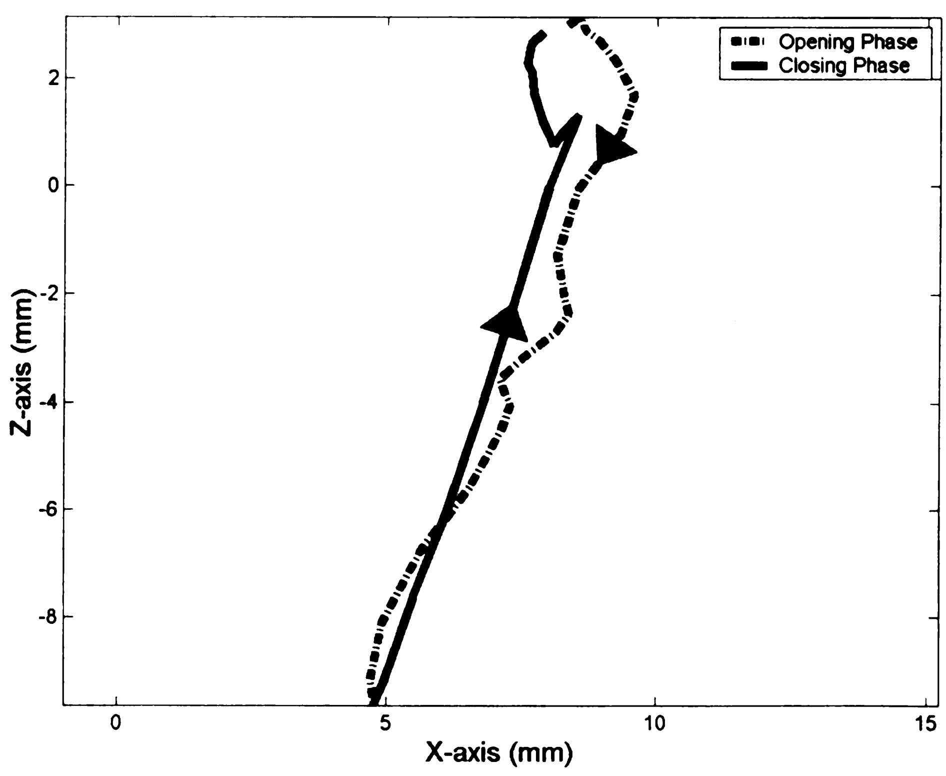

Figure 21: Characteristic chewing patters of the normalized midline-mandibular marker location from one chewing cycle of horse #4 chewing hay on the left, viewed in the z-x plane. Arrows indicate the direction the mandible moves.

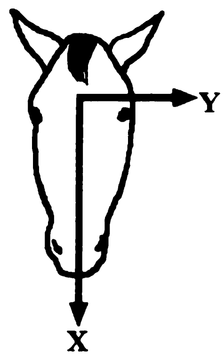

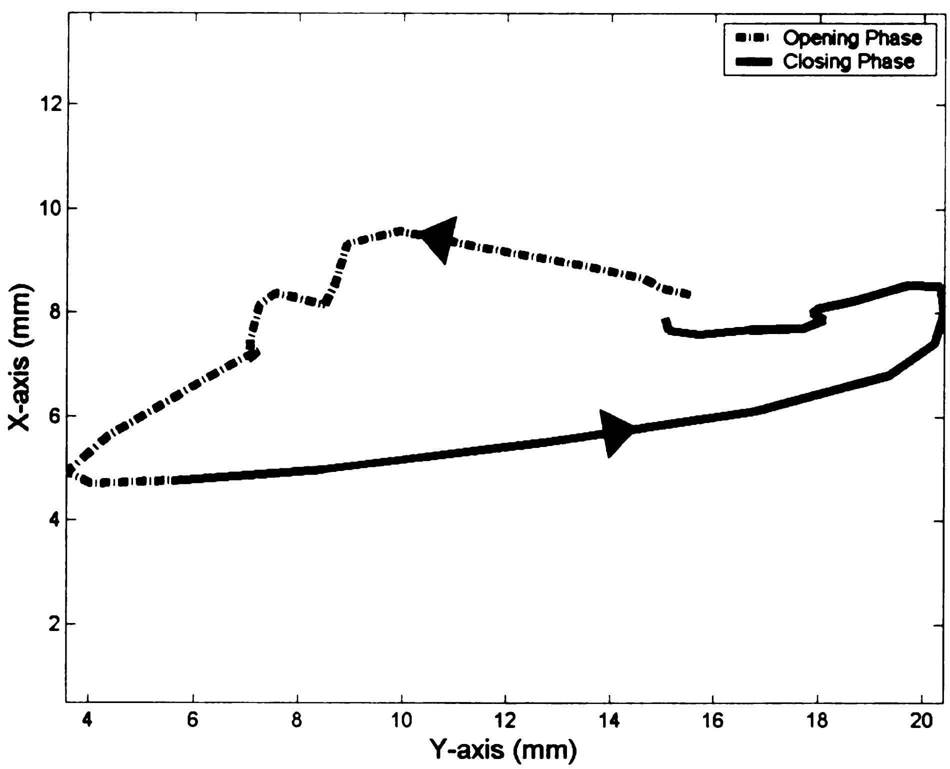

Figure 22: Characteristic chewing patters of the normalized midline-mandibular marker location from one chewing cycle of horse #4 chewing hay on the left, viewed in the x-y plane. Arrows indicate the direction the mandible moves.

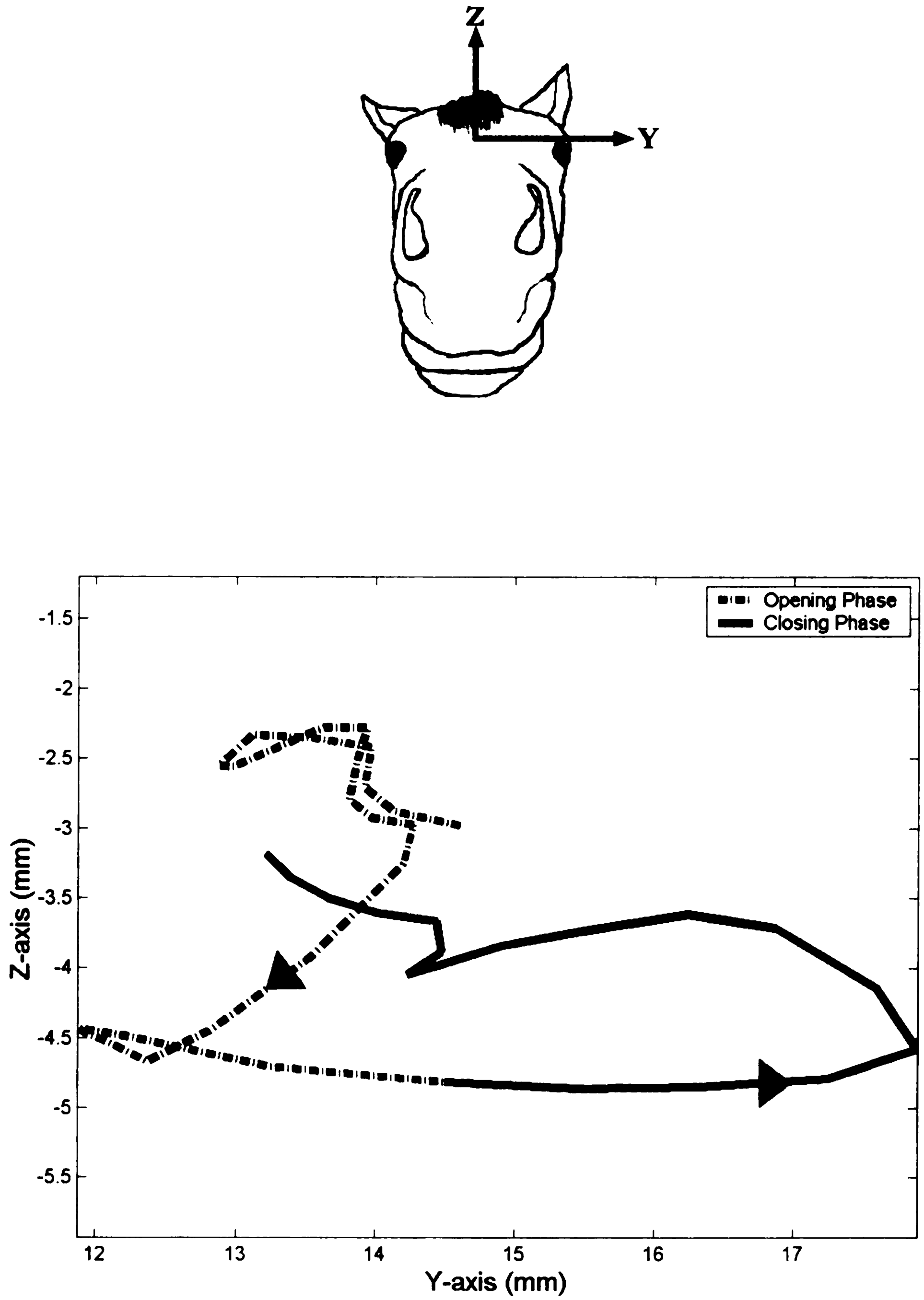

Figure 23: Location of mandible coordinate system during one sample chewing cycle from horse #4 chewing hay on the left viewed in the z-y plane. Arrows indicate the direction the mandible moves.

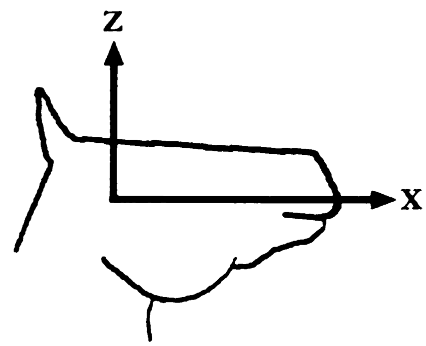

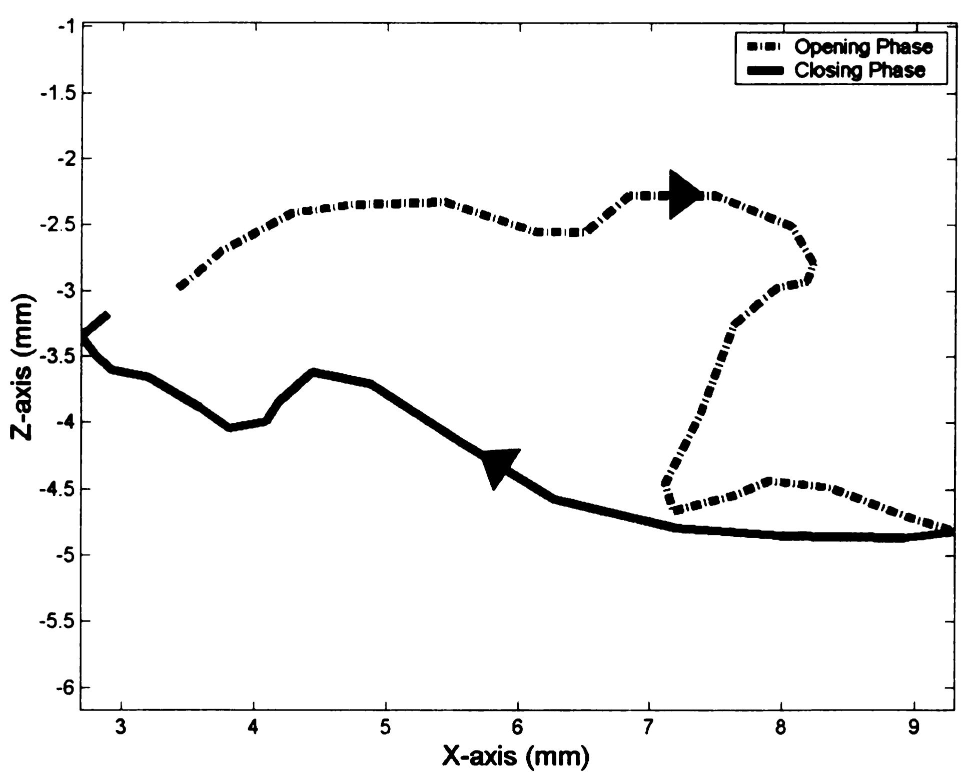

Figure 24: Location of mandible coordinate system during one sample chewing cycle from horse #4 chewing hay on the left viewed in the z-x plane. Arrows indicate the direction the mandible moves.

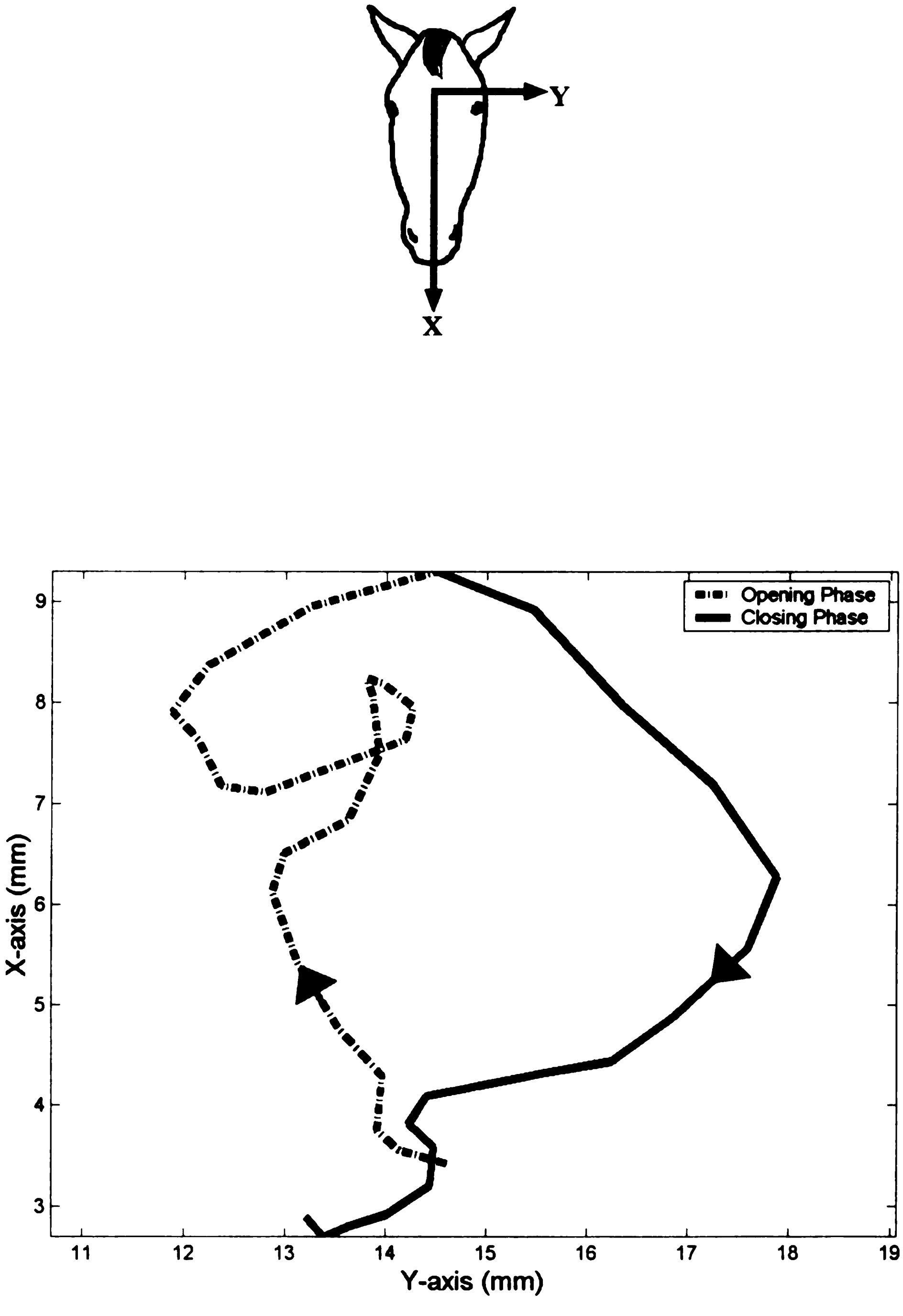

Figure 25: Location of mandible coordinate system during one sample chewing cycle from horse #4 chewing hay on the left viewed in the x-y plane. Arrows indicate the direction the mandible moves.

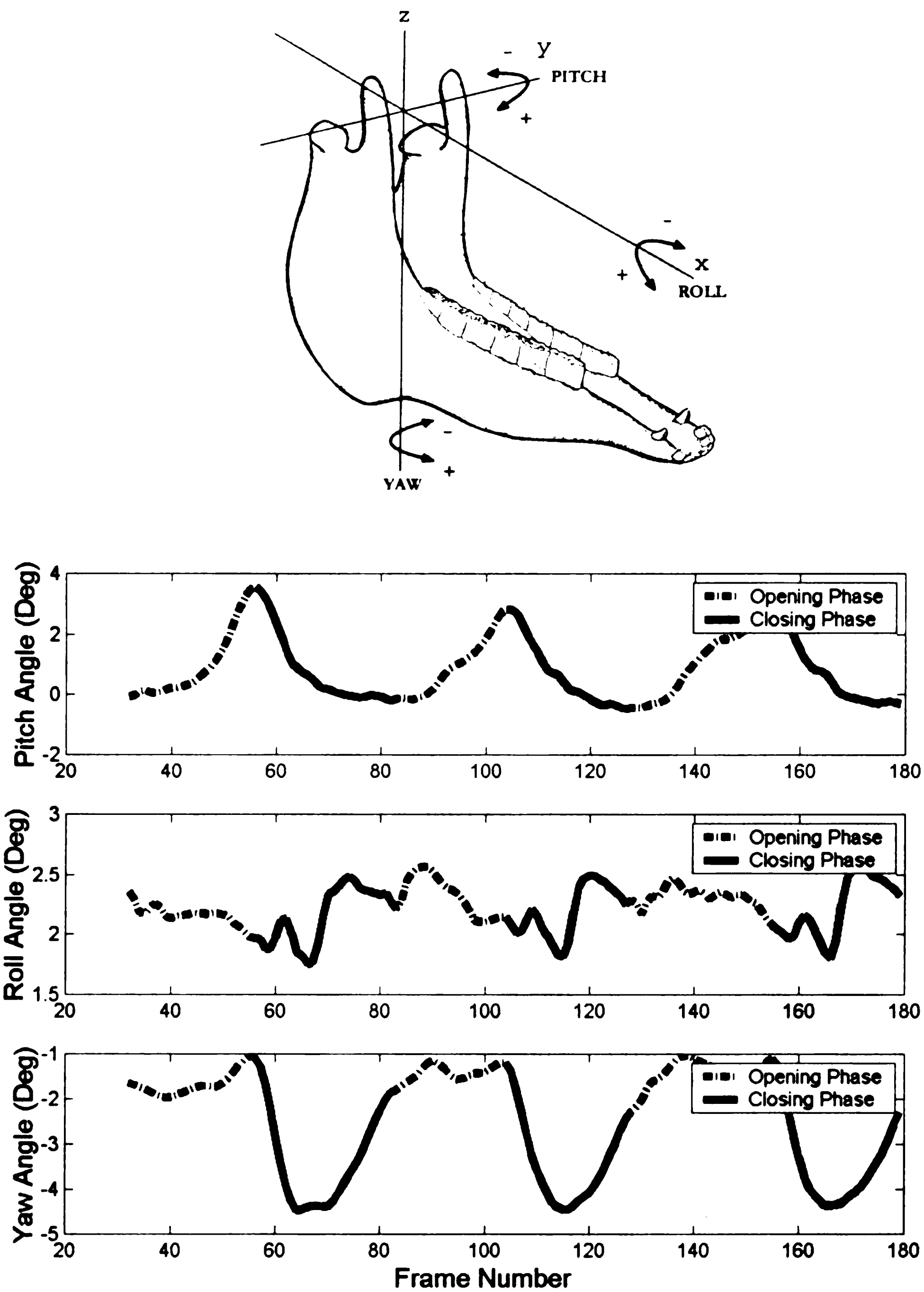

Figure 26: Euler angles for one trial from horse #1 chewing hay on the right: pitch (top), roll (middle), and yaw (below)

4. Discussion:

In the realm of equine medicine, dentistry has received relatively little attention compared with other areas, such as infectious diseases. This is at least partly due to the lack of an accurate method for studying chewing movements and the development of dental wear patterns. This study described a method of measuring the kinematics of chewing and has demonstrated the value of the technique in characterizing the kinematic differences between chewing two types of food.

4.1 Significance of Marker Placement:

The principle of virtually all modern kinematic analysis techniques is the marking of the skin overlying certain anatomically defined landmarks, with subsequent recording of the trajectories of these markers (van Weeren, 1989). This was the technique applied in evaluating the kinematics of the mandible during chewing. The use of skin markers in kinematic analysis introduces an uncontrollable source of biological error since movements of the skin are recorded and not those of the underlying skeletal structures, which are the real subjects of study. There always exists a certain degree of sliding of the skin over the underlying bone, the amplitude and direction of which can be expected to vary per site. As the skin displacement is cyclic with the same frequency as the skeletal cycle, it cannot be detected in the raw data (Capozzo et. al, 1988).

Because skin displacement is a systematic error, it is important to either adhere skin markers to regions with minimal soft tissue motion or correct for skin displacement. Often, in studies that have received a lot of attention, such as human knee and ankle kinematics, algorithms have been developed to account for skin displacement. Algorithms can be generated by inserting a pin into the bone under the skin being evaluated and comparing the relative displacement of a skin marker with the bone pin on the segment while the motion being evaluated is taking place. Reinschmidt et al. (1997) for example, examined human knee kinematics and quantified the difference between skin and bone marker kinematics using the average root mean square difference and the maximal difference between the knee rotations.

There have not been any bone pin studies to analyze the skin displacement relative to the equine skull and mandible during chewing. The actual skin displacement can be determined by inserting a bone pin into the mandible with the marker set in place. Since the pin is a rigid structure fixed rigidly to the bone, it provides an accurate representation of the movement of the bone. Comparisons between the movement of the bone with the movement of the skin marker allow the amount of skin displacement relative to the bone to be quantified and correction algorithms to be developed. Other, less invasive, techniques such as attaching magnets to the incisors and tracking their motion with a magnetometer mounted on the skull would also provide pure mandibular kinematics that can be compared to the motion of the markers (Plesh *et al.*, 1993). This technique would be suitable as long as the horse's natural chewing pattern is not influenced by a magnet adhered to the incisors. Salomen and Waysenson (1979) tracked the three-dimensional motion of a small radioactive source, cemented into the position of interest. The radiation emitted by the source is detected by a scintillation detector, which counts the amount of radiation falling on its surface by transforming the radiation into a proportional electric current. This technique would provide the pure mandibular motion, however, the scintillation detector would need to be mounted on the skull in order to determine the mandibular motion relative to the skull, which may not be feasible.

In the absence of correction algorithms for the equine mandible, the skin markers were placed in sites where skin displacement was expected to be small based on the fact that skin was tightly adhered to the underlying bone without the intervention of copious loose soft tissue. Pilot studies helped determine these locations. Markers were placed on the rigid portion of the mandible and a software package, provided by Motion Analysis, was employed to evaluate the relative displacement between the markers. The locations with the least amount of displacement were chosen in the study.

Previous studies (Baker and Easley, 1999; Collinson, 1994) have attempted to measure the displacement of the mandible by observing how a point on the midline of the mandible moved relative to a point on the midline of the skull. Problems with this technique will be discussed later. In the present study, in order to track the mandibular motion in a similar manner and make comparisons to Baker and Easley's and Collinson's results, a marker needed to be placed along the midline of the mandible. However, the only bony structure on the midline of the mandible is at the mandibular symphysis, just caudal to the lower lip. Unfortunately, this location is not suitable for marker placement due to the high amount of skin displacement that occurs at that location while chewing. The motion of the lips displaces the skin in that region due to their close proximity. Therefore, a virtual marker was created along the midline of the mandible using the average x-coordinates of the rostral facial crest markers and the z-coordinates of the markers placed on the notch on the mandible from the standing file. The y-coordinate was set equal to zero to place this virtual marker on the midline of the mandible. This virtual marker was then tracked relative to the skull's coordinate system and the mandibular motion measured in this manner can be compared to previous studies, such as Leue's (1941) and Collinson's (1994).

The transformation matrix obtained through the algorithm by Soderkvist and Wedin (1993) more accurately represents the motion of the segment if the marker set is well configured. Well-configured marker placement requires that the markers have a broad distribution, that they are not placed colinearly. If a segment's markers are placed in a straight line and the segment rotates about that line, the motion cannot be detected because the linear arrangement of markers does not appear to move to the detection system. Therefore, the more distributed the marker placement, the more accurately the transformation matrix will represent the actual motion.

The coordinate systems for both the skull and mandible were created from markers placed on the skin overlying bony, anatomical landmarks. The coordinate systems' locations are highly sensitive to marker placement, especially those on the articular tubercles and condyles, which define the y-axis of the skull and mandibular coordinate systems, respectively. The y-axis was also utilized to define the z-axis through principles of cross products. Consequently, the correct marker placement was critical to produce results that adequately represented the chewing motion.

The relatively small bony prominence at the tubercles and condyles required the use of markers with a base that had a slightly smaller surface area compared to the markers at all other locations. A disadvantage to using markers with a small base is that it allowed the markers to sag away from the landmarks they were placed on under the influence of gravity, which shifted the y-axis ventrally by as much as 1 cm. This issue did not affect the data trends, but it is possible that the origins of the skull and mandibular coordinate system could have been shifted slightly below the anatomical axes.

In addition, if the glue holding the markers in place was not completely set at the start of data acquisition, or if the underlying skin was dirty, the markers occasionally fell off and had to be re-glued in place. Typically, the markers were glued precisely at the location they fell from because the glue remaining on the skin indicated the location, but it is possible that minor deviations did occur. The consequence of this shift did not influence a given trial, but may have introduced small variations in the results between trials recorded before and after the marker relocation.

The author has not discovered any human TMJ kinematic investigations that used surface skin markers, however, magnetic resonance imaging, optoelectronic systems, and magnetometers have been used. MRI units are not designed to be functional for horses and a magnetometer system requires placing magnets on the incisors, which would likely disrupt a horse's natural chewing pattern. Neither system is as accurate as the Motion Analysis System. Optoelectronic systems function by tracking light-emitting diodes, which is similar to the Motion Analysis tracking system.

4.2 Diet Effects on Dentition

As horses were domesticated, their natural, grazing diet was modified by feeding more concentrated feeds to supplement the reduced roughage intake and provide adequate nutrition. Not only does this diet change effect the chewing patterns of horses, but it also requires the gastrointestinal system to process large quantities of concentrate (such as grain and pellets) rather than roughage consumed continuously throughout the entire day, as it is designed to do. In addition, horses lack the ruminant's ability to regurgitate and remasticate food, and thus are more dependent on a dentition that can effectively break down forages to release cell contents for nutritional uptake. Given complete freedom on pastures, horses spend as much as sixteen hours a day nibbling, chewing, swallowing, and digesting food, little by little to prevent their small stomachs from becoming empty (Duncan, 1992).

The folded layers of dentin, cement, and enamel that construct the horse's teeth provide a self-grinding mechanism that wear-down the opposing occlusal surface. When the horse chews, the jaws separate to the maximum pitch angle followed by the lower jaw moving laterally as the pitch angle decreases until occlusal contact is again established. The teeth abrade against each other in order to grind food particles, which also wears down the occlusal surface as the lower jaw moves medially to the neutral position. A horse that chews with maximal lateral excursion will make complete occlusal contact and will wear the molar table evenly and adequately. If a horse regularly chews with inadequate lateral excursion, overgrowths will develop on the buccal side of the upper molar table and on the lingual side of the lower molar table. Initially, sharp enamel points form, which can evolve into more serious malocclusions that will further inhibit mandibular lateral excursion.

Gobel and Duffner (1954, cited by Dixon 2000) noted that overgrowths could be reduced by a high roughage diet and conversely were encouraged by feeding a high concentrate diet, such as pellets. Becker (1962, cited by Dixon 2000) also noted that such overgrowths are rarely found in species that are constantly grazing, such as zebras, Przewalski's horses, mules, or African donkeys and are very slight when they do occur. Brunner (1941, cited by Dixon 2000) found no evidence of enamel overgrowths in fossil equine skulls. Becker (1942, cited by Dixon 2000) examined 1000 domesticated horses and found sharp enamel overgrowths in 99.2% and buccal trauma in 78.8%. A later study of 32,000 cavalry horses showed enamel overgrowths in 91.7% and shear mouth in 0.3% (Becker 1945, cited by Dixon 2000). These findings indicate that the dental health of domesticated horses is much worse than that of non-domesticated equids, which insinuates that an ample, high roughage diet that a non-domesticated horse would eat is more desirable for improved dental health.

Properly maintaining a horse's overall health, especially for an active performance horse, should consider the effects of concentrate feeds. Racehorses, for example, have a considerable workload and must therefore maintain a high calorie diet. Eating concentrate feeds provides the necessary nutrient density in a smaller volume. A horse would have to consume an extremely high volume of hay to obtain the calorie requirements and maintain body weight if concentrates were not given. In addition, the bulky mass of food that would accumulate within the large intestines on a hay-only diet is not desirable for high-exertion performance horses. Consequently, the equine manager must be sure that an equine dentist maintains proper dental occlusion with routine treatments as chewing large amounts of concentrate feeds can attribute to malocclusions.

Horses chew on one side at a time. In this study, four horses chewed on the right and three on the left and they did not change chewing sides during data collection. The number of cycles a horse will chew on one side before switching to the other side has not been documented to the author's knowledge. However, horses without malocclusions have been observed to chew on both sides. If a malocclusion restricts a horse from chewing on one side, continuous chewing on the other side will cause the malocclusion to worsen. It is necessary for an equine dentist to remove these restricting malocclusions in order to allow the horse to chew with adequate lateral excursion. If problematic dentition is neglected, malocclusions can propagate into more serious problems such as buccal and lingual trauma and peridontal disease.

4.3 Mandibular Euler Angles During Chewing:

In biomechanics, movement descriptions provide a transition from mechanical terminology to anatomically meaningful terms. For example, when evaluating the motion of the tibia relative to the femur, the first joint rotation is described as flexion/extension, the second as ab/adduction, and the third as internal/external rotation. This terminology, however, is not applicable when describing the motion of the mandible relative to the skull since rigid fusion of the mandibular symphysis precludes independent motion of the left and right sides. The opening and closing of the jaw can logically be call flexion and extension, but the rami of the mandible cannot show ab/adduction, which refers to motion away from or towards the midline of the body or internal and external rotation, which refers to a rotation towards and away from the midline of the body. Pitch, roll, and yaw are commonly used in the aerospace field to describe the 3-D motion of aircrafts. In equine biomechanics, Fredrickson *et al.* (1971) used this terminology to describe the three-dimensional orientation and motion of the equine hoof during locomotion. Ostry *et al.* (1997) and used pitch, roll, and yaw to describe the rotations of the human mandible.

The masticatory cycle in herbivorous mammals is generally considered to consist of three events: the opening stroke, the closing stroke, and the power stroke. Collinson (1994) described the opening stroke as a downward hinge movement of the mandible, mediated by the gliding action of both condyles and the closing stroke as an upward movement combined with a rotation of each condyle in its glenoid cavity. This study showed that not only is there a downward hinge movement (a pitch rotation α about the transverse horizonal axis) during the opening phase, but slight rotations also occur about the other two axes.

As the horses chewed, the pitch angular velocity was positive as the jaws opened and negative as the jaws closed. The roll and yaw angles were small compared to the pitch angle during the opening phase of a horse chewing on the right. The roll rate was negative, which was a negative rotation about the longitudinal axis resulting in a clockwise roll of the mandible when viewed from the front of the horse, and the yaw rate was positive (a slight positive rotation about the vertical axis). In one horse, the yaw was negative early in the opening phase, but then became positive near the end of the opening phase. During the closing phase, the extent of roll was small compared to pitch and yaw and was generally positive for a horse chewing on the right, corresponding to a counter-clockwise rotation when observed from the front. The yaw of a horse chewing on the right was negative during the first portion of the closing phase, followed by a positive yaw during the second portion of the closing phase. The positive yaw corresponded to the grinding portion, or power stroke, of the cycle where the pitch angle was small and had little variation. The slope of molar table angle likely dictates the extent of roll angle during the power stroke: a steeper molar table angle will result in more extensive mandibular roll and a more level molar table will have less.

A horse chewing on the left (**Figure 69** in Appendix C, for example) had a positive roll rate (mandible rolled counter-clockwise when viewed from the front) and a negative yaw rate (mandible moves to the right) during the cycle's opening phase. During the closing phase, the roll rate was generally negative (mandible rolled clockwise) and its magnitude was small compared to pitch and yaw. The yaw angle increased during the first portion of the closing phase, followed by a negative yaw rate during the second portion, again corresponding to the grinding phase. The left molar table is sloped in the opposite direction to the right molar table and consequently, the mandible rolls in the opposite manner when compared to the right. Similar to chewing on the right, the negative yaw corresponded to the power stroke of the cycle.

In order to completely describe the mandibular motion, not only do the rotations of the mandibular coordinate system need to be provided, but also the displacement of the coordinate system.

4.4 Mandibular Coordinate System Displacement:

During the opening phase of a horse chewing on the left, as seen in **Figures 23-25**, the origin of the mandibular coordinate system moved in the negative z-direction (ventrally) and slightly in the positive x-direction (rostrally). In general, there was little displacement in the y-direction. During the closing phase, the mandibular coordinate system displaced in the positive z-direction (dorsally) and slightly in the negative x-direction (caudally). The coordinate system displaced in the positive y-direction early in the closing phase, followed by a displacement in the negative y-direction. The change in displacement direction likely corresponds to the power stroke of the chewing cycle.

A horse chewing on the right has the same general trends as a horse chewing on the left, except the sign of the y-displacement is reversed.

In order to completely describe a rigid body's orientation in space, the three rotation and three displacements need to be described. The mandibular rotations and displacements sufficiently describe the mandible's orientation during the chewing cycle. However, the location of the midline mandibular marker provides an additional visual aid in describing the motion.

4.5 Midline-Mandibular Marker Displacement:

Plotting the midline-mandible marker serves as a visual aid in describing the mandibular motion. The mandible's motion is completely described by the three rotation and three translations; however, the resulting motion is not obvious. The location of the virtual midline-mandible marker was plotted in all three planes. During the opening phase, the midline-mandible marker of a horse chewing on the right moved in the negative z-direction (ventrally) and in some horses, slightly to the left (positive y-direction) until the maximum pitch angle was obtained. The displacement in the x-direction was minimal, but tended to be in the negative direction (caudally). During the closing phase, the midline-mandible marker moved to the right (negative y- and positive z-directions) until the maximum lateral excursion was obtained and occusal contact was established. The mandible then slid to the left (positive y-direction), back to the original position during the grinding process. The midline-mandible marker slightly moved either in the positive x-direction (rostrally) during the entire closing phase (two horses), or continued in the negative x-direction (caudally) for the beginning portion of the closing phase, then moved in the positive x-direction (five horses). When observing the midline-mandibular marker motion in the z-y plane **(Figures 18-19)**, it is likely that the slope of the cheek teeth's occlusal surface determines the slope of the path from location #3 to #1. This can be confirmed by comparing actual measurements of the horse's teeth to the slope on the graphs. These patterns were more clearly indicated in some horses than others, but the general trends were similar. These results indicate that the mandible's center of rotation is slightly rostral and ventral to the mandibular coordinate system.

A horse chewing on the left has the same general trends as a horse chewing on the right, except the sign of the y-displacement is reversed.

4.6 Comparisons to Previous Work:

4.6.1 Lateral Mandibular Displacement (Y-displacement):

Two previous studies have examined the lateral excursion of the equine mandible. Leue (1941) created a molograph that fitted over the rostral portion of the horse's upper and lower jaws and traced the mandibular path while chewing grass, oats, and bran **(Figure 4)**. The mandible location that the sketches were created from is not indicated nor are the excursion values in Becker's (1962) citation of Leue's study. Dixon (2000) stated that the excursion values were 60, 38, and 23 mm while chewing grass, oats, and bran respectively. These values were obtained by simply measuring the distances on the sketch provided in Becker (1962). Unfortunately, the sketch does not necessarily represent the actual excursion values as the curves are much too smooth and the sketch could have been resized for publication purposes. Therefore, the sketch appears to be just a representation of the general chewing pattern rather than an actual chewing cycle. The sketch can be used to make basic comparisons between three different feeds.

Using the relative excursion values of the excursion based on Leue's study provided by Dixon (2000), the lateral excursion while chewing bran was 38% of the lateral excursion while chewing grass. In the present study, the lateral excursion while chewing pellets was 77% of the lateral excursion while chewing hay. Leue stated that a horse would chew with more lateral excursion when the moisture content of the food is increased and with a less when the fiber content is increased (cited by Baker and Easley, 1999). Grass has a much higher moisture content than hay and bran has more fiber than pellets. In addition, the particle size of bran is smaller than the size of pellets. Leue (1941, cited by Dixon, 2000) suggested that fibrous food such as hay or grass required the mandible to move laterally to its full extent to allow complete grinding, whereas smaller particles could be more easily retained on the occlusal surface and therefore required less lateral excursion to adequately grind the food. This combination of factors probably contributed to more extensive lateral excursion while chewing grass compared to hay, and reduced lateral excursion while chewing bran compared to pellets. Consequently, the lateral excursion while chewing pellets was a greater percentage of the excursion while chewing hay compared to the relationship between bran and grass in Leue's study.

Collinson (1994) reported incisor displacement to be 44-45 mm while chewing forages. The displacement was measured by marking the upper and lower lips with a continuous line at the junction between the first incisors, recording the mastication sequences with a video camera, and measuring the displacement from the recording. As stated previously in regards to Baker and Easley's (1999) efforts to track the mandibular motion during chewing, the lips consist of highly mobile soft tissue and cannot be classified as rigid bodies. Therefore, this method of measuring the incisor displacements is regarded as an approximation only.

The mean lateral displacement (y-displacement) in this study, measured at the virtual midline mandibular marker, was 19.87 mm and 15.38 mm while chewing hay and pellets, respectively. As previously described, the virtual midline-mandible marker was created at approximately the level of the first molars. Therefore, this virtual marker does not represent the motion of the incisors. The x-distance between the condyles and virtual marker is approximately half the distance between the condyles and the incisors. Consequently, obtaining lateral excursions of the virtual marker that are approximately half of those measured at the incisors by Collinson is reasonable and proportional.

Collinson (1994) reported the mean width of the lower fourth premolar, the largest tooth in the molar row, to be 1.64 cm measured from 16 horses. Although the upper cheek teeth are slightly wider than the lower, the lateral excursion while chewing hay was approximately 2 cm, which is sufficient to wear nearly the entire occlusal surface. The lateral excursion while chewing pellets, however, was approximately 1.5 cm, which is insufficient to completely wear the opposing occlusal surface and consequently, sharp enamel points can develop. If the horse's diet primarily comes from concentrates, an equine dentist must regularly treat the horse to prevent malocclusions from developing. **Figure 27** depicts the interaction between the upper and lower enamel ridges of a left cheek tooth while chewing on the left.

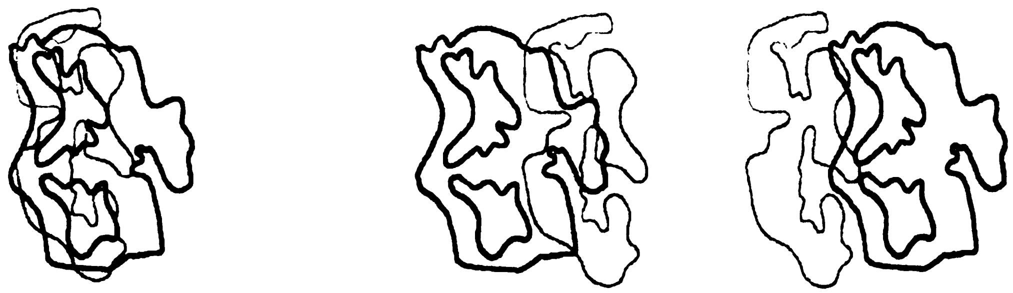

(a) (b) (c)

Figure 27: Schematic of enamel ridges for a left cheek tooth while chewing on the left. Black = upper molar, Grey = lower molar (a) maximum lateral excursion (start of grinding phase) (b) mid grinding phase (c) end of grinding phase (resting position)

4.6.2 Mandibular X and Z-Displacements:

As discussed above, lateral excursions obtained in this study comply with Collinson's study (1994) that measured lateral excursion at the incisors. The author is not aware of studies that also measured the displacements in the x and z-directions. The displacements in the x, y, and z-directions were significantly larger while chewing hay than pellets. This is likely due to the feed-particle size as Leue (1941) described since the dry matter contents are similar. In order to completely grind large food particles, the mandible must open and displace more than when chewing smaller particles. This study shows that not only does more lateral excursion occur while chewing hay, but there is also more mandibular displacement rostro-caudally and dorso-ventrally when compared to chewing pellets. Accordingly, the area encompassed by a cycle is significantly larger while chewing hay compared to pellets.

4.6.3 Mandibular Chewing Velocity and Frequency:

Collinson (1994) reported the absolute velocity measured at the fourth premolar to range from 104 mm/sec for high fiber hay (75% fiber) to 85 mm/sec for low fiber hay (55% fiber). These values are average velocities for the entire chewing cycle, obtained by using the displacement values measured from the lips and cycle duration values to estimate the velocity at the incisors. Incisor tooth velocity values were then used to estimate the velocity attained by individual molar teeth during mastication (Collinson, 1994). Collinson found molar velocity to be proportional to the distance from the TMJ, whereby the velocity of the third molar was approximately half the velocity of the second premolar. The fourth premolar is the tooth just rostral to the first molar, which is where the velocity of the virtual midline-mandible marker was measured. This study obtained mean absolute velocity values, measured at the virtual midline-mandibular marker, of 77.63 mm/sec for hay with 44.6% fiber and 79.03 mm/sec for pellets with 30% fiber, which follows the trend that Collinson described. There was no significant difference in the velocities of hay versus pellets.

The chewing frequency reported by Collinson ranged from 1.14 Hz for high fiber (75%) forages, 1.15 Hz for medium fiber (65%) forages and 1.16 Hz for low fiber (55%) forages. By measuring masseter muscle activity with electromyography, chewing frequency was determined. The chewing frequencies Collinson reported were not highly dependent on fiber content. The forage length was 3-12 cm, a typical range for hay. In this study, the mean frequency was 1.18 Hz while chewing hay, which is similar to Collinson's findings, and 1.48 Hz while chewing pellets. Chewing frequency appears to be dependent on particle size; the larger particle size of hay requires more time to completely grind on the occlusal surface compared to pellets.

4.6.4 Mandibular Coordinate System Translation and Rotation:

The author is unaware of any previous study that examines the translation or rotation of the equine TMJ.

4.6.5 Human Studies

In a study performed by Visscher *et al.* (2000), the kinematics of the human mandible for different head postures was investigated. The head position was found to influence the mandibular kinematics, probably due to the differences in mandibular loading. Although the horses were fed from the same location, future studies should record chewing cycles for different head postures to determine if the motion varies with head position. Gallo *et al.* (2000) described the mandibular motion during mastication through the helical axis pathway. In this study, three translations and three rotations described the mandibular motion because the results give a more intuitive description of the motion. Yatabe *et al.* (1997) used the kinematic center of the right and left condyles as a reference point for the reconstruction of condylar movement paths. In the present study, the mandibular kinematic center was established halfway between the two condyles and the motion of that location was observed relative to the skull coordinate system. In order to make comparisons to human condylar motion based on Yatabe's findings, the equine condylar motion can be observed by creating a mandibular coordinate system at each condyle and observing translations and rotations at that point.

5. Conclusions and Recommendations:

A limited number of veterinarians and specialists have dedicated their lives to improving equine dental health and understanding the development of malocclusions. On-line equine dentistry groups are flooded with discussions on dentistry techniques and theories as to what the primary contributing factors that lead to malocclusions are. Most professional equine dentists would agree that horses chew forages such as hay differently than concentrate feeds and they believe that the degree of lateral excursion is an important factor in minimizing malocclusions.

This study quantified the three-dimensional motion of the equine TMJ while chewing hay and pellets. The results provide base-line data, including the angular and linear displacements of the TMJ during the chewing cycle. The location of a virtual midline-mandible marker was plotted to serve as a visual aid in describing the mandibular motion. The horses examined did not have any malocclusion and they encompassed a broad range of breeds, sizes, and ages. In addition, the three-dimensional Motion Analysis tracking system is much more accurate than the tracking points on the lips as Collinson (1994) and Baker and Easley (1999) have done in two dimensions. Therefore, the results from this study more adequately represent the general, normal 3-D motion of the equine TMJ.

The paired t-test tested the null hypothesis, that there is not a significant difference between the mean values of the variables that measure mandibular motion in horses chewing hay versus pellets, and the results allow the null hypothesis to be rejected.

Therefore, the experimental hypothesis is accepted. While the results indicate that chewing motion is influenced by feed-particle size, the data collected did show that for some horses in the sample, this was not the case. Nevertheless, the measured variables were significantly different when statistics were run over the complete group of seven horses. Coarse, fibrous feeds show a more extensive chewing motion than pellets.

The knowledge gained through this study can be useful to the feed industry. Products with larger feed particle size and the current nutritional value per kilogram need to be developed to encourage horses to chew with more lateral excursion while maintaining adequate nutrition. Current products are designed for their nutritional value, but the small particle size of most concentrates does not encourage horses to chew with the extent of lateral excursion that would prevent sharp enamel points from developing.

Having a description of the TMJ motion during normal chewing, it would be interesting to now examine horses with malocclusions. The malocclusions would be evaluated and categorized by an equine dentist, and the deviations from the normal patterns would be noted. The dentist would then treat the horse to remove the malocclusions and the horse would be re-evaluated at post-treatment intervals to observe any changes in the chewing pattern. The techniques that resulted in improved chewing (more extensive lateral excursion) would be documented and shared with the equine dentistry community to promote equine dental health.

In the future, kinematic studies should include a broader range of feed types with varying fiber and moisture content to determine how fiber and moisture influence the chewing cycle. Bone pin, magnetometer, or 3-D fluoroscopic studies should be performed to determine how the skin displaces over the bony landmarks selected for marker placement during chewing. By adjusting for skin displacement, the results will more accurately represent the TMJ motion.

Appendix A:

Location of midline-mandibular marker relative to skull coordinate system viewed in all three planes for all horses.

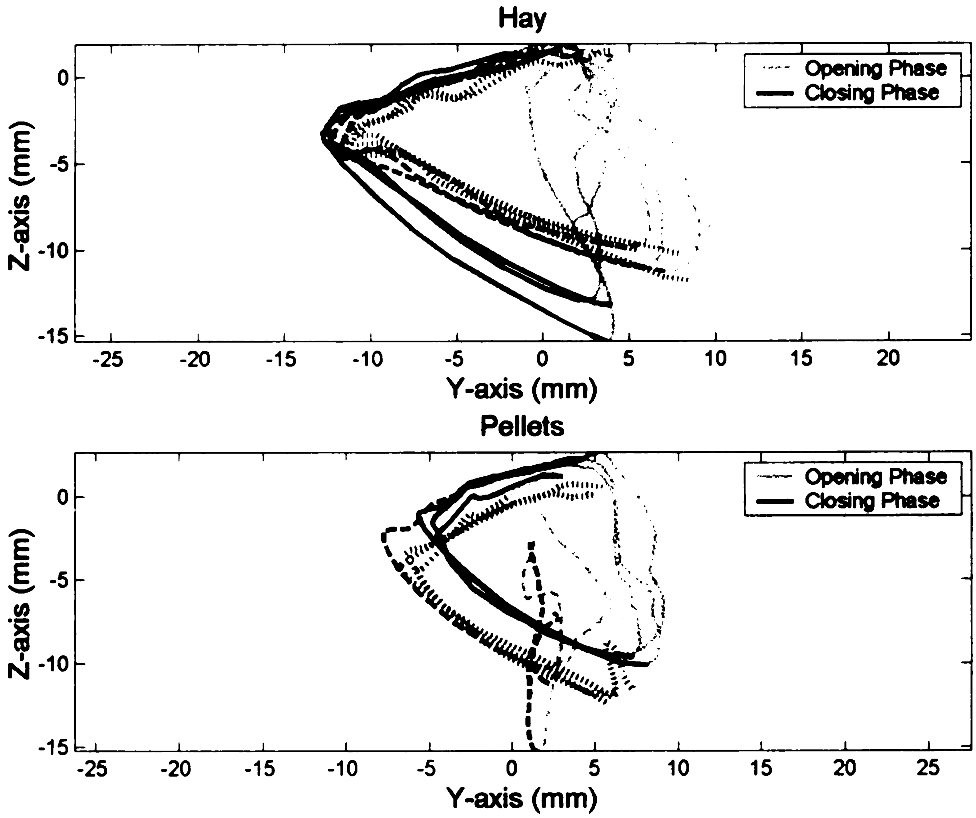

Figure 28: z-y location of midline-mandibular marker
for horse #1 chewing on the right
Solid line = Trial 1
Dashed line = Trial 2
Hatched line = Trial 3

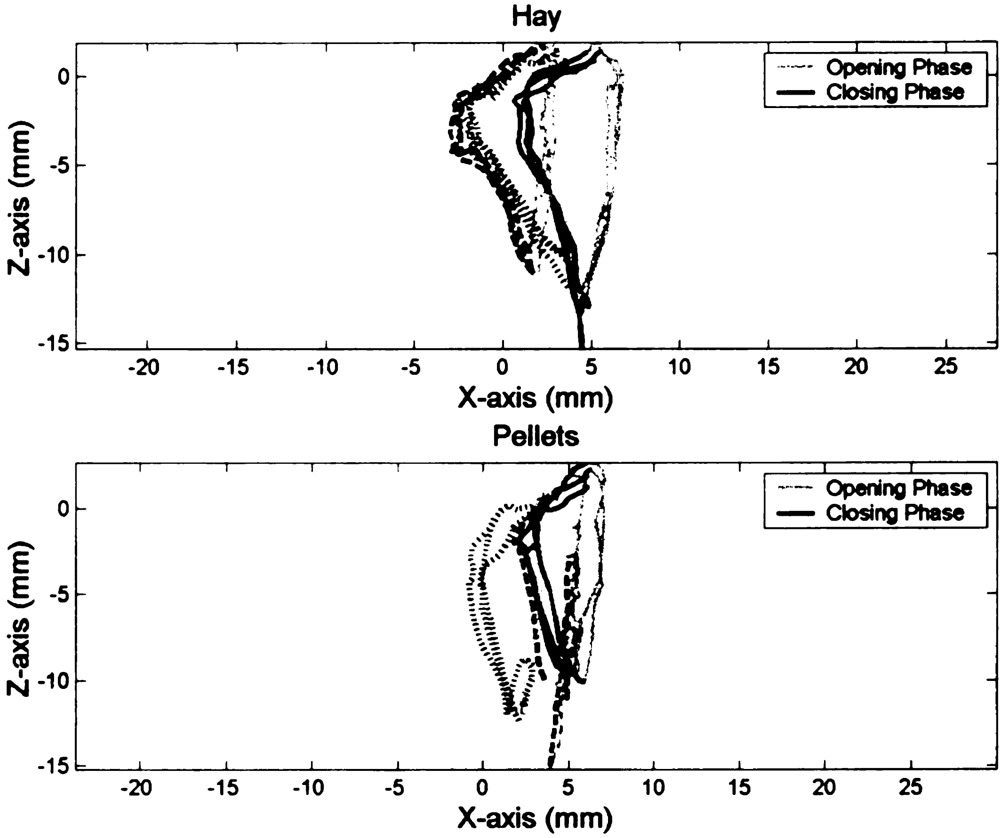

Figure 29: z-x location of midline-mandibular marker
for horse #1 chewing on the right
Solid line = Trial 1
Dashed line = Trial 2
Hatched line = Trial 3

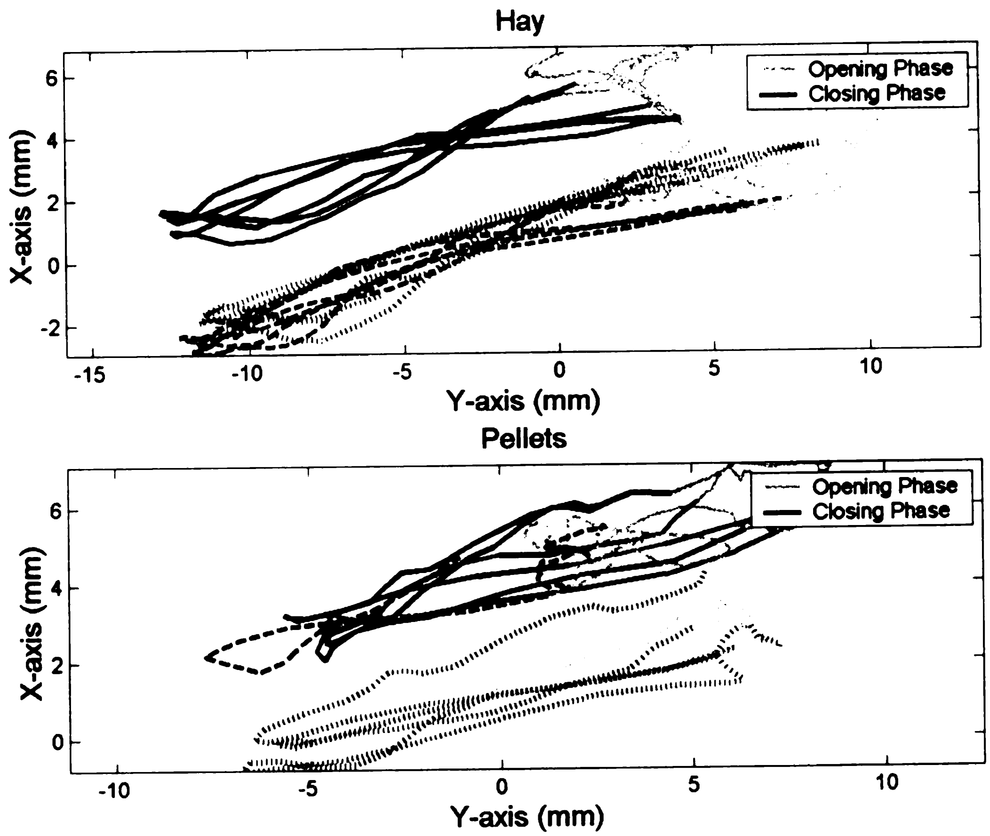

Figure 30: x-y location of midline-mandibular marker
for horse #1 chewing on the right
Solid line = Trial 1
Dashed line = Trial 2
Hatched line = Trial 3

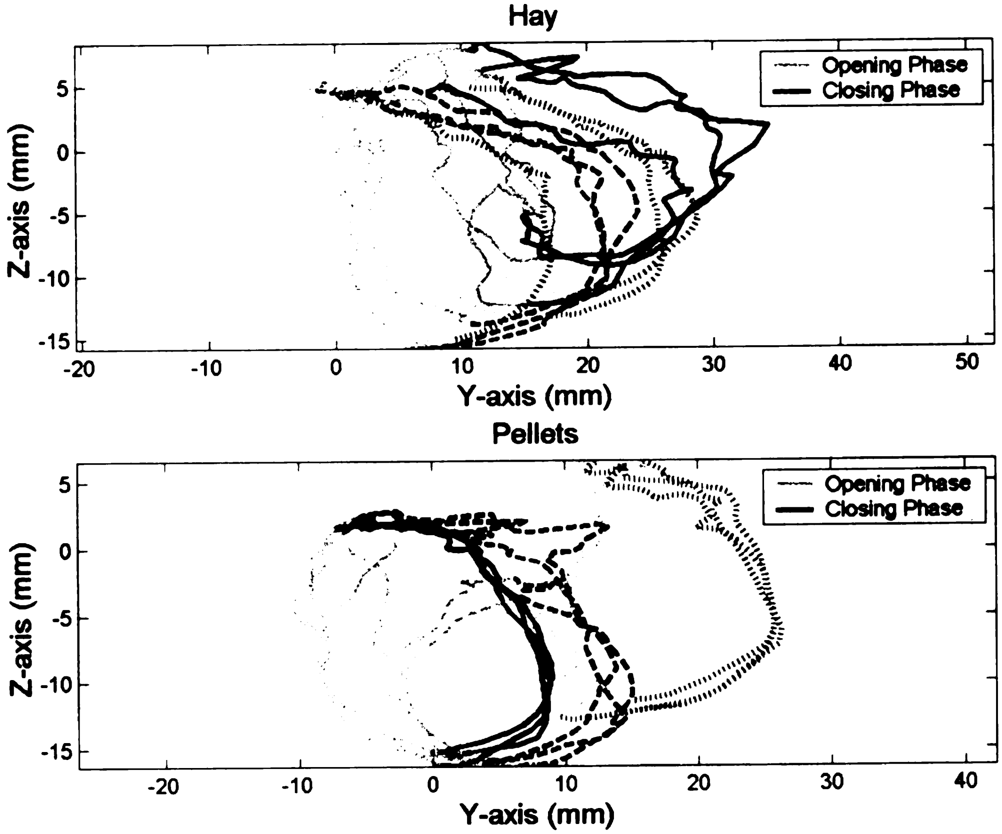

Figure 31: z-y location of midline-mandibular marker
for horse #2 chewing on the left
Solid line = Trial 1
Dashed line = Trial 2
Hatched line = Trial 3

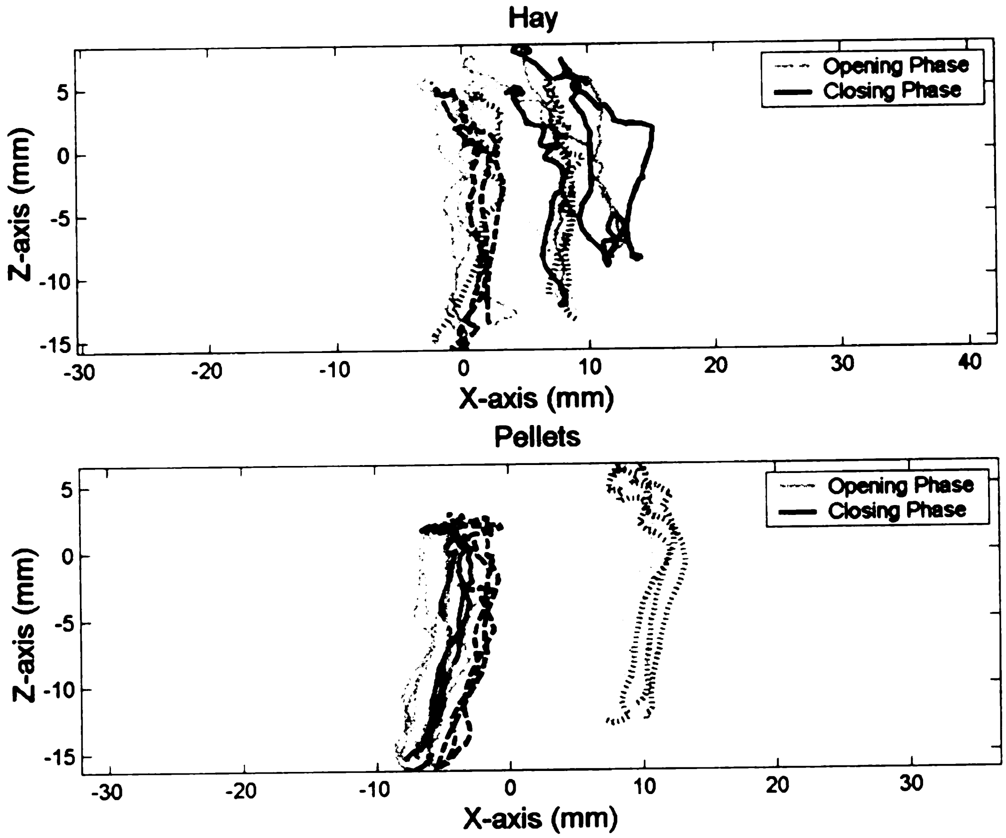

Figure 32: z-x location of midline-mandibular marker
for horse #2 chewing on the left
Solid line = Trial 1
Dashed line = Trial 2
Hatched line = Trial 3

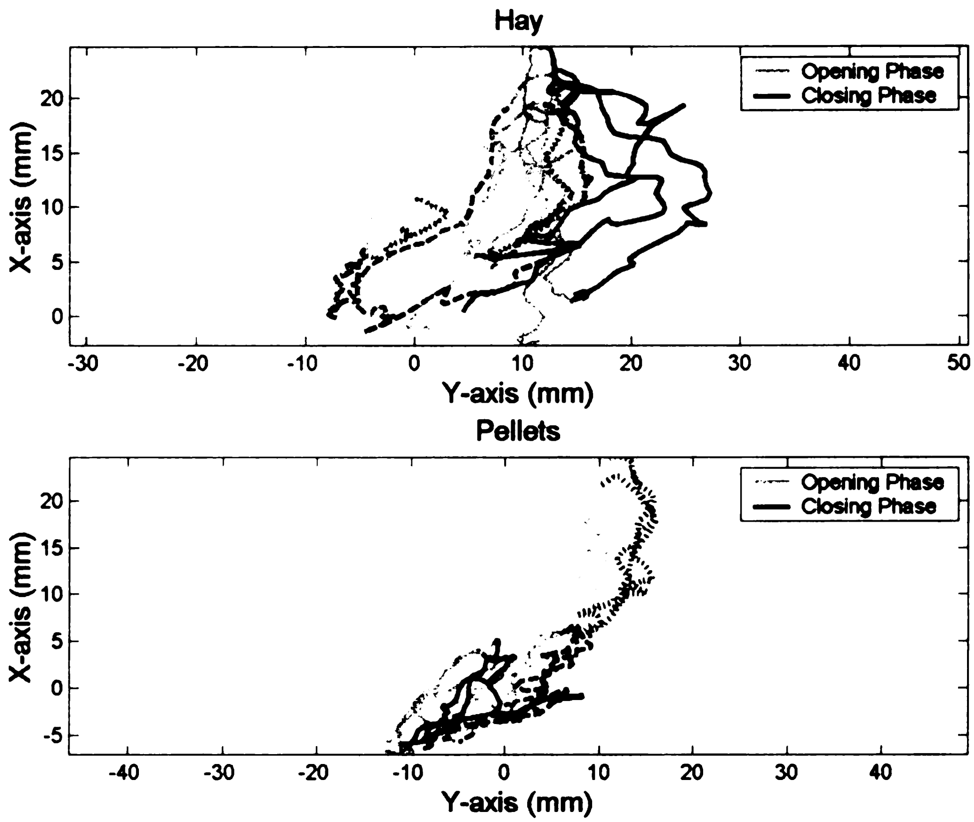

Figure 33: x-y location of midline-mandibular marker
for horse #2 chewing on the left
Solid line = Trial 1
Dashed line = Trial 2
Hatched line = Trial 3

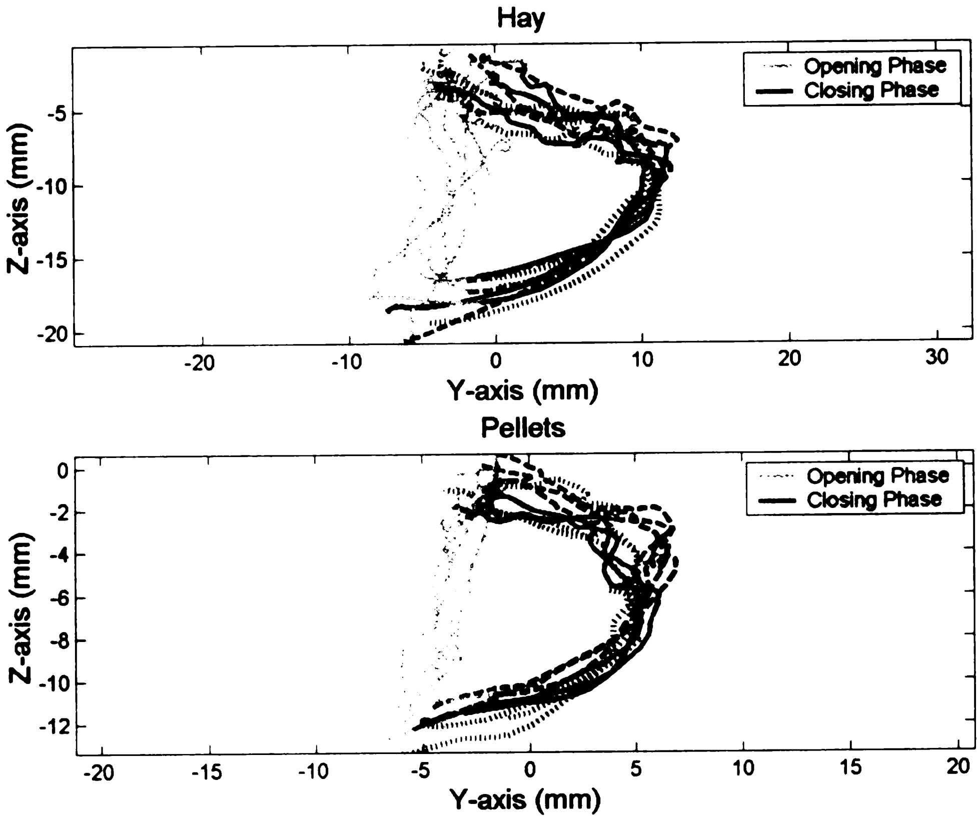

Figure 34: z-y location of midline-mandibular marker for horse #3 chewing on the left
Solid line = Trial 1
Dashed line = Trial 2
Hatched line = Trial 3

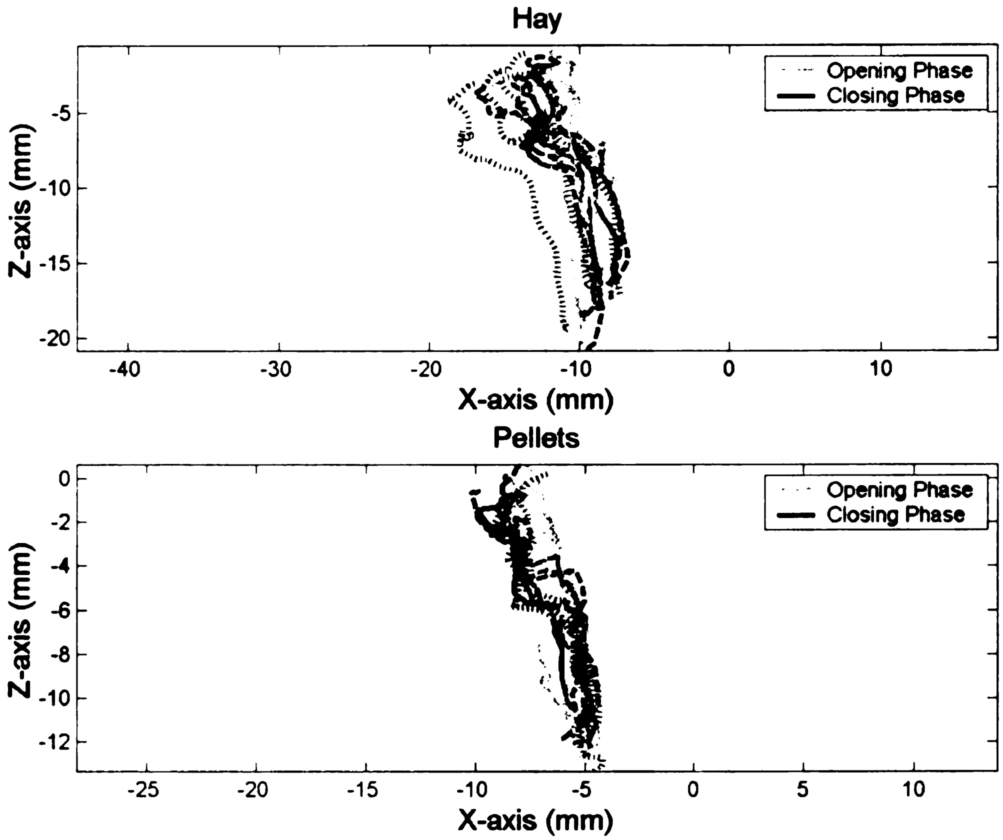

Figure 35: z-x location of midline-mandibular marker
for horse #3 chewing on the left
Solid line = Trial 1
Dashed line = Trial 2
Hatched line = Trial 3

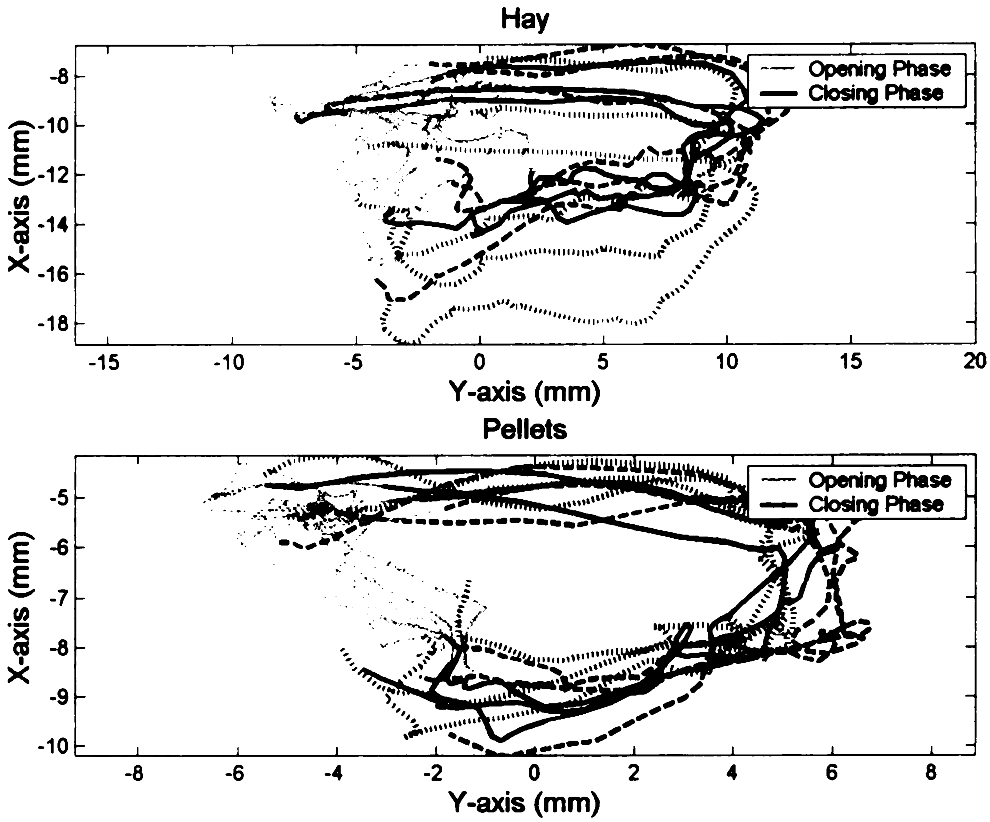

Figure 36: x-y location of midline-mandibular marker
for horse #3 chewing on the left
Solid line = Trial 1
Dashed line = Trial 2
Hatched line = Trial 3

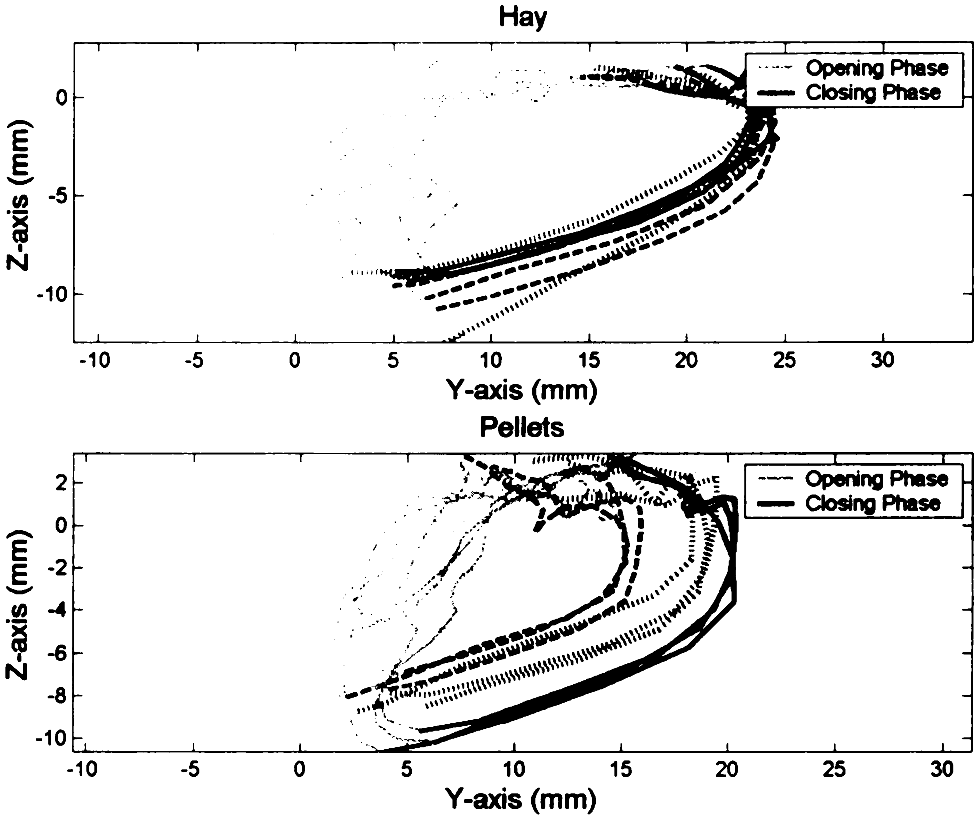

Figure 37: z-y location of midline-mandibular marker
for horse #4 chewing on the left
Solid line = Trial 1
Dashed line = Trial 2
Hatched line = Trial 3

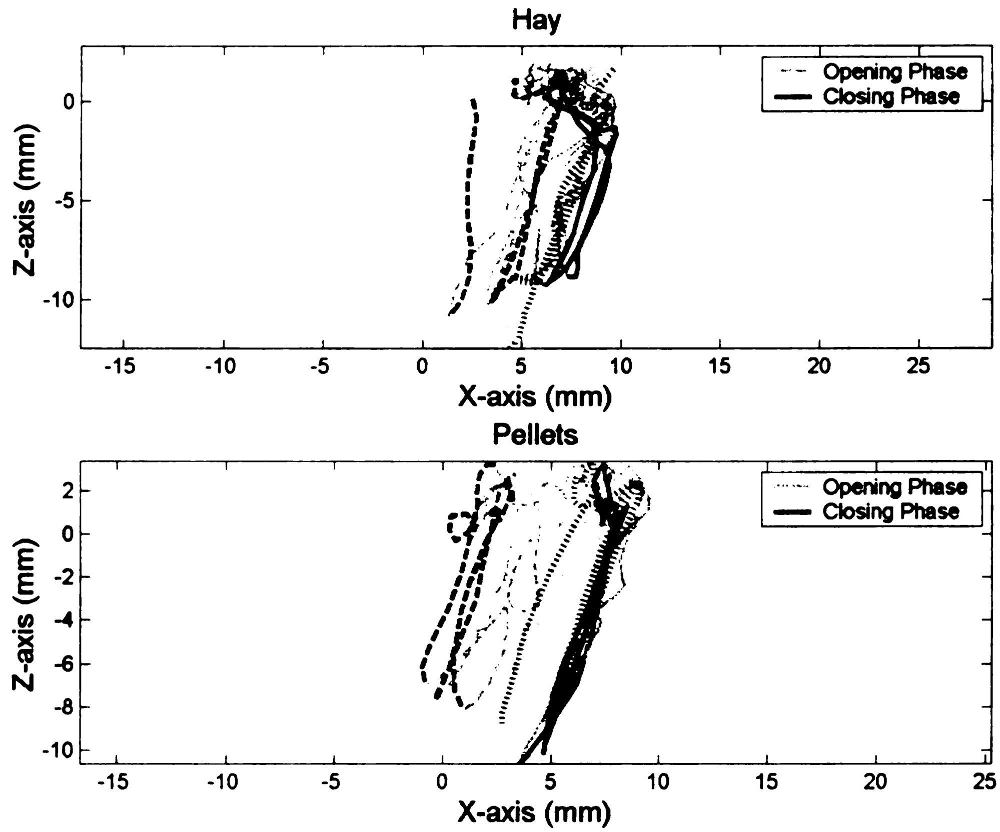

Figure 38: z-x location of midline-mandibular marker
for horse #4 chewing on the left
Solid line = Trial 1
Dashed line = Trial 2
Hatched line = Trial 3

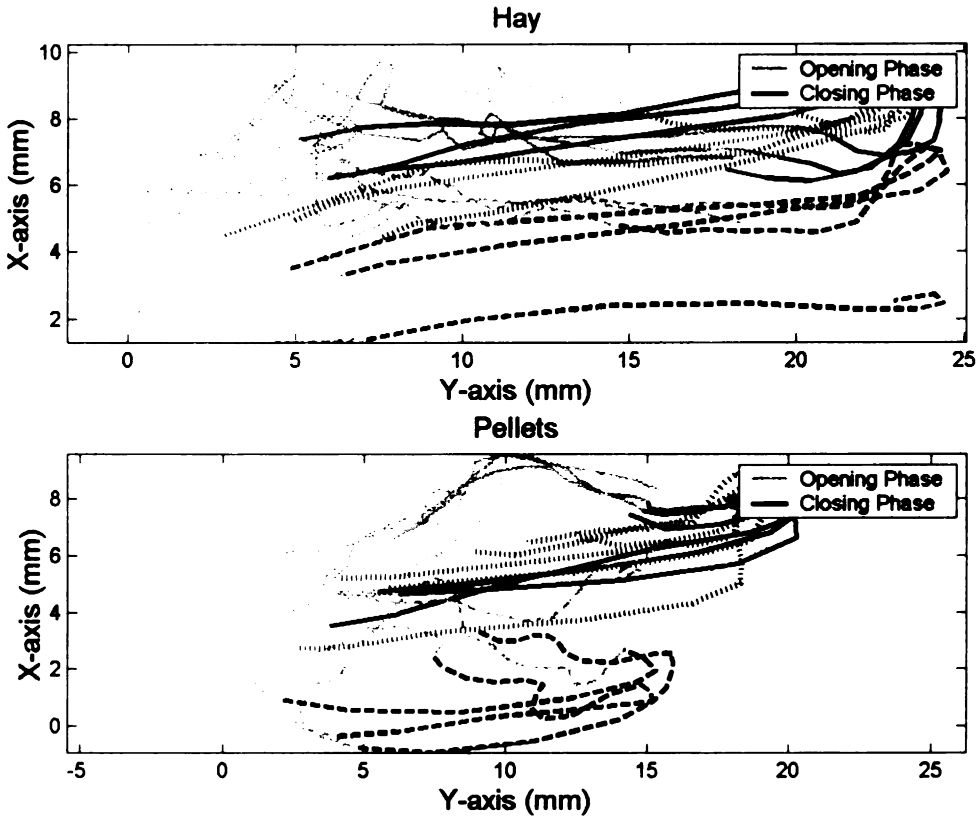

Figure 39: x-y location of midline-mandibular marker
for horse #4 chewing on the left
Solid line = Trial 1
Dashed line = Trial 2
Hatched line = Trial 3

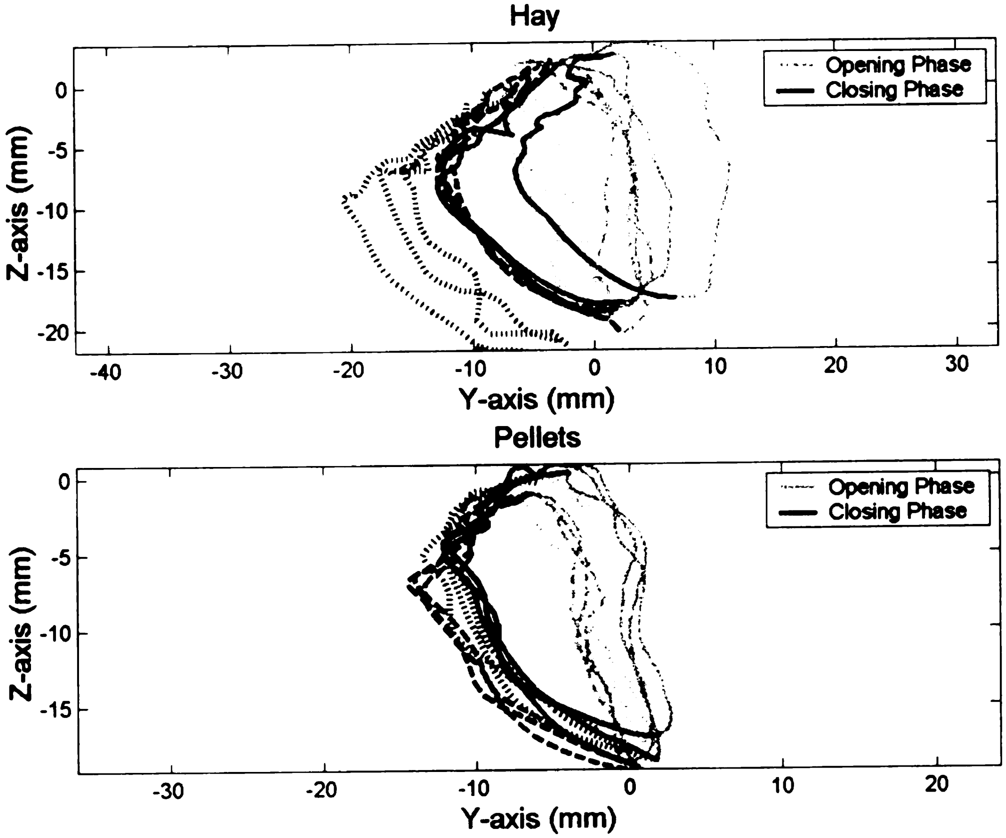

Figure 40: z-y location of midline-mandibular marker
for horse #5 chewing on the left
Solid line = Trial 1
Dashed line = Trial 2
Hatched line = Trial 3

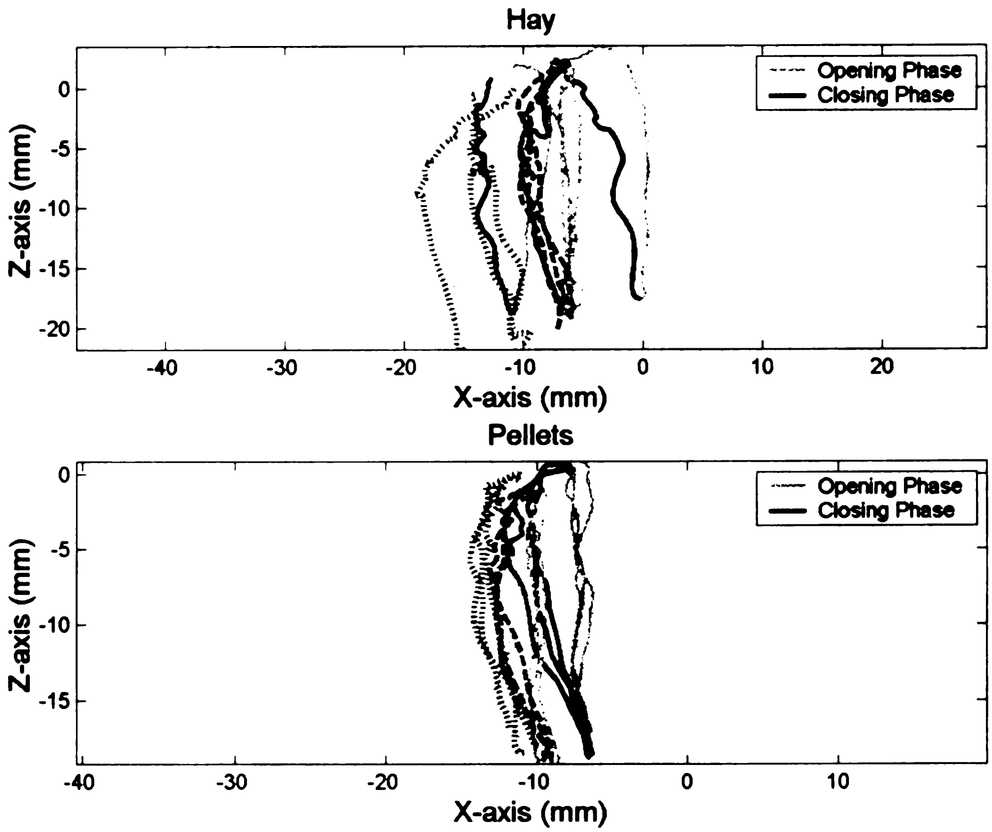

Figure 41: z-x location of midline-mandibular marker
for horse #5 chewing on the left
Solid line = Trial 1
Dashed line = Trial 2
Hatched line = Trial 3

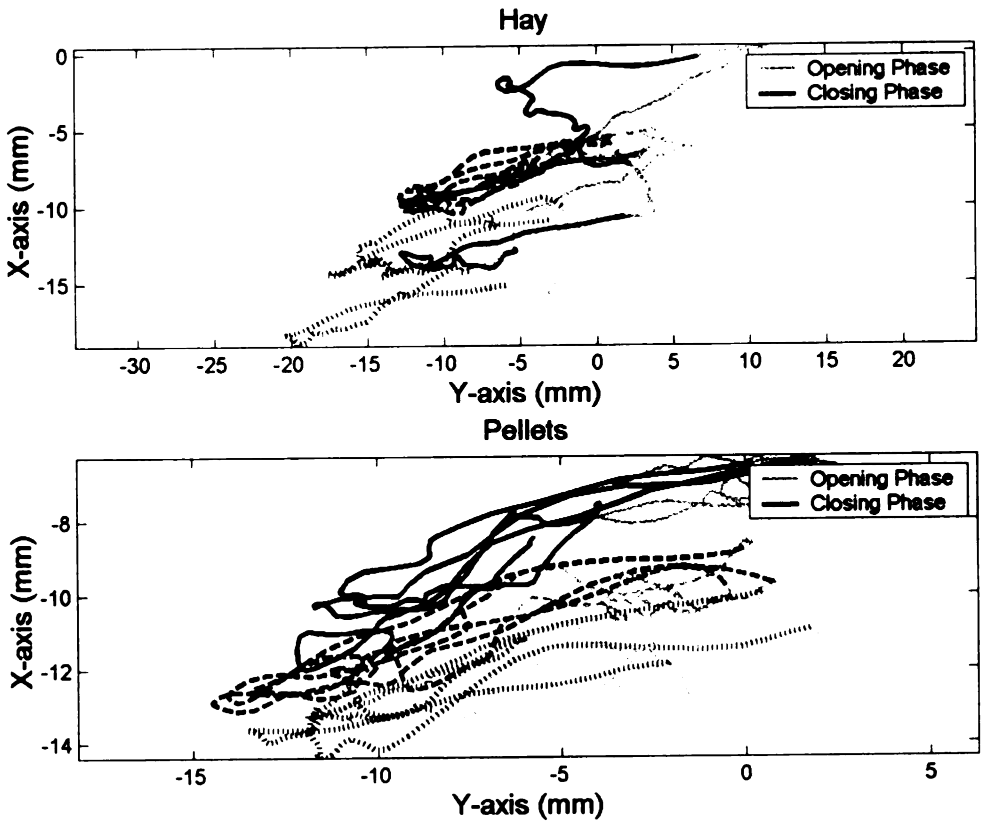

Figure 42: x-y location of midline-mandibular marker
for horse #5 chewing on the left
Solid line = Trial 1
Dashed line = Trial 2
Hatched line = Trial 3

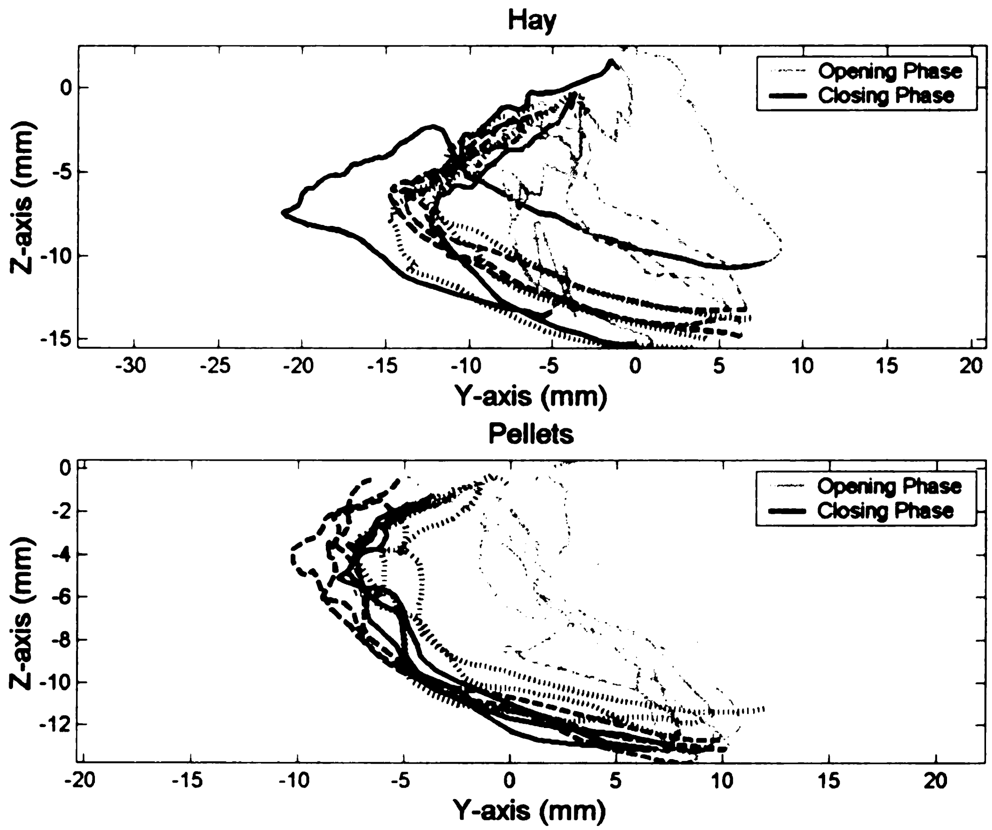

Figure 43: z-y location of midline-mandibular marker
for horse #6 chewing on the left
Solid line = Trial 1
Dashed line = Trial 2
Hatched line = Trial 3

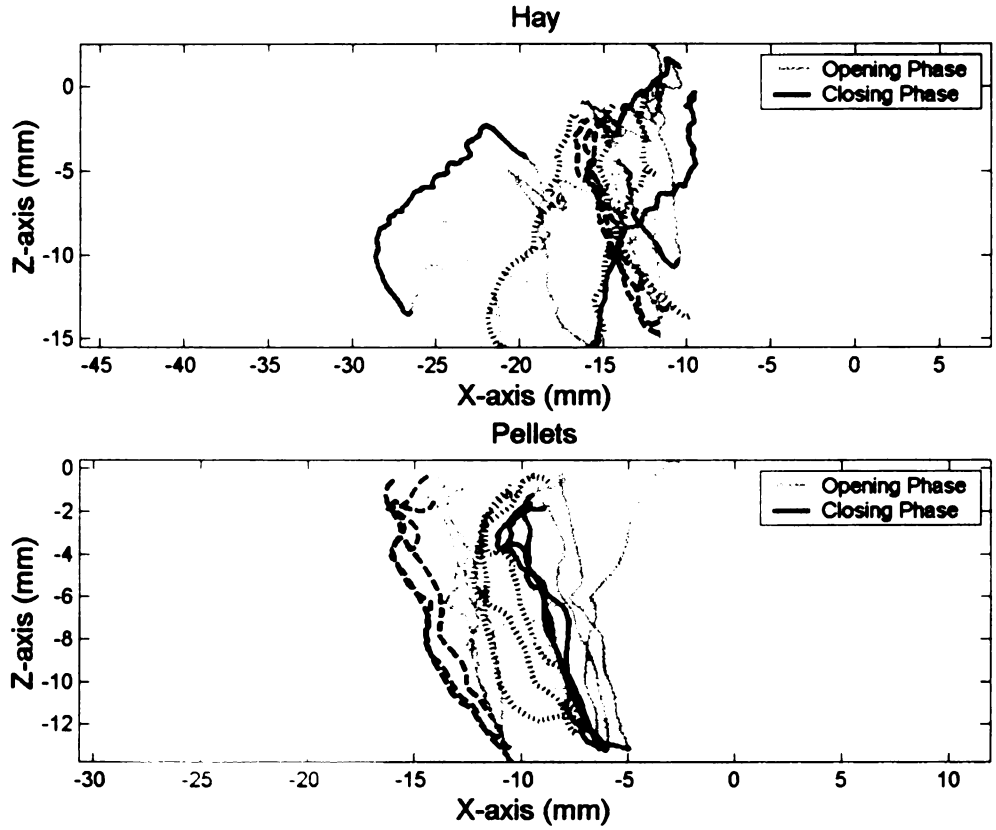

Figure 44: z-x location of midline-mandibular marker
for horse #6 chewing on the left
Solid line = Trial 1
Dashed line = Trial 2
Hatched line = Trial 3

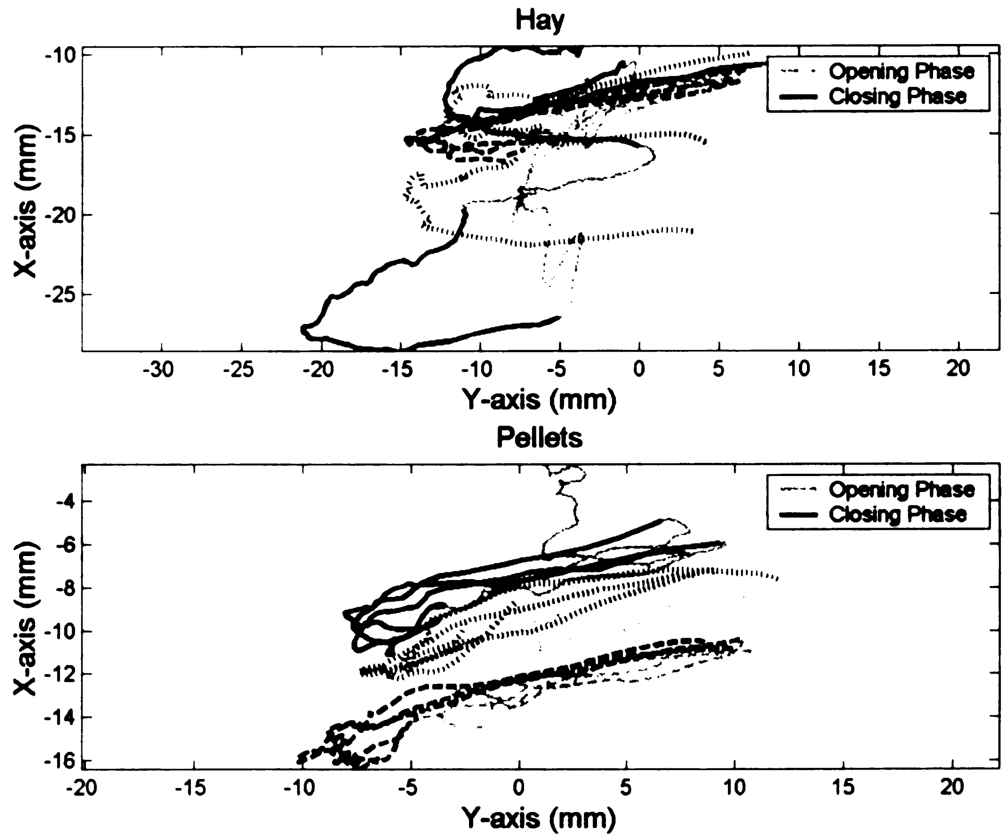

Figure 45: x-y location of midline-mandibular marker
for horse #6 chewing on the left
Solid line = Trial 1
Dashed line = Trial 2
Hatched line = Trial 3

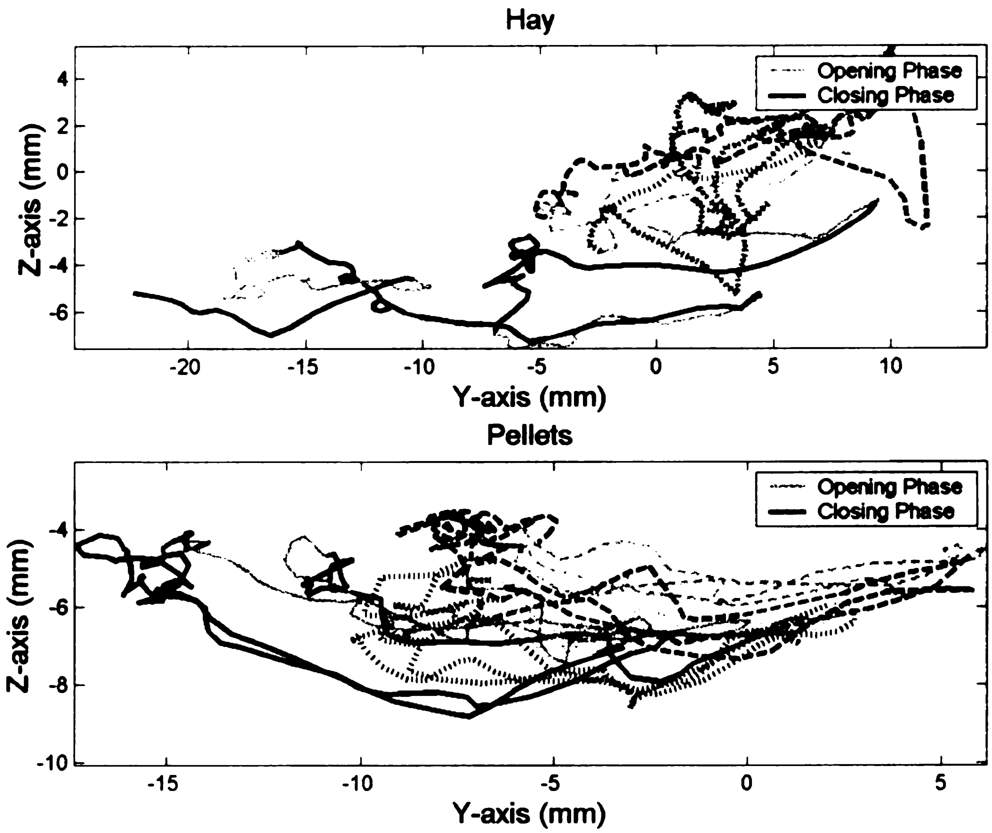

Figure 46: z-y location of midline-mandibular marker
for horse #7 chewing on the left
Solid line = Trial 1
Dashed line = Trial 2
Hatched line = Trial 3

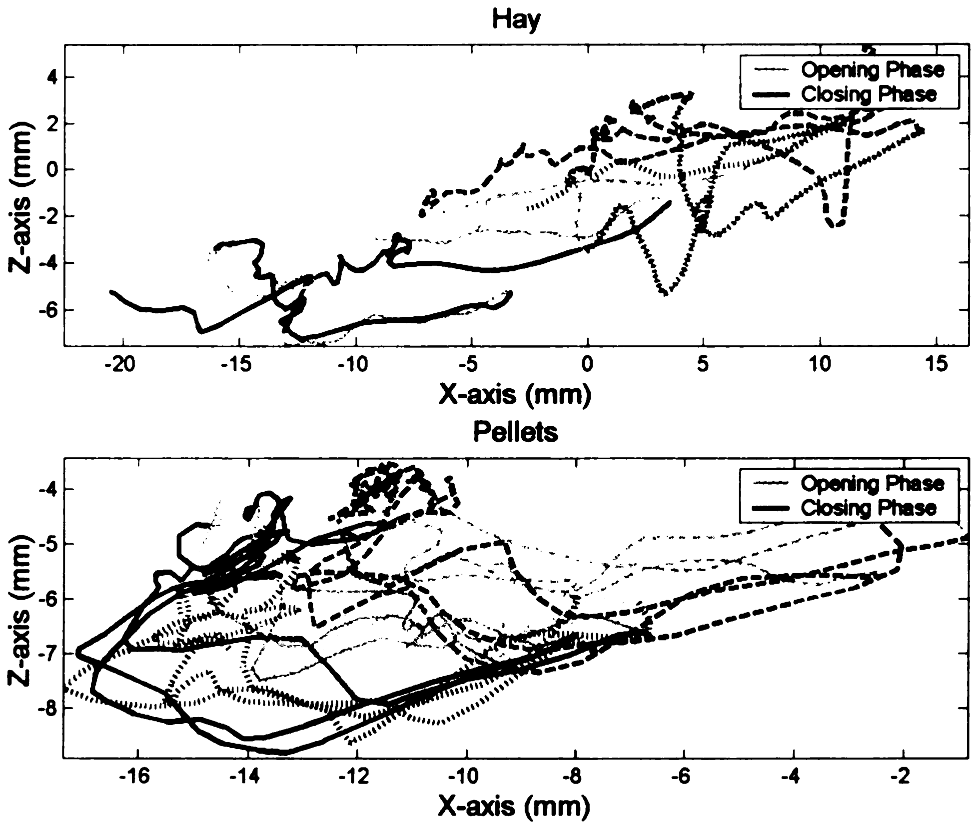

Figure 47: z-x location of midline-mandibular marker
for horse #7 chewing on the left
Solid line = Trial 1
Dashed line = Trial 2
Hatched line = Trial 3

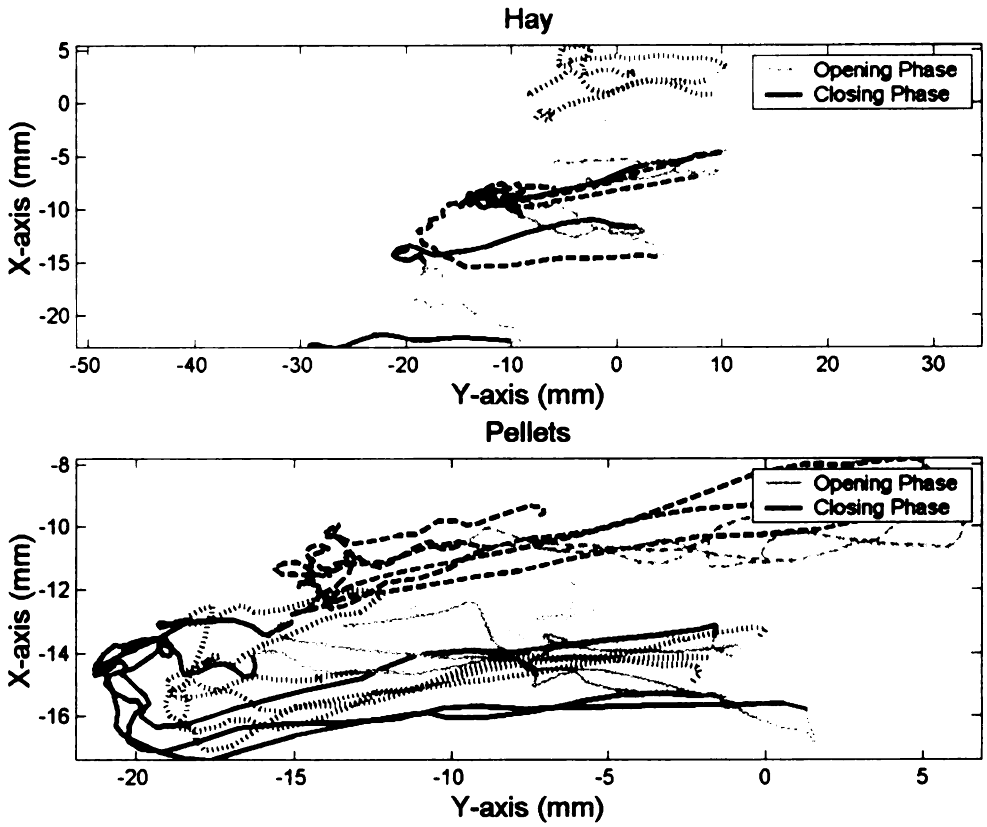

Figure 48: x-y location of midline-mandibular marker for horse #7 chewing on the left
Solid line = Trial 1
Dashed line = Trial 2
Hatched line = Trial 3

Appendix B:

Location of mandibular coordinate system relative to skull coordinate system viewed in all three planes for all horses.

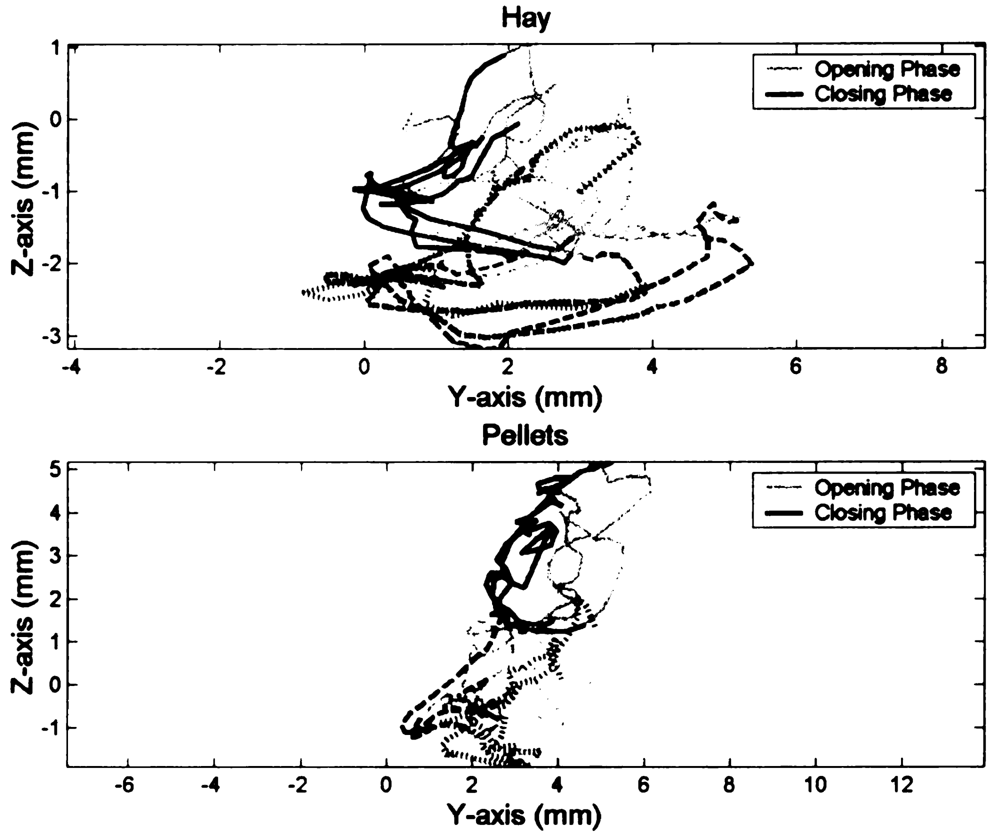

Figure 49: z-y location of mandibular coordinate system
for horse #1 chewing on the right
Solid line = Trial 1
Dashed line = Trial 2
Hatched line = Trial 3

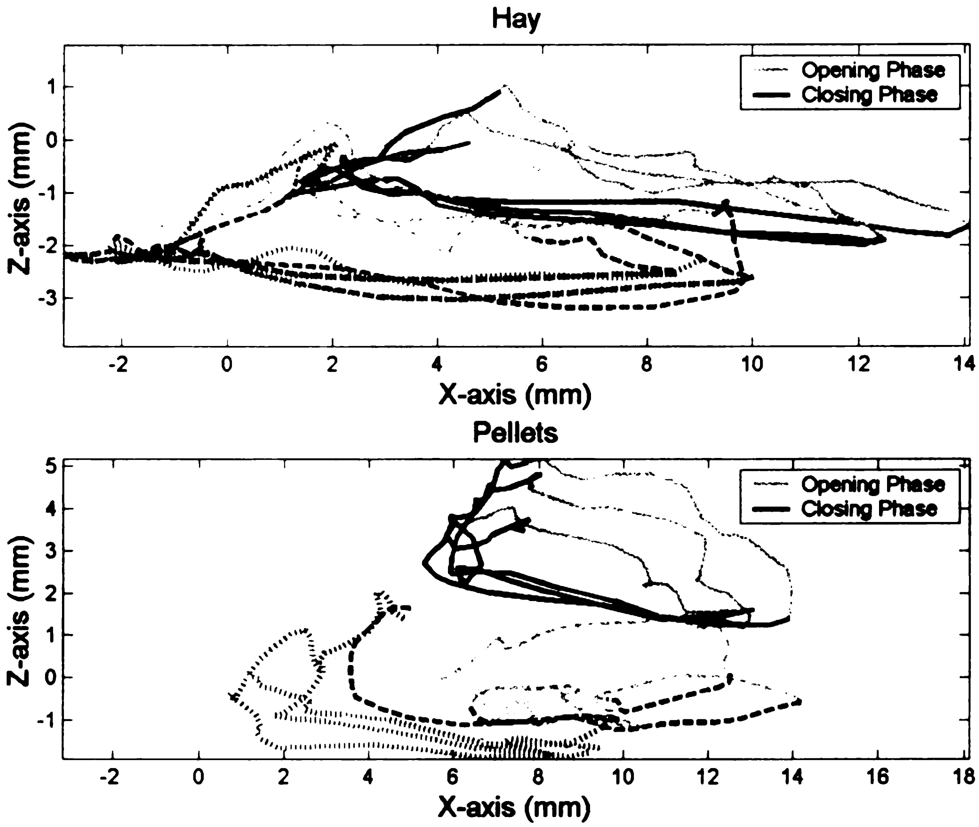

Figure 50: z-x location of mandibular coordinate system for horse #1 chewing on the right
Solid line = Trial 1
Dashed line = Trial 2
Hatched line = Trial 3

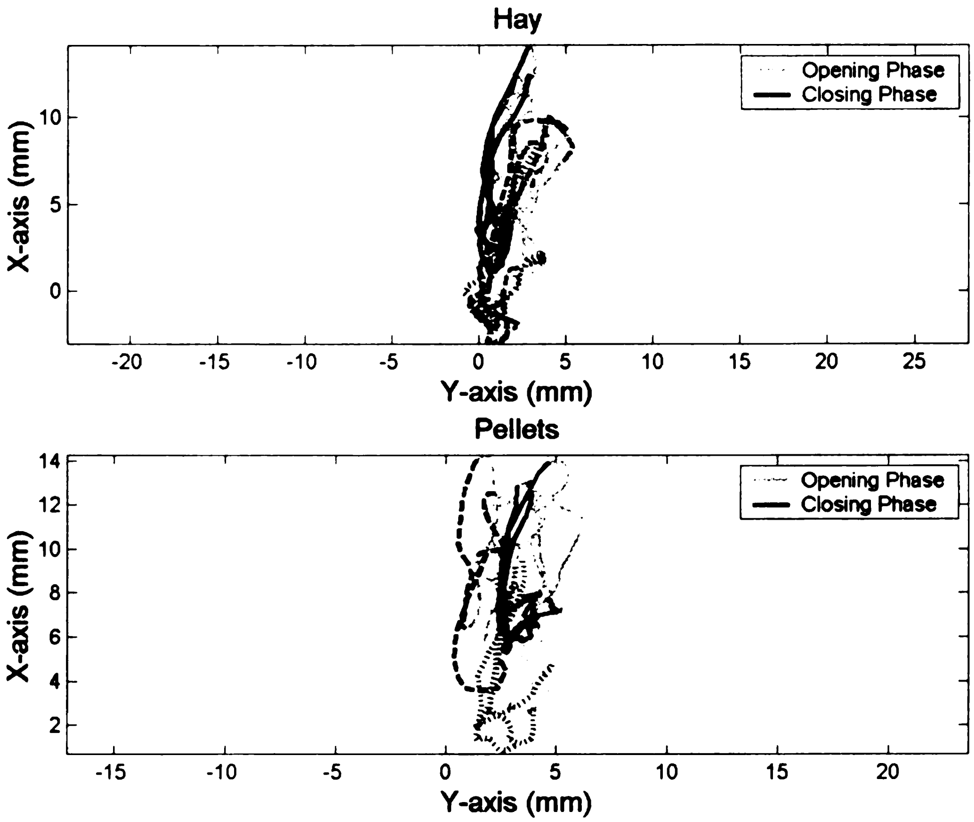

Figure 51: x-y location of mandibular coordinate system for horse #1 chewing on the right
Solid line = Trial 1
Dashed line = Trial 2
Hatched line = Trial 3

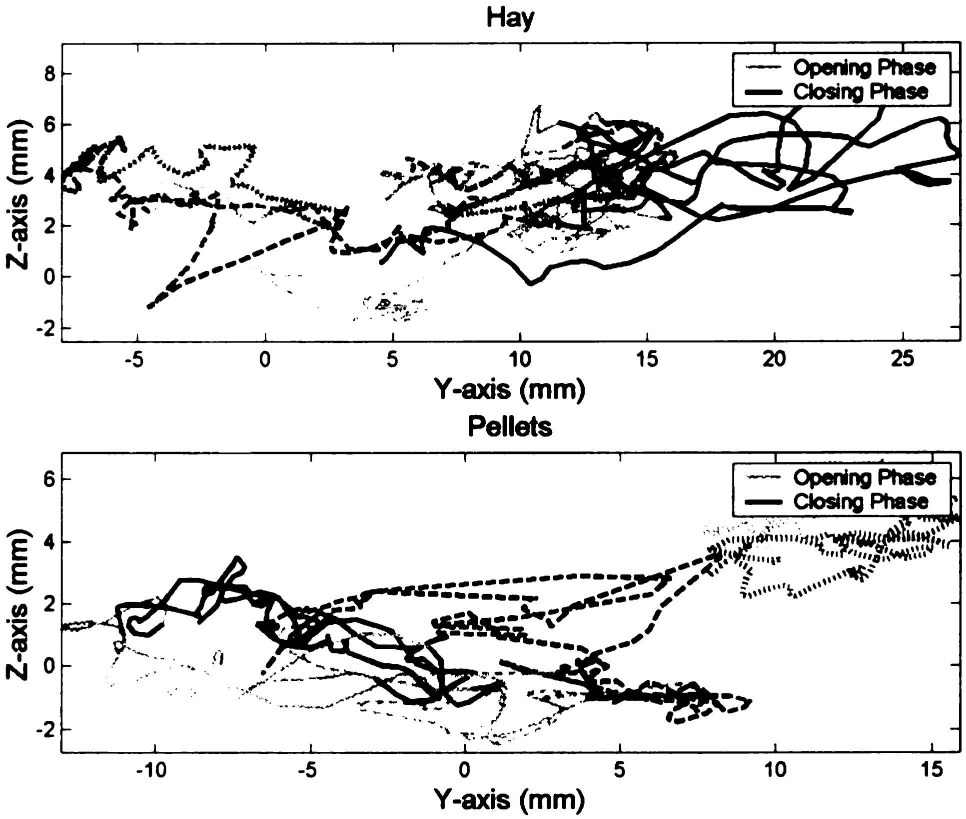

Figure 52: z-y location of mandibular coordinate system
for horse #2 chewing on the left
Solid line = Trial 1
Dashed line = Trial 2
Hatched line = Trial 3

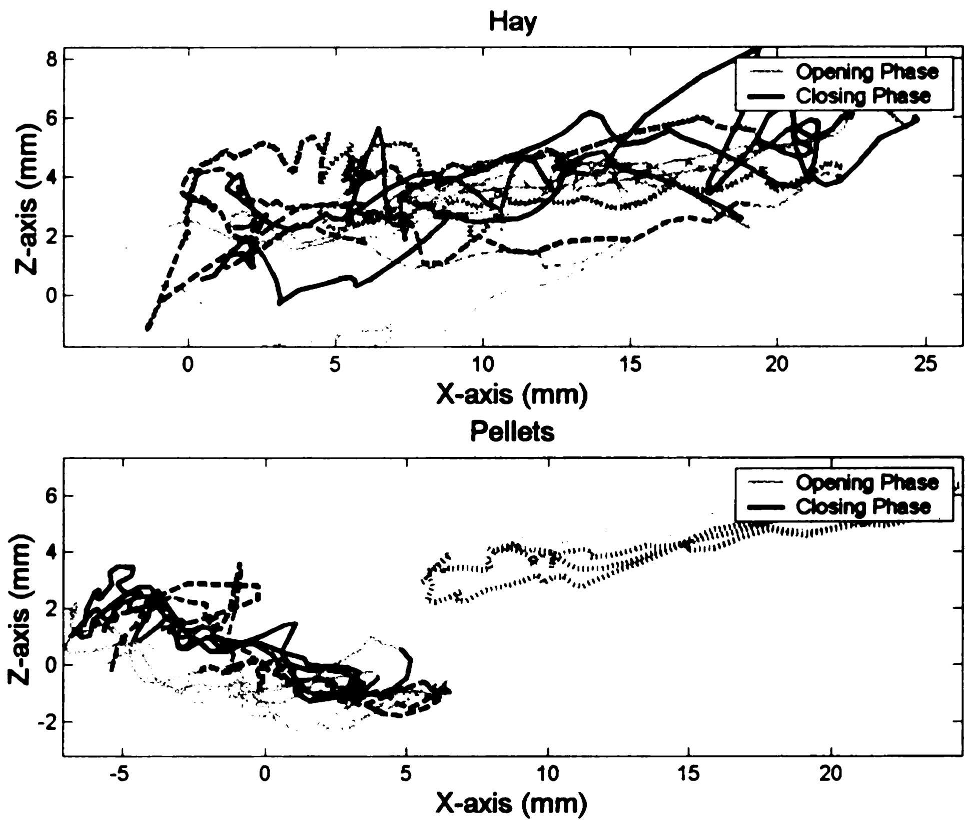

Figure 53: z-x location of mandibular coordinate system for horse #2 chewing on the left
Solid line = Trial 1
Dashed line = Trial 2
Hatched line = Trial 3

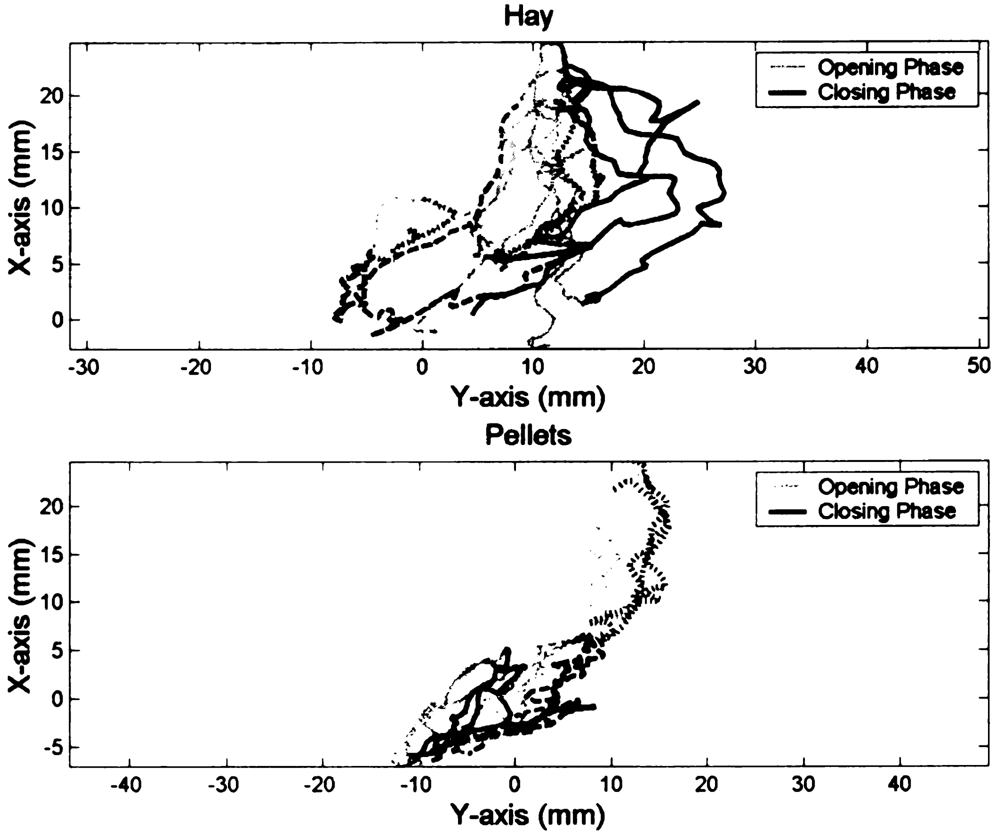

Figure 54: x-y location of mandibular coordinate system for horse #2 chewing on the left
Solid line = Trial 1
Dashed line = Trial 2
Hatched line = Trial 3

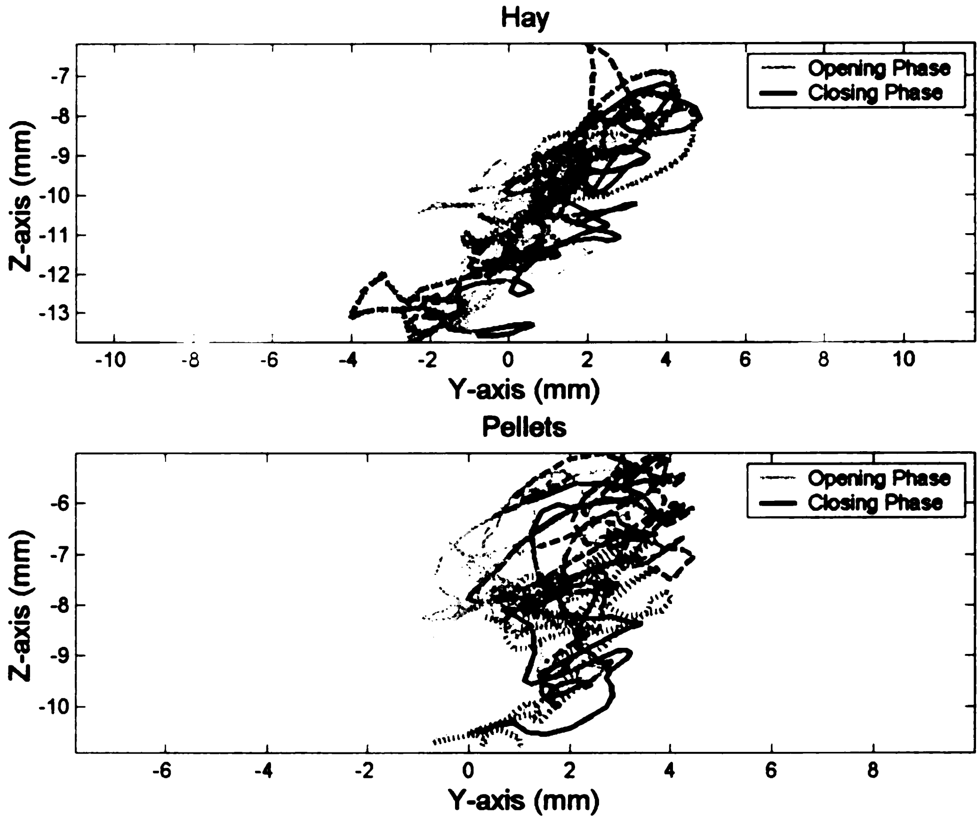

Figure 55: z-y location of mandibular coordinate system
for horse #3 chewing on the left
Solid line = Trial 1
Dashed line = Trial 2
Hatched line = Trial 3

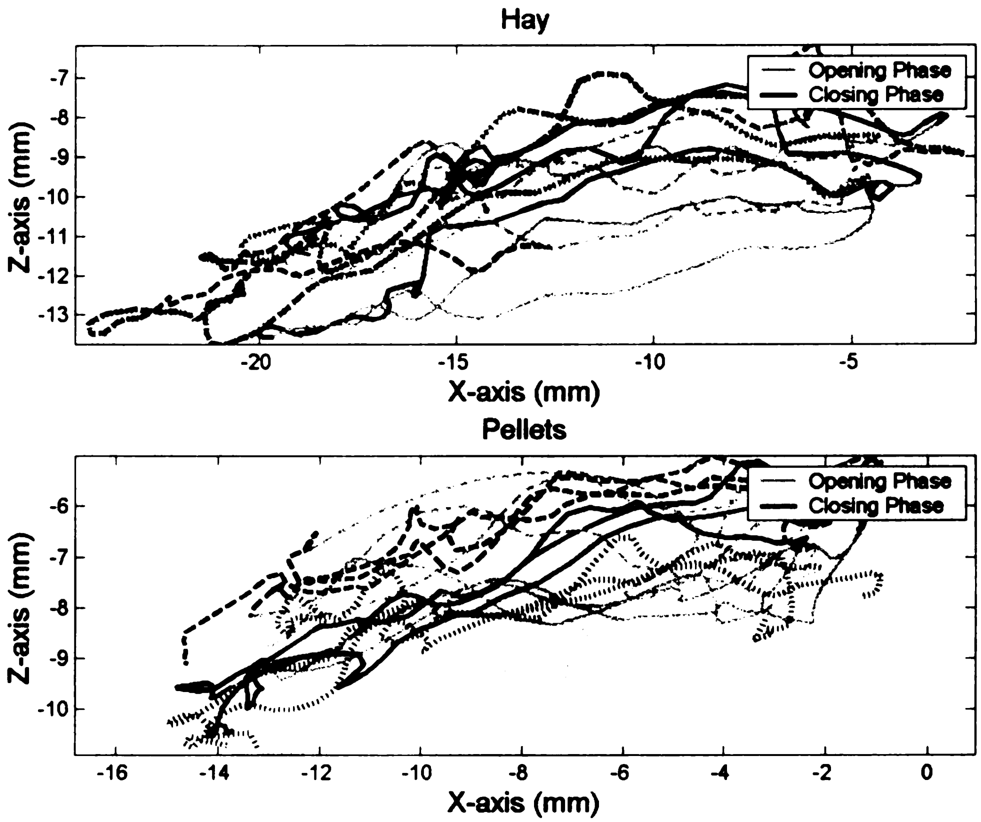

Figure 56: z-x location of mandibular coordinate system
for horse #3 chewing on the left
Solid line = Trial 1
Dashed line = Trial 2
Hatched line = Trial 3

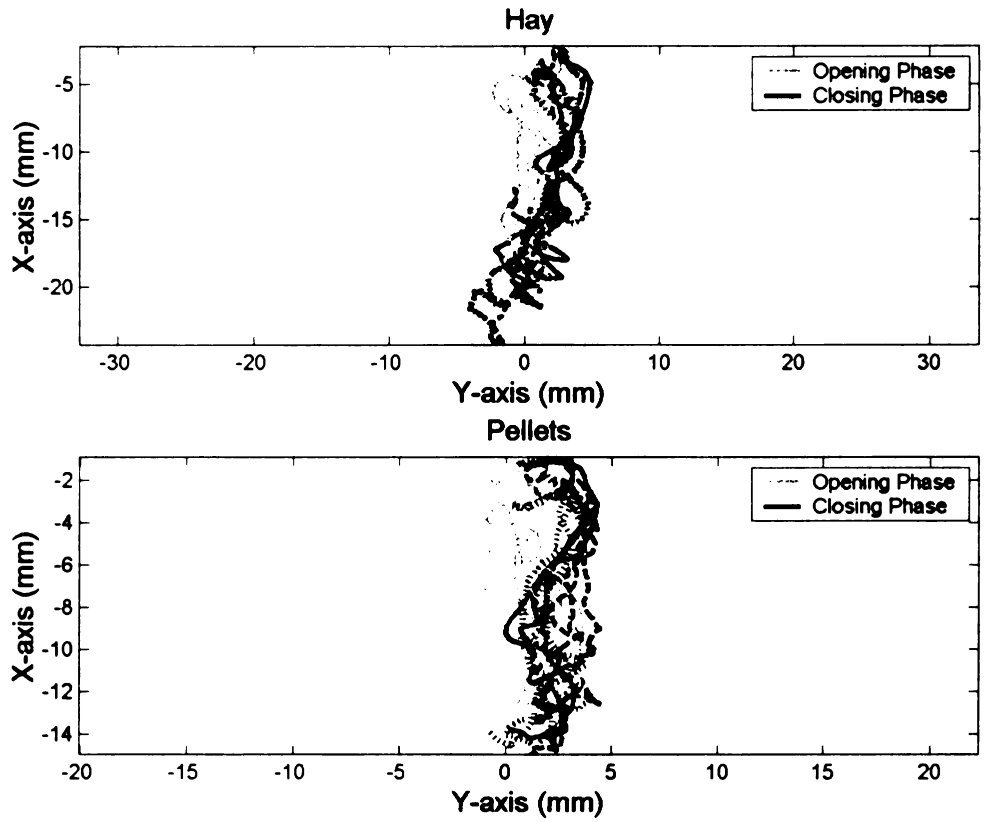

Figure 57: x-y location of mandibular coordinate system
for horse #3 chewing on the left
Solid line = Trial 1
Dashed line = Trial 2
Hatched line = Trial 3

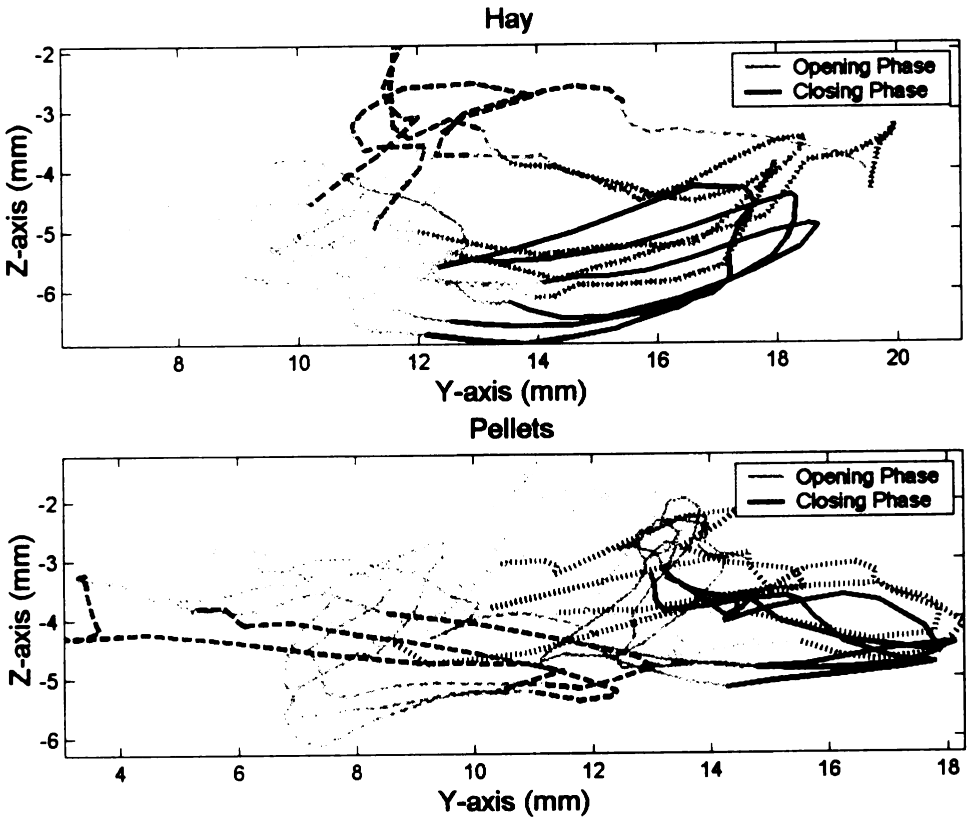

Figure 58: z-y location of mandibular coordinate system
for horse #4 chewing on the left
Solid line = Trial 1
Dashed line = Trial 2
Hatched line = Trial 3

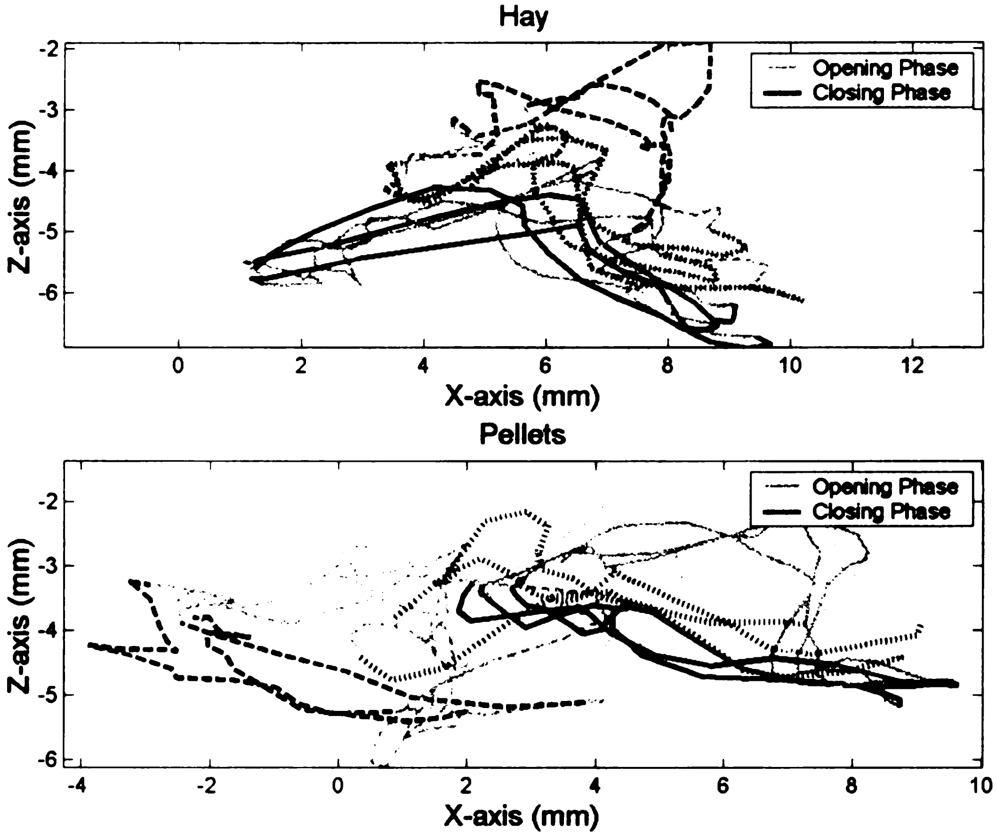

Figure 59: z-x location of mandibular coordinate system
for horse #4 chewing on the left
Solid line = Trial 1
Dashed line = Trial 2
Hatched line = Trial 3

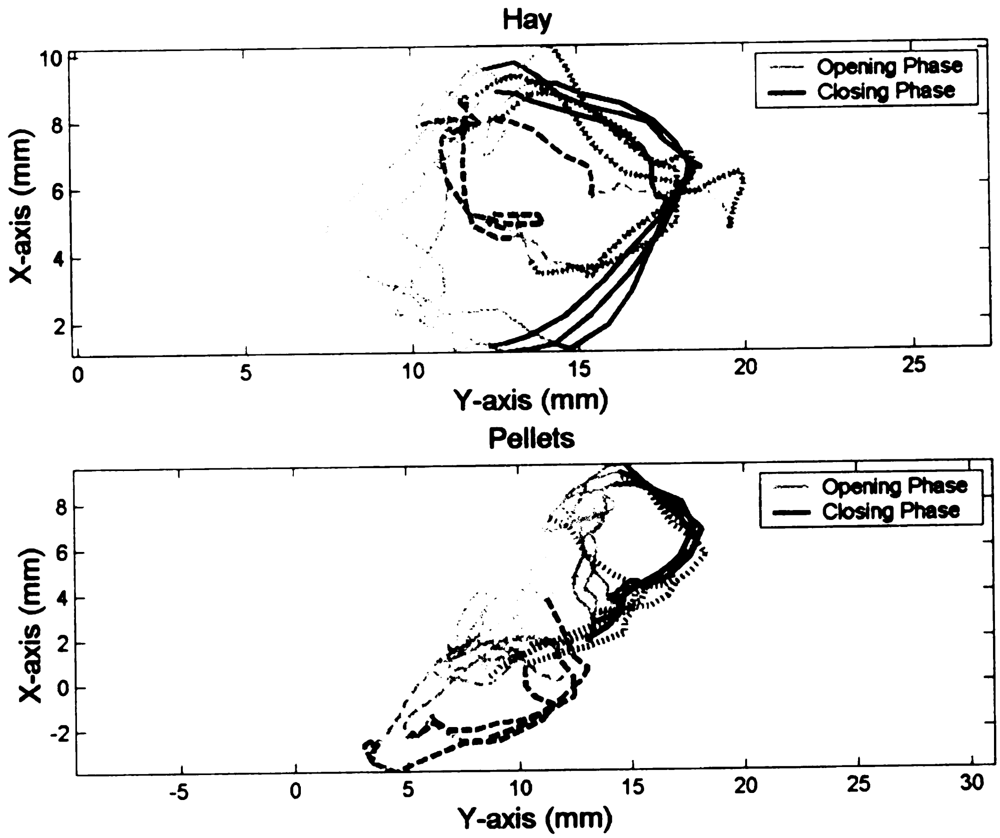

Figure 60: x-y location of mandibular coordinate system for horse #4 chewing on the left
Solid line = Trial 1
Dashed line = Trial 2
Hatched line = Trial 3

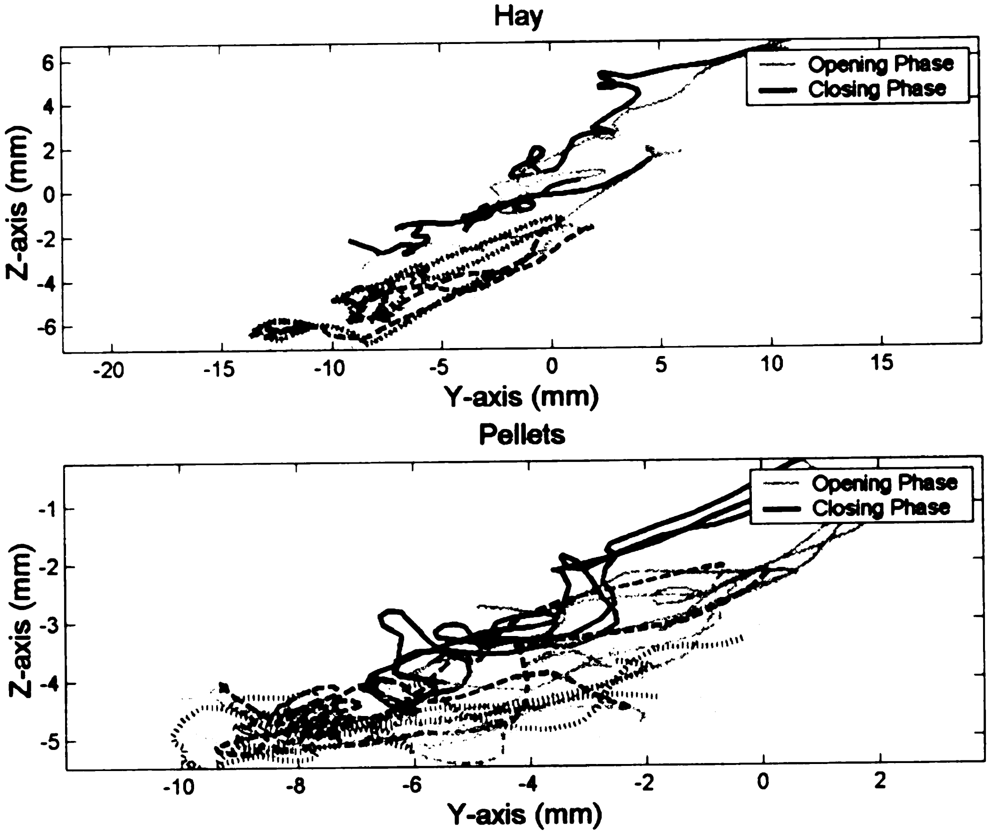

Figure 61: z-y location of mandibular coordinate system for horse #5 chewing on the right
Solid line = Trial 1
Dashed line = Trial 2
Hatched line = Trial 3

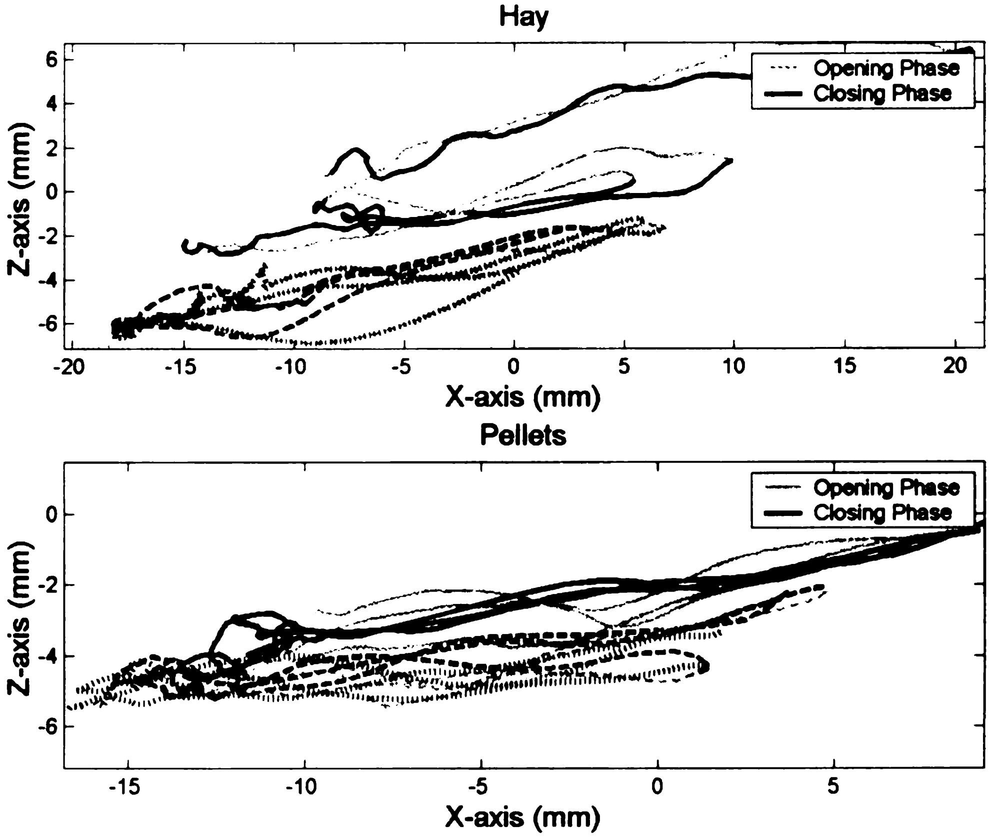

Figure 62: z-x location of mandibular coordinate system
for horse #5 chewing on the right
Solid line = Trial 1
Dashed line = Trial 2
Hatched line = Trial 3

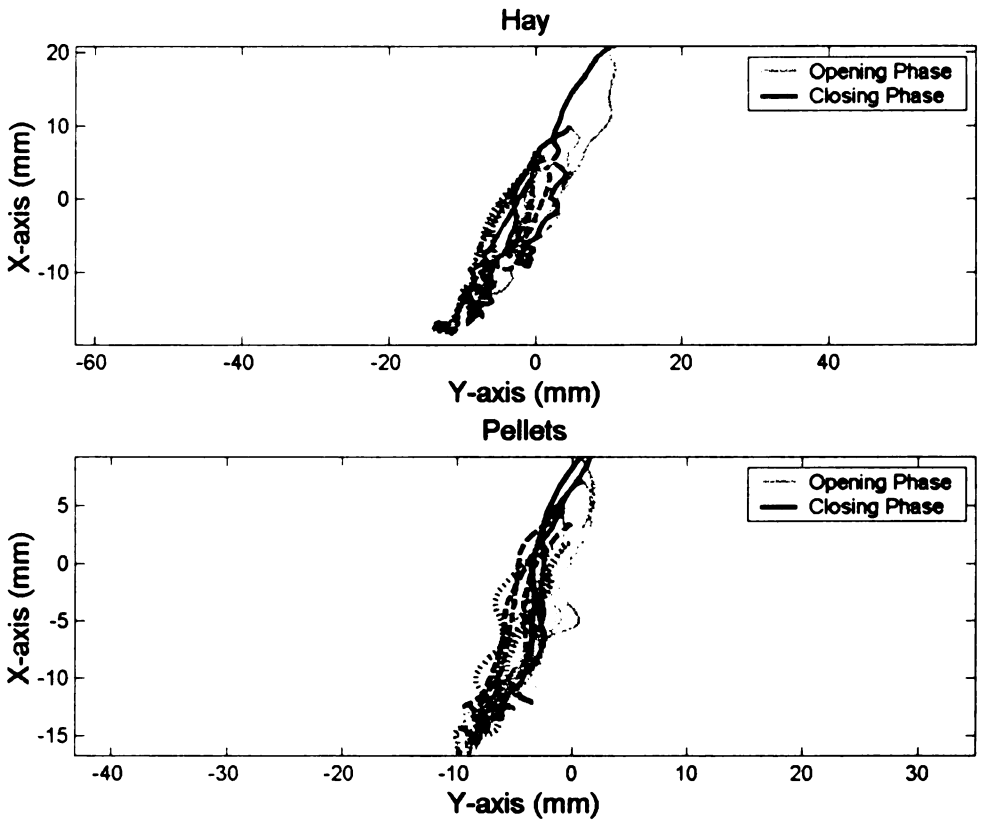

Figure 63: x-y location of mandibular coordinate system
for horse #5 chewing on the right
Solid line = Trial 1
Dashed line = Trial 2
Hatched line = Trial 3

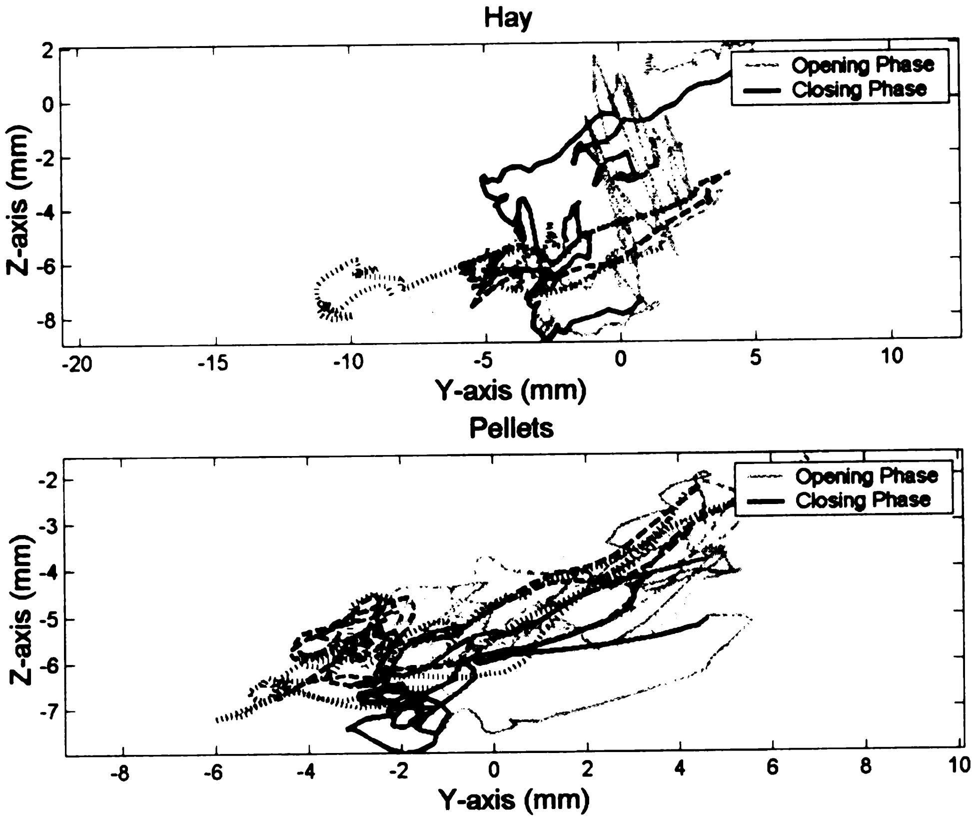

Figure 64: z-y location of mandibular coordinate system
for horse #6 chewing on the right
Solid line = Trial 1
Dashed line = Trial 2
Hatched line = Trial 3

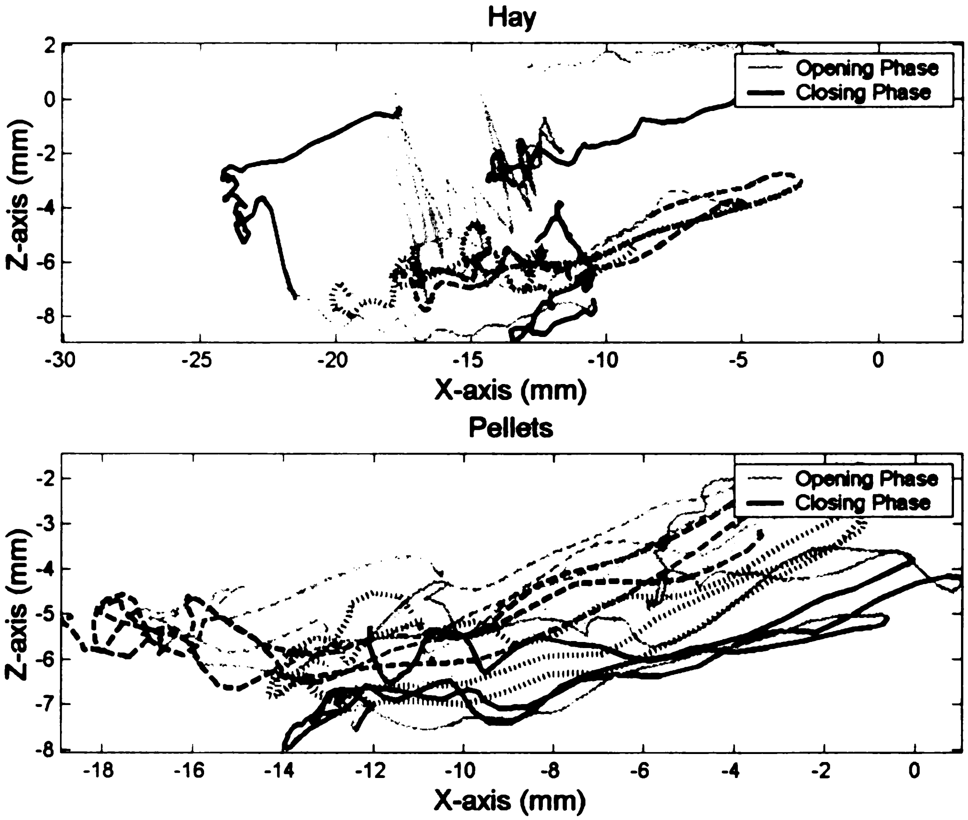

Figure 65: z-x location of mandibular coordinate system for horse #6 chewing on the right
Solid line = Trial 1
Dashed line = Trial 2
Hatched line = Trial 3

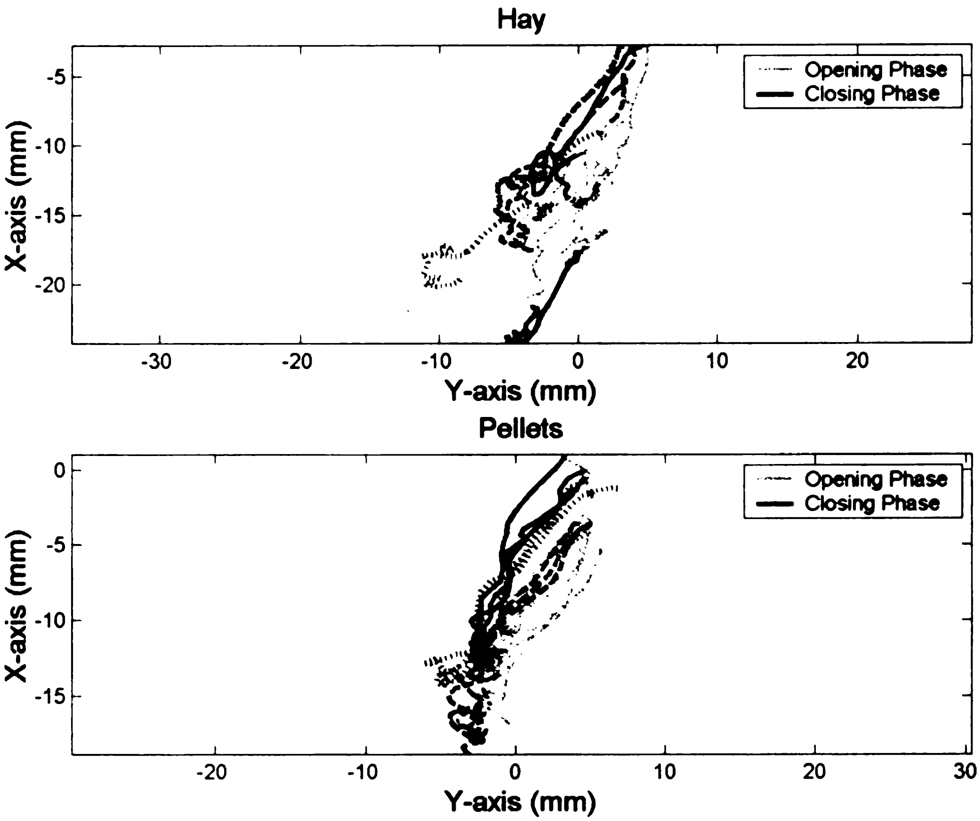

Figure 66: x-y location of mandibular coordinate system
for horse #6 chewing on the right
Solid line = Trial 1
Dashed line = Trial 2
Hatched line = Trial 3

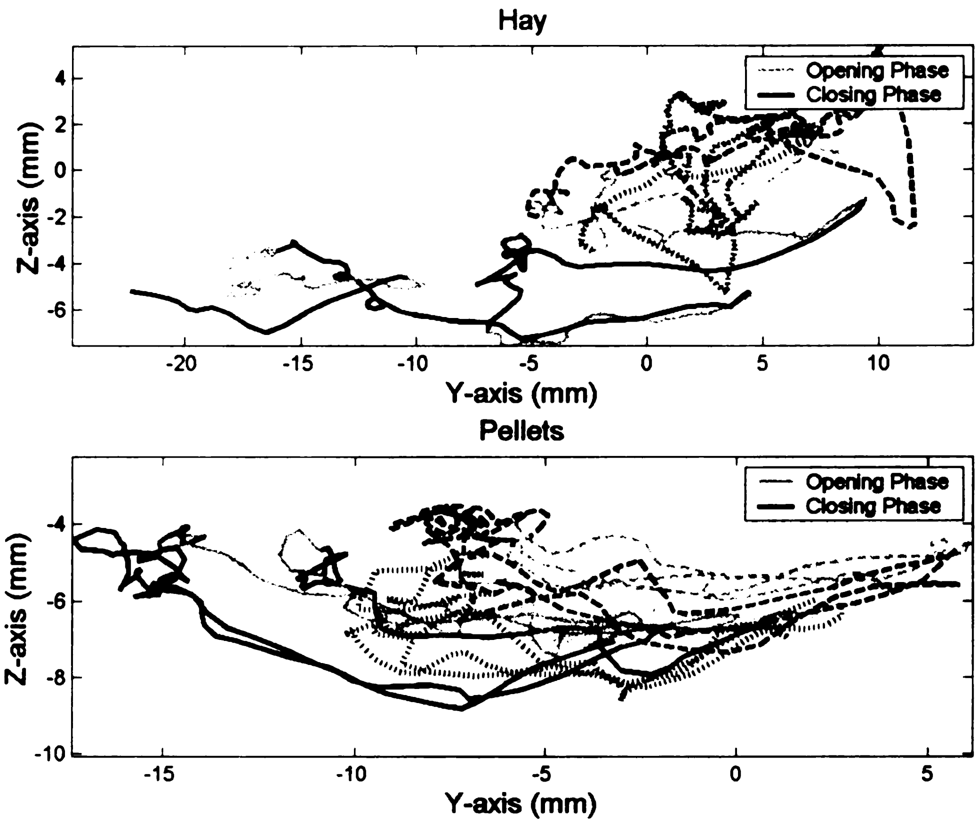

Figure 67: z-y location of mandibular coordinate system
for horse #7 chewing on the right
Solid line = Trial 1
Dashed line = Trial 2
Hatched line = Trial 3

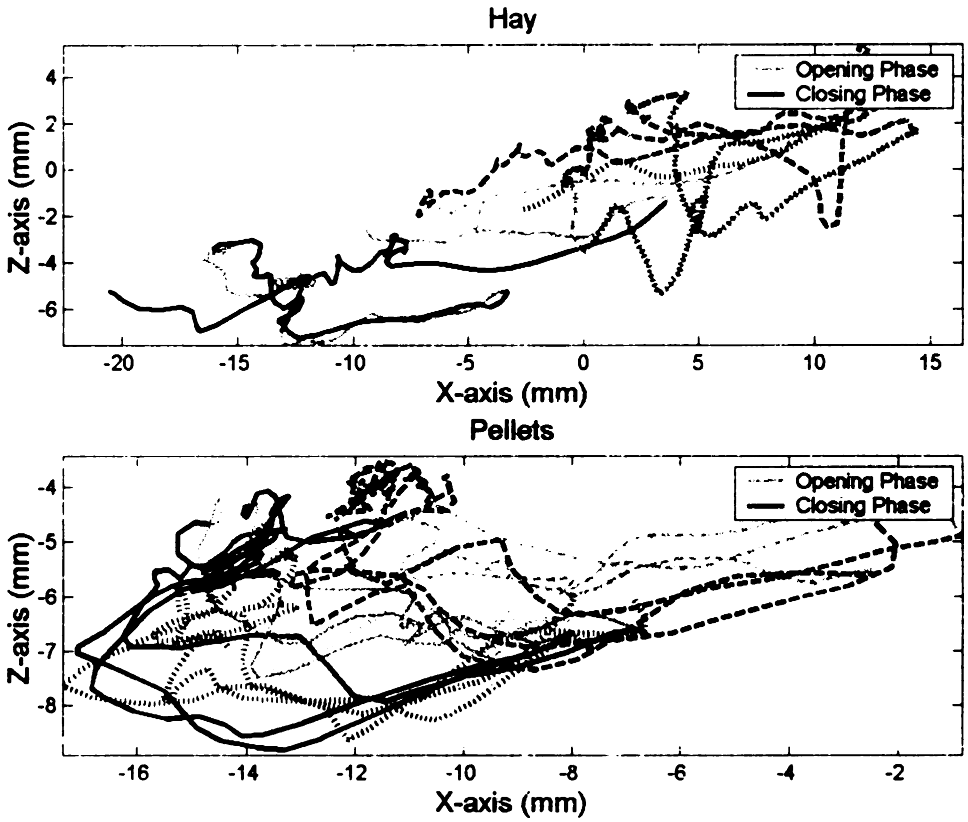

Figure 68: z-x location of mandibular coordinate system
for horse #7 chewing on the right
Solid line = Trial 1
Dashed line = Trial 2
Hatched line = Trial 3

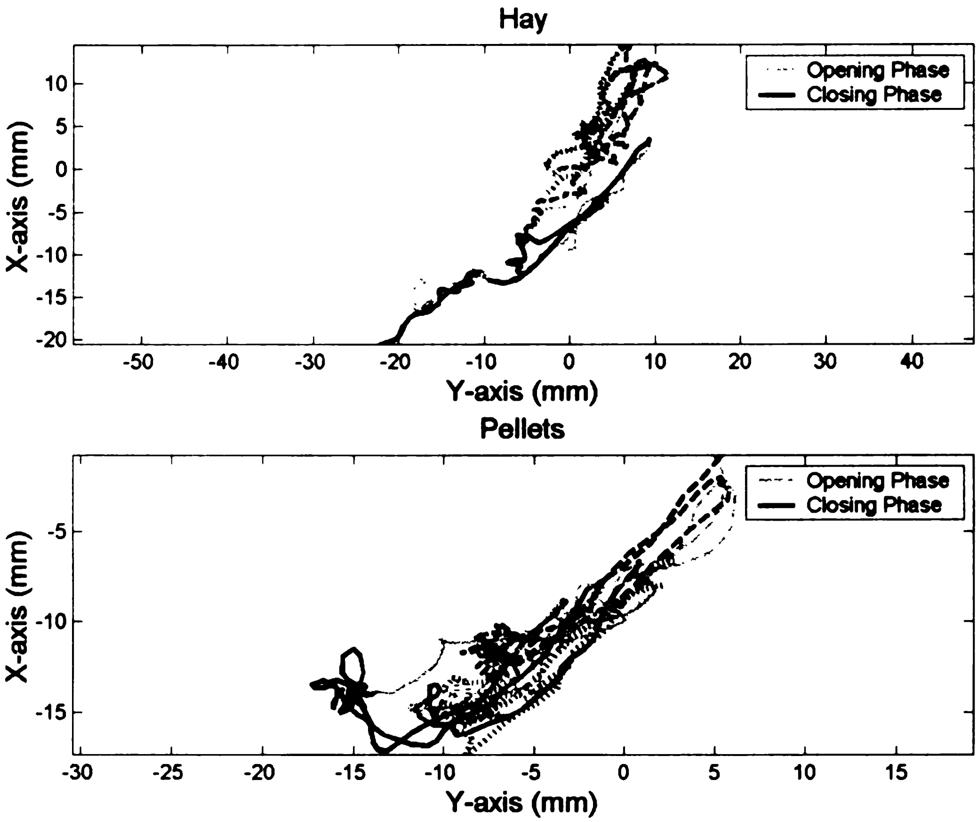

Figure 69: x-y location of mandibular coordinate system
for horse #7 chewing on the right
Solid line = Trial 1
Dashed line = Trial 2
Hatched line = Trial 3

Appendix C:

Mandibular Euler angles for all horses

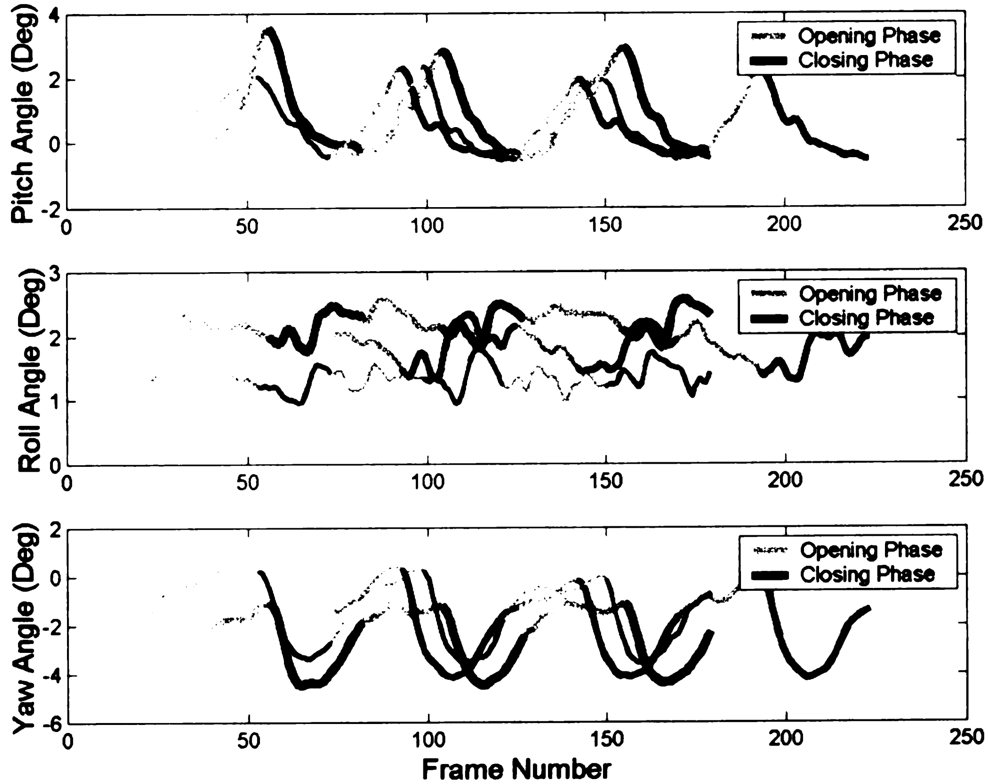

Figure 70: Euler angles for horse #1
while chewing hay on the right

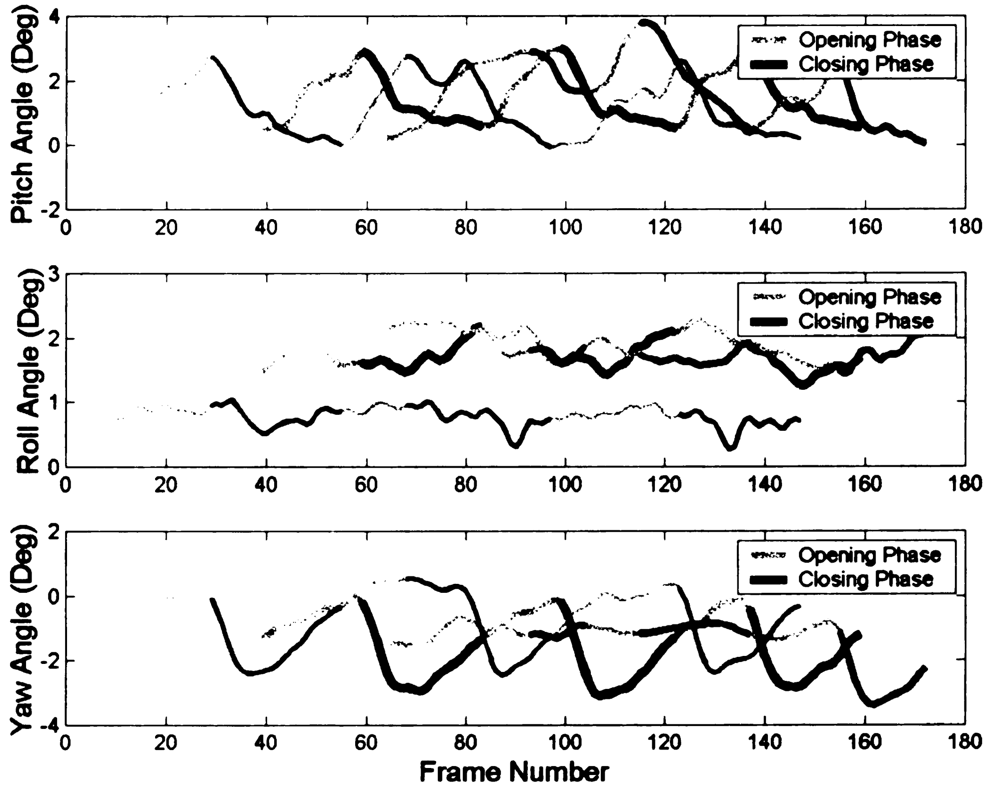

Figure 71: Euler angles for horse #1
while chewing pellets on the right

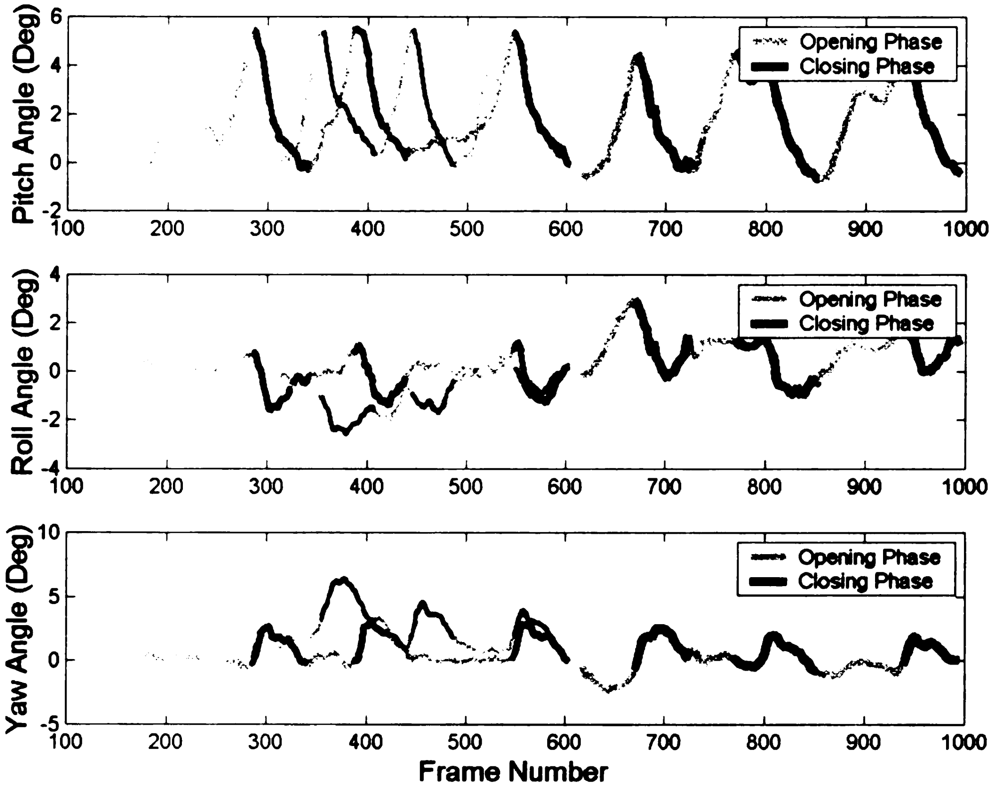

Figure 72: Euler angles for horse #2
while chewing hay on the left

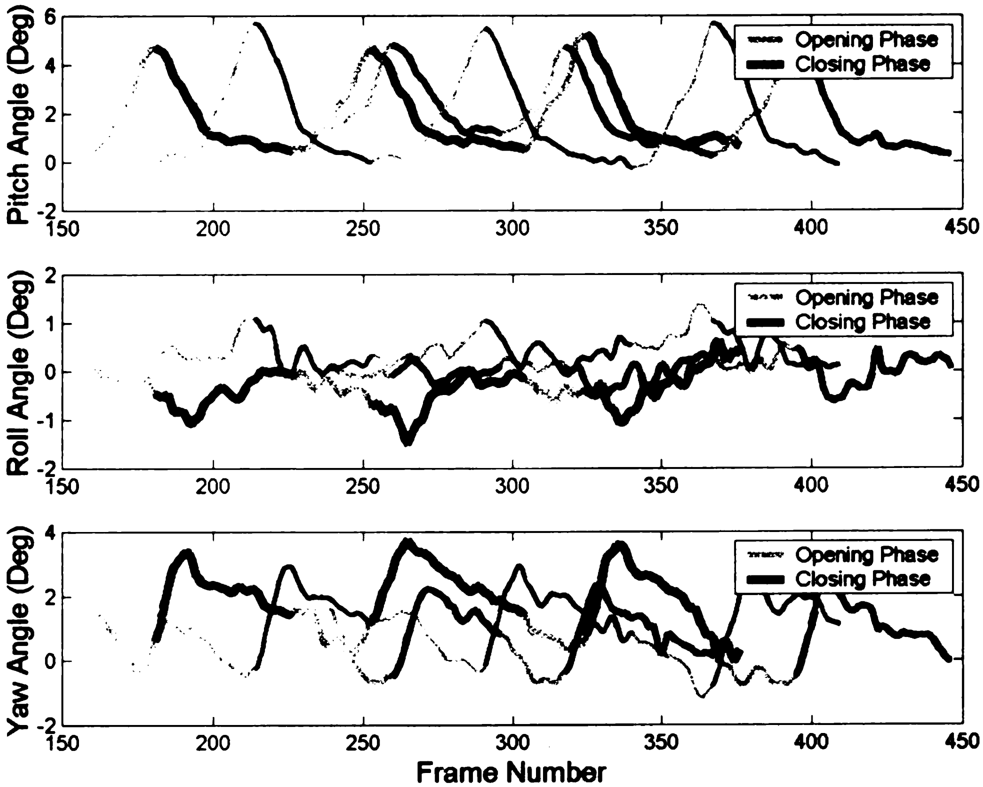

Figure 73: Euler angles for horse #2
while chewing pellets on the left

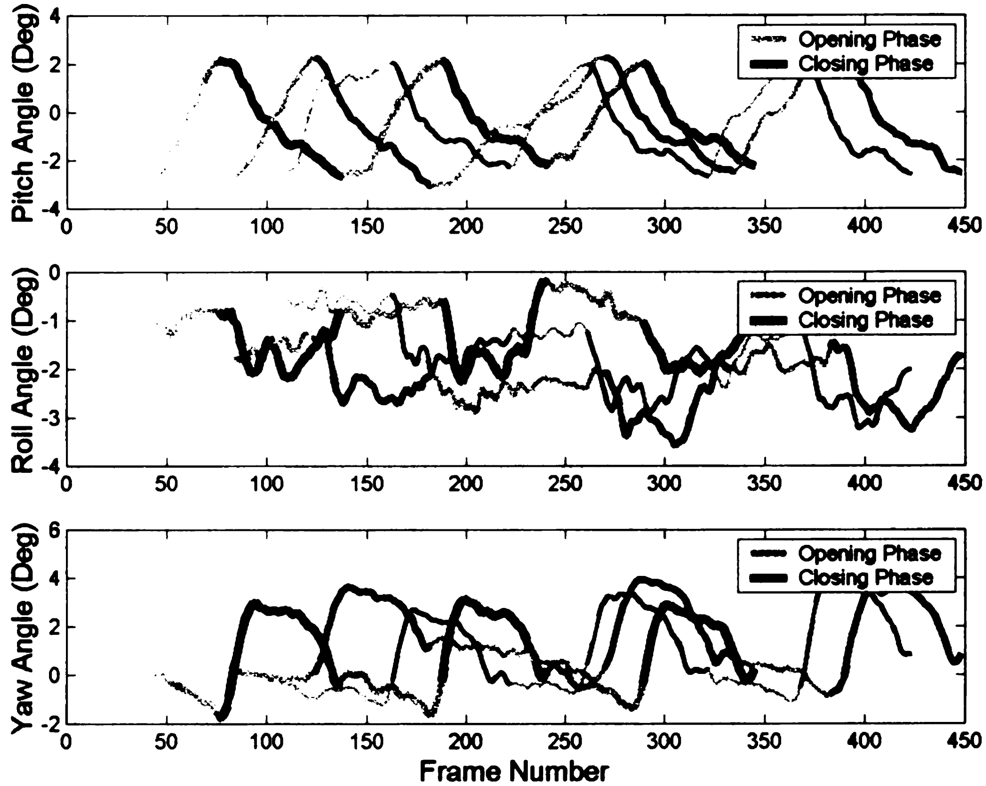

Figure 74: Euler angles for horse #3
while chewing hay on the left

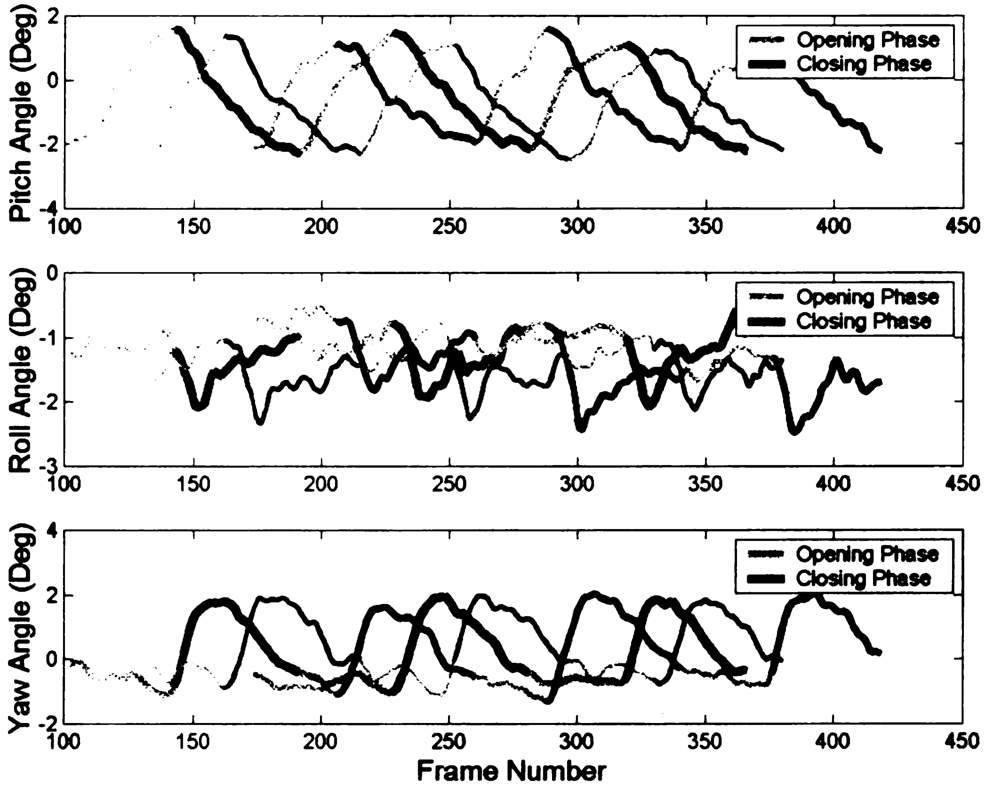

Figure 75: Euler angles for horse #3 while chewing pellets on the left

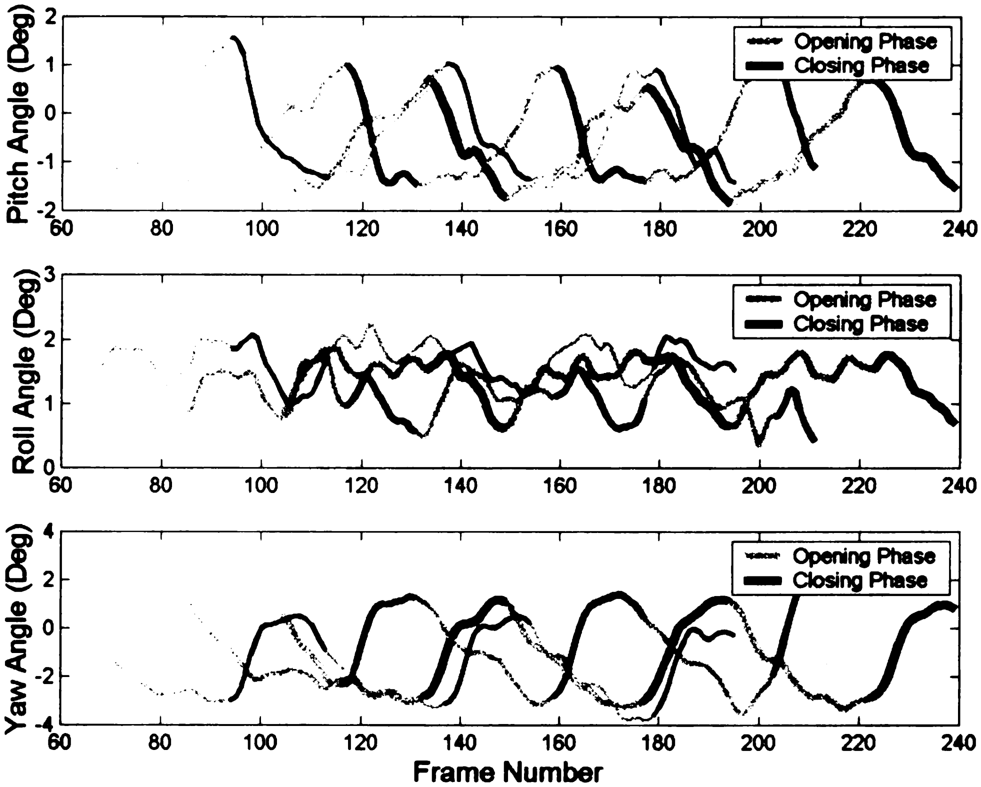

Figure 76: Euler angles for horse #4
while chewing hay on the left

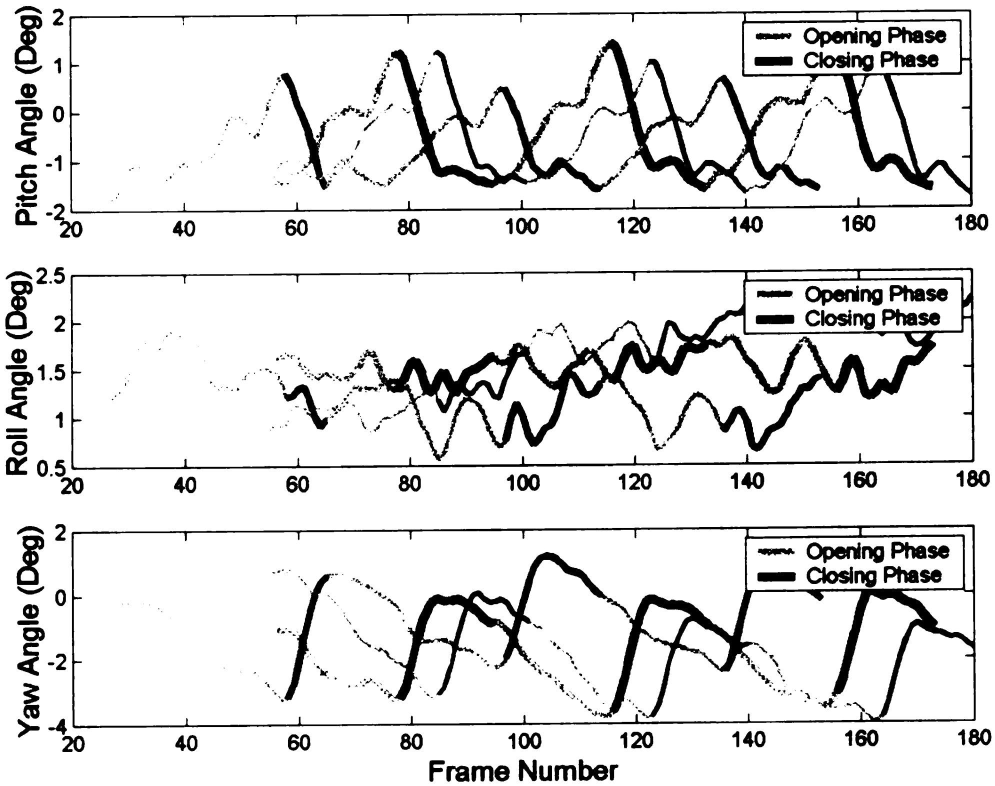

Figure 77: Euler angles for horse #4
while chewing pellets on the left

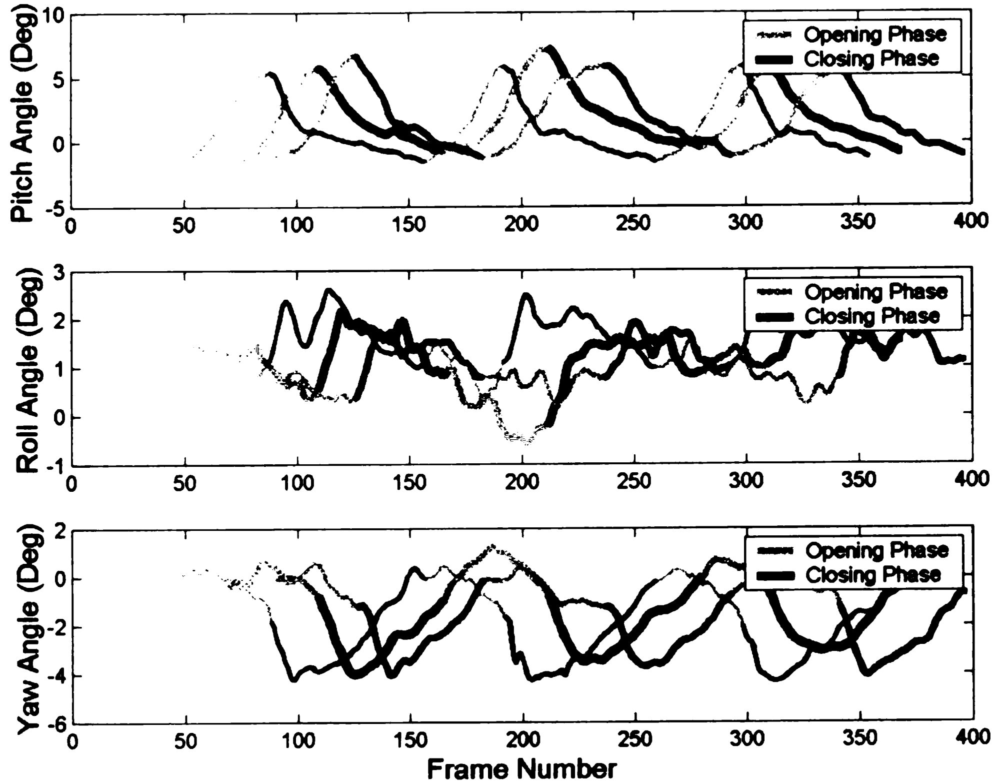

Figure 78: Euler angles for horse #5 while chewing hay on the right

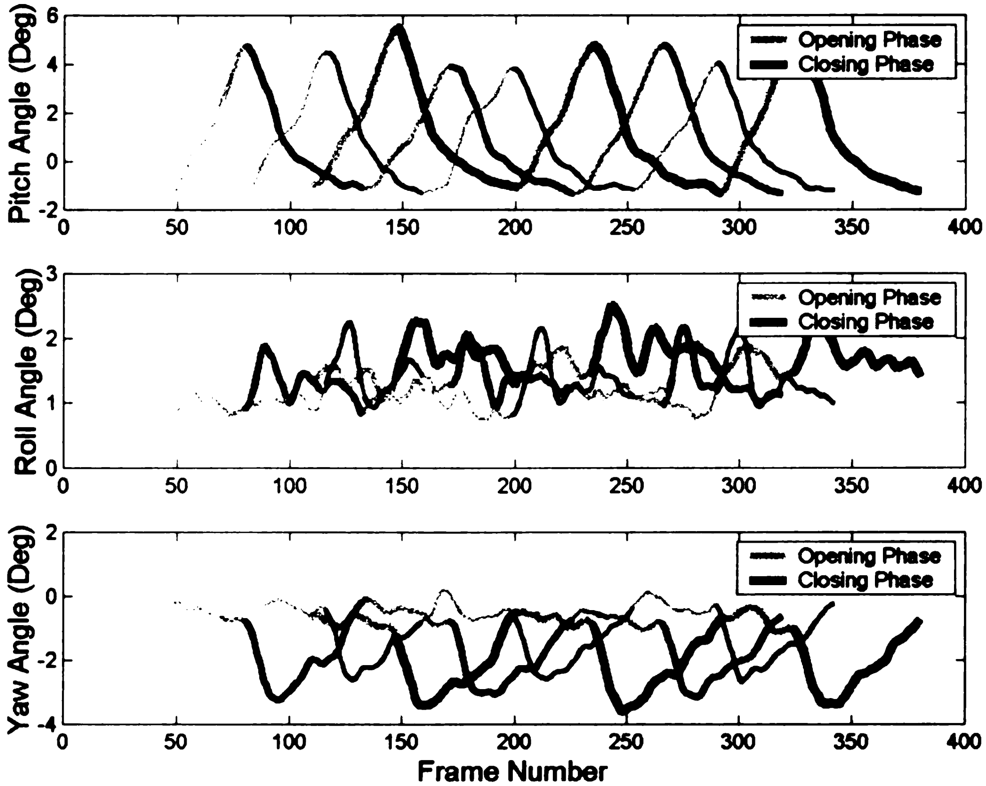

Figure 79: Euler angles for horse #5
while chewing pellets on the right

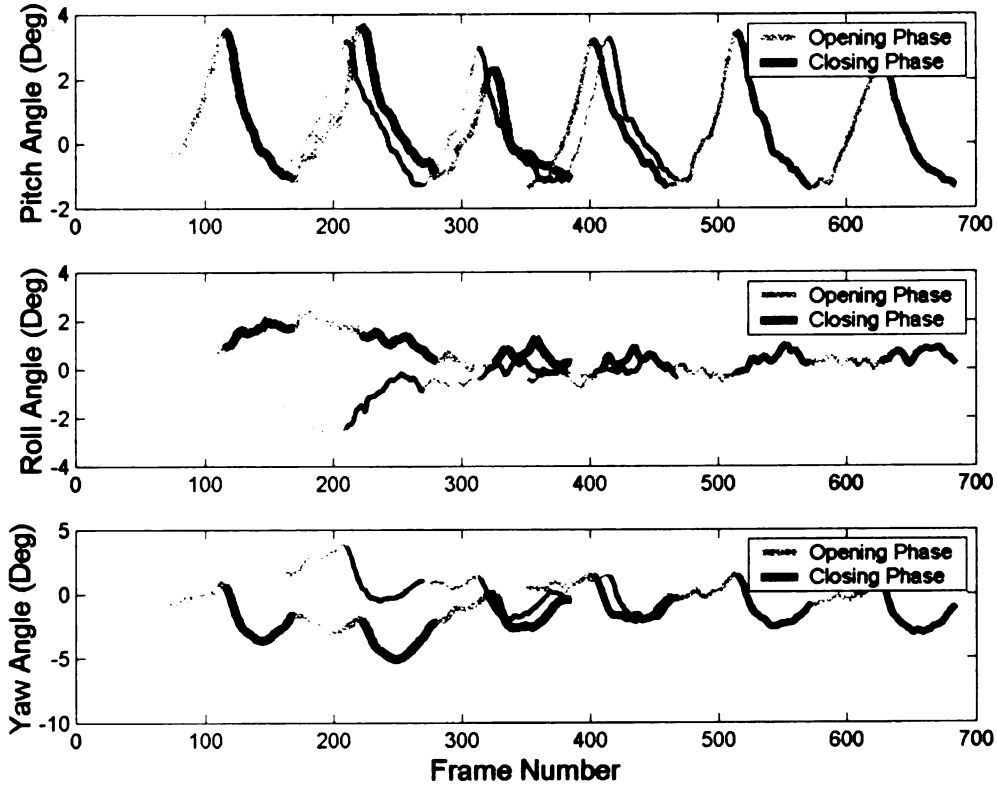

Figure 80: Euler angles for horse #6
while chewing hay on the right

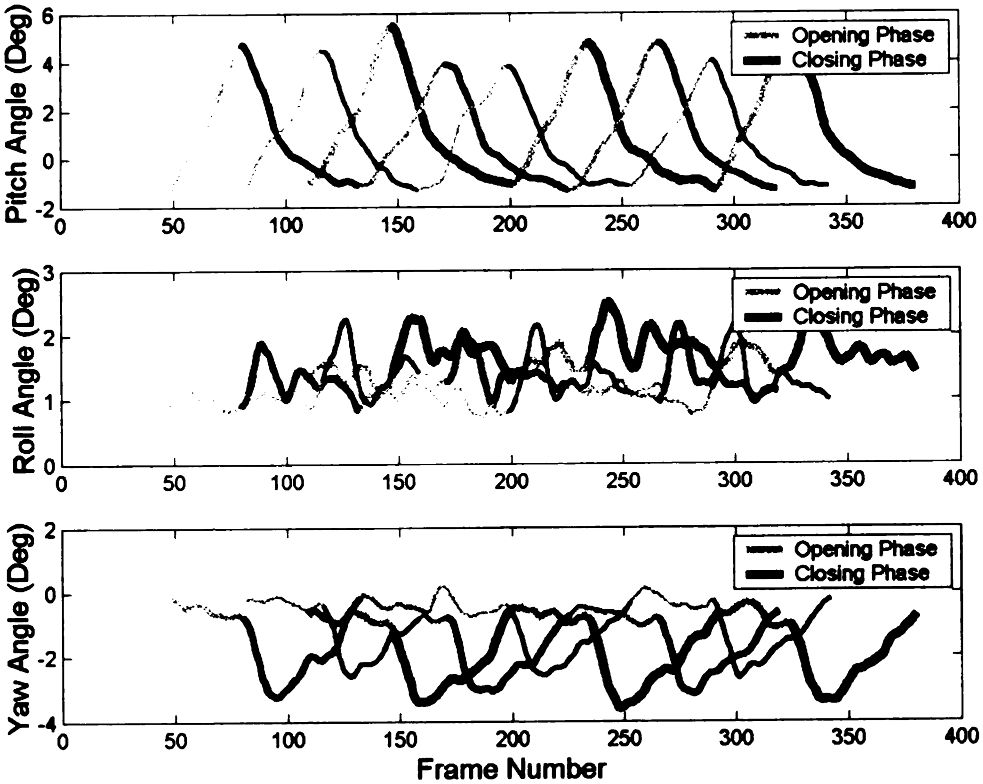

Figure 81: Euler angles for horse #6
while chewing pellets on the right

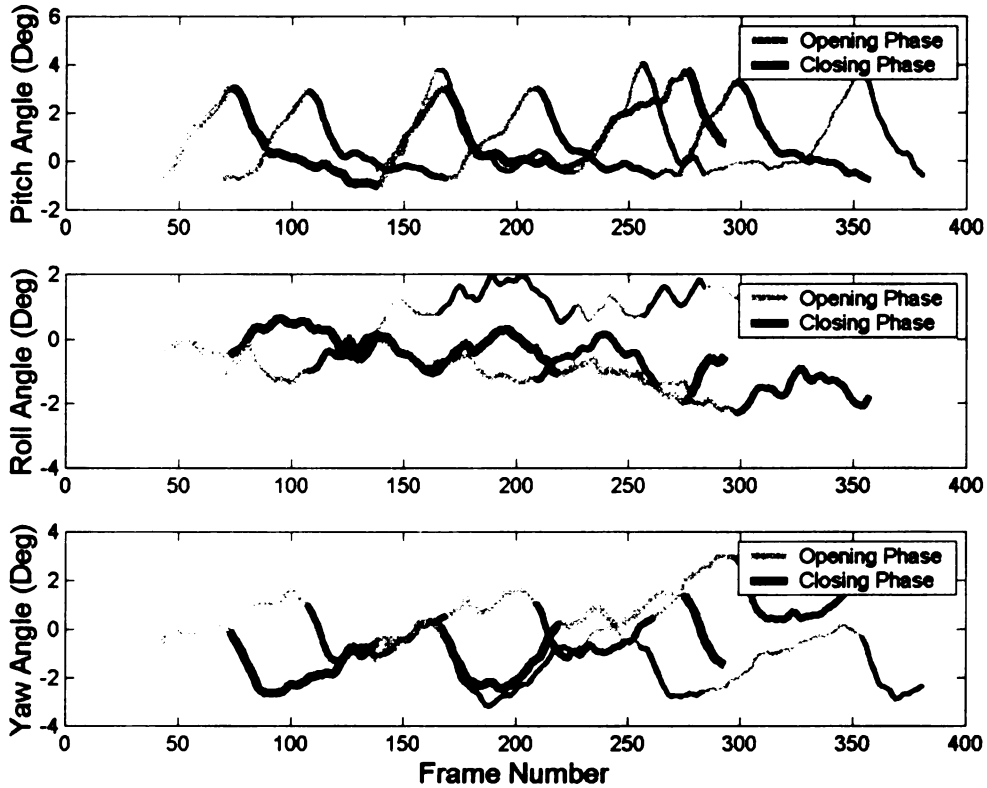

Figure 82: Euler angles for horse #7
while chewing hay on the right

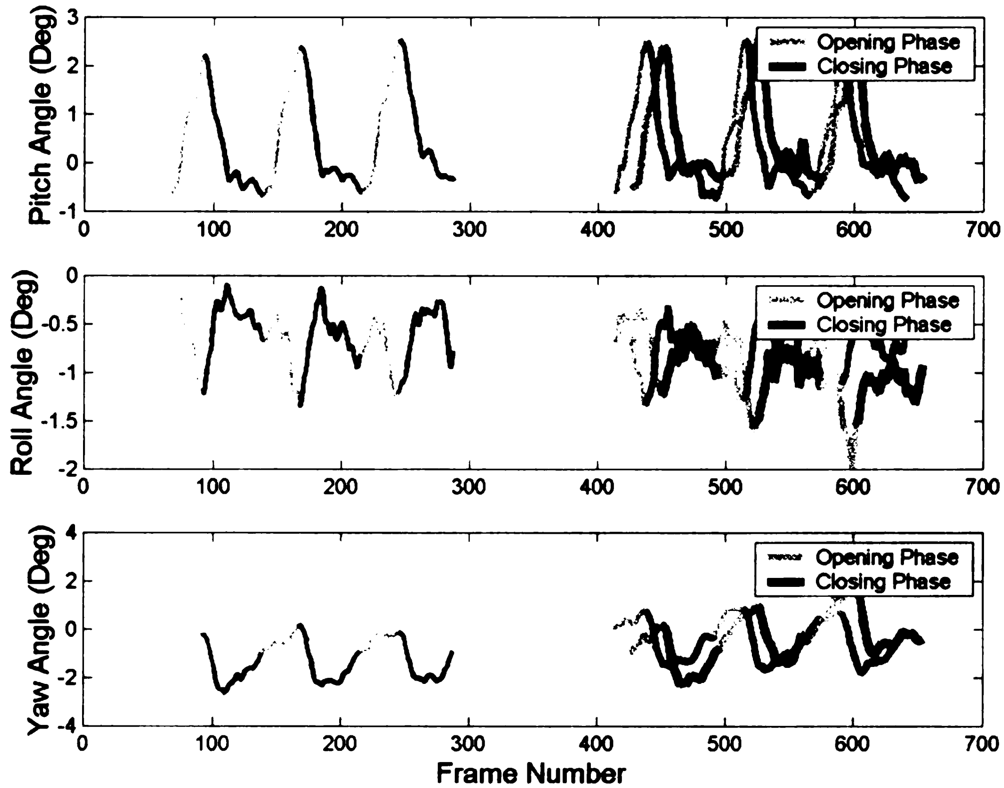

Figure 83: Euler angles for horse #7 while chewing pellets on the right

Bibliography

Baker G. and Easley J (1999) Equine Dentistry. W.B. Saunders Company Ltd. New York. pp. 30-32

Becker E (1962) Cited by Dixon PM (2000) Equine dental disease Part 3: a long-term study of 400 cases: disorders of wear, traumatic damage and idiopathic fractures, tumors and miscellaneous disorders of the cheek teeth. Equine Veterinary Journal Vol. 32, No. 1, pp. 9-18.

Brunner J (1941) Cited by Dixon PM (2000) Equine dental disease Part 3: a long-term study of 400 cases: disorders of wear, traumatic damage and idiopathic fractures, tumors and miscellaneous disorders of the cheek teeth. Equine Veterinary Journal Vol. 32, No. 1, pp. 9-18.

Capozzo A, Gazzani F, and Macellari V (1988) Skin marker artifacts in gait analysis. Proceedings of the 6th meeting European Society of Biomechanics. Butterworth, London. p. C23

Chen J and Buckwater K (1992) Motion analysis of the mandibular condyle from magnetic resonance images. Advances in Bioengineering Vol. 22, pp. 545-548.

Christiansen E, Thompson J, Hasso A, Hinshaw D, Moore R, Roberts D, and Kopp S (1987) CT number characteristics of malpositioned TMJ menisci diagnosis with CT number highlighting (blinkmode). Investigative Radiology Vol. 22, No. 4, pp. 315-321.

Collinson M (1994) Food processing and digestibility in horses (Equus caballus). BSc dissertation, Monash University.

Dyce KM, Sack WO, and Wensing, CJG (1987) Textbook of Veterinary Anatomy. W.B. Saunders Company Ltd. Philadelphia. pp. 61-65, 111-113.

Duncan P (1992) Horses and Grass: The nutritive ecology of equids and their impact on the carmargue. Springer-Verlag, New York.

Encyclopedia Britannica (2001) Britannica.com, Chicago, IL.

Fredricson I and Drevemo S (1971) A new method of investigating equine locomotion. Equine Veterinary Journal Vol. 3, No. 4, pp. 137-140.

Gallo LM, Fushima K, and Palla S (2000) Mandibular helical axis pathway during mastication. Journal of Dental Research Vol. 79, No. 8, pp. 1566-1572.

Gobel F and Duffner K (1954) Cited by Dixon PM (2000) Equine dental disease Part 3: a long-term study of 400 cases: disorders of wear, traumatic damage and idiopathic fractures, tumors and miscellaneous disorders of the cheek teeth. Equine Veterinary Journal Vol. 32, No. 1, pp. 9-18.

Grood ES and Suntay WJ (1983) A joint coordinate system for the clinical description of three simensional motions: application to the knee. Journal of Biomechanical Engineering Vol. 105, pp. 136-144.

Haug EJ (1989) Computer-Aided Kinematics and Dynamics of Mechanical Systems. Volume I: Basic Methods. Allyn and Bacon. Boston. pp.305-328

Jeffrey D (1986) Equine Dentistry Manual, Volume II. Leatherwork & Horse Tack & World Wind Equine Dental Supply Company. Waverly, NE. p. 1.

Joest E (1970) Handbuch der Speziellen Pathologischen Anatomie der Haustiere, Band V, Digestionsapparat, I. Teil. Verlag Paul Parey. Berlin. pp131-132

Johnson TJ (2000) Advanced Equine Dentistry. Recorder #114.

Kadaba MP, Ramakrishnan HK, and Wooten ME (1990) Measurement of lower extremity kinematics during level walking. Journal of Orthopaedic Research Vol. 8, No. 3, pp. 383- 392.

Koolstra JH and van Eijden TMGJ (1992) Application and validation of a three-dimensional mathematical model of the human masticatory system in vivo. Journal of Biomechanics Vol. 25, No. 2, pp. 175-187.

Leue G (1941) Cited by Becker, E (1962) Zahne. In: Handbuch der Speziellen Pathologischen Anatomie der Haustiere, Eds: J Dobberstein, G. Pallaske and H. Stunzi, Band V, 3rd edn, Verlag Paul Parey, Berlin. pp.131-132.

Leue G (1941) Cited by Dixon PM (2000) Equine dental disease Part 3: a long-term study of 400 cases: disorders of wear, traumatic damage and idiopathic fractures, tumors and miscellaneous disorders of the cheek teeth. Equine Veterinary Journal Vol. 32, No. 1, pp. 9-18.

Ostry D, Vatikiotis-Bateson E, and Gribble P (1997) An examination of the degrees of freedom of human jaw motion in speech and mastication. Journal of Speech, Language and Hearing Research Vol. 40, pp. 1341-1351.

Patterson LJ, Shappell KK, and Hurtig MB (1989) Mandibular condylectomy in a horse. Journal of American Veterinary Medical Association Vol. 195, No. 1, pp.101-102.

Paz M, Carter L, Westesson P, Katzberg R, Tallents R, Subteiny D, and Goldin B (1990) CT dentistry of the TMJ disk: Correlation with histological observations of hyalinization, metaplastic cartilage, and calcification in autopsy specimens. American Journal of Orthodontics Dentofacial Orthopaedics Vol. 98, No. 4, pp. 354-357.

Plesh O, Bishop B, and McCall WD (1993) Kinematics of jaw movements during chewing at different frequencies. Journal of Biomechanics Vol. 26, No. 8, pp. 243-250.

Ramakrishnan HK and Kadaba MP. (1991) On the estimation of joint kinematics during gait. Journal of Biomechanics Vol. 24, No. 10, pp. 969-977.

Raustia AM and Pyhtinen J (1990) Morphology of the condyles and mandibular fossa as seen by computed tomography. The Journal of Prosthetic Dentistry Vol. 63, No. 1, pp. 77-82.

Reinschmidt C, van den Bogert AJ, Nigg BM, Lundberg A, and Murphy N (1997). Effect of skin movement on the analysis of skeletal knee joint motion during running. Journal of Biomechanics Vol. 30, No. 7, pp.729-732.

Rosenstein DS, Bullock MF, Ocello PJ, and Clayton HM (2001). Arthrocentesis of the temporomandibular joint in adult horses. American Journal of Veterinary Research Vol. 62, No. 5, pp. 729-733.

Salomon JA, Waysenson BD (1979) Computer-monitored radionuclide tracking of three-dimensional mandibular movements. Part I: Theoretical approach. Journal of Prosthetic Dentistry Vol. 41, No. 3, pp. 340-344.

Sisson S and Grossman JD (1975) <u>The Anatomy of Domestic Animals, Volume I</u> W.B. Saunders Company. Philadelphia. pp. 318-342, 384-386.

Soderkvist I and Wedin P (1993) Determining the movements of the skeleton using well-configured markers. Journal of Biomechanics Vol. 26, No. 12, pp. 1473-1477.

Triola MF (1998) <u>Elementary Statistics Seventh Edition</u>. Addison-Wesley. New York. pp. 288-308.

Visscher CM, Huddleston Slater JJR, Lobbezoo F, and Naeje M (2000) Kinematice of the human mandible for different head postures. Journal of Oral Rehabilitation Vol. 27, pp. 299-305.

Warmerdam EPL, Klein WR, and van Herpen BPJM (1997) Infectious temporomandibular joint disease in the horse: computed tomographic diagnosis and treatment of two cases. Veterinary Record Vol. 141, pp. 172-174.

Woltring HJ (1986) A FORTRAN package for generalized, cross-validatory spline smoothing and differentiation. Advances in Engineering Software Vol. 8, No. 2, pp. 104-113.

Weller R, Cauvin ER, Bowen IM, and May SA (1999) Comparison of radiography, scintigraphy and ultrasonography in the diagnosis of a case of temporomandibular joint arthropathy in a horse. Veterinary Record Vol. 144, pp. 377-379.

Yatabe M, Zwijnengurg A, Megens CCEJ, Naeije M (1997) Movements of the mandibular condyle kinematic center during jaw opening and closing. Journal of Dental Research Vol. 76, No. 2, pp. 714-719.

Zhang X, Ashton-Miller JA, and Stohler CS (1995) Three-dimensional unilateral method for the bilateral measurement of condylar movements. Journal of Biomechanics Vol. 28, No. 8, pp. 1007-1011.